

**Subunits of highly fluorescent protein R-phycoerythrin
as probes for cell imaging and single-molecule detection**

by

Dragan Isailovic

A dissertation submitted to the graduate faculty
in partial fulfillment of the requirements for the degree of

DOCTOR OF PHILOSOPHY

Major: Analytical Chemistry

Program of Study Committee:
Edward. S. Yeung, Major Professor
Gregory J. Phillips
Mei Hong
Robert S. Houk
Marc D. Porter

Iowa State University

Ames, Iowa

2005

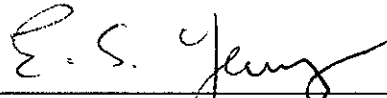
Copyright © Dragan Isailovic, 2005. All rights reserved.

Graduate College
Iowa State University

This is to certify that the doctoral dissertation of

Dragan Isailovic

has met the dissertation requirements of Iowa State University


Major Professor

For the Major Program

To
My family

TABLE OF CONTENTS

ABSTRACT	vi
CHAPTER 1. GENERAL INTRODUCTION	1
Dissertation Organization.....	1
Single-Cell Analysis.....	1
Single-Molecule Detection.....	2
High-Resolution and High-Contrast Light Microscopy and Spectroscopy for Imaging of Cells and Molecules.....	4
High-Throughput Spectral Analysis of Single-Molecules and Single-Cells.....	14
Fluorescent Proteins.....	16
Localization and Expression of Proteins in <i>Escherichia coli</i> (<i>E. coli</i>).....	22
Our Goal.....	27
References.....	28
CHAPTER 2. ISOLATION AND CHARACTERIZATION OF R-PHYCOERYTHRIN SUBUNITS AND ENZYMATIC DIGESTS	35
Abstract.....	35
Introduction.....	36
Experimental.....	38
Results and discussion.....	43
Acknowledgements.....	49
References.....	50
CHAPTER 3. FORMATION OF FLUORESCENT PROTEINS BY NON-ENZYMATIC ATTACHMENT OF PHYCOERYTHROBILIN TO APO-SUBUNITS OF R-PHYCOERYTHRIN <i>IN VITRO</i> AND <i>IN VIVO</i> (<i>IN ESCHERICHIA COLI</i>)	70
Summary.....	70
Introduction.....	71
Material and methods.....	74
Results.....	78
Discussion.....	82
References.....	84
Footnotes.....	86

CHAPTER 4. HIGH-THROUGHPUT SINGLE-CELL FLUORESCENCE

SPECTROSCOPY	112
Abstract.....	112
Introduction.....	113
Experimental.....	115
Results and discussion.....	117
Conclusion.....	120
Acknowledgements.....	120
References.....	121

CHAPTER 5. GENERAL CONCLUSIONS	130
---	-----

ACKNOWLEDGEMENT	134
------------------------------	-----

ABSTRACT

The purposes of our research were:

1. To characterize subunits of highly fluorescent protein R-Phycoerythrin (R-PE) and check their suitability for single-molecule detection (SMD) and cell imaging,
2. To extend the use of R-PE subunits through design of similar proteins that will be used as probes for microscopy and spectral imaging in a single cell, and
3. To demonstrate a high-throughput spectral imaging method that will rival spectral flow cytometry in the analysis of individual cells.

We first demonstrated that R-PE subunits have spectroscopic and structural characteristics that make them suitable for SMD. Subunits were isolated from R-PE by high-performance liquid chromatography (HPLC) and detected as single molecules by total internal reflection fluorescence microscopy (TIRFM). In addition, R-PE subunits and their enzymatic digests were characterized by several separation and detection methods including HPLC, capillary electrophoresis, sodium dodecyl sulfate-polyacrylamide gel electrophoresis (SDS-PAGE) and HPLC-electrospray ionization mass spectrometry (ESI-MS). Favorable absorption and fluorescence of the R-PE subunits and digest peptides originate from phycoerythrobilin (PEB) and phycourobilin (PUB) chromophores that are covalently attached to cysteine residues. High absorption coefficients and strong fluorescence (even under denaturing conditions), broad excitation and emission fluorescence spectra in the visible region of electromagnetic spectrum, and relatively low molecular weights make these molecules suitable for use as fluorescence labels of biomolecules and cells.

We further designed fluorescent proteins both *in vitro* and *in vivo* (in *Escherichia coli*) based on the highly specific attachment of PEB chromophore to genetically expressed apo-subunits of R-PE. In one example, apo-alpha and apo-beta R-PE subunits were cloned from red algae *Polysiphonia boldii* (*P. boldii*), and expressed in *E. coli*. Although expressed apo-subunits formed inclusion bodies, fluorescent holo-subunits were formed after incubation of *E. coli* cells with PEB. Spectroscopic characterization of holo-subunits confirmed that the attachment of PEB chromophore to apo-subunits yielded holo-subunits containing both PEB and urobilin (UB). Fluorescence and differential interference contrast (DIC) microscopy showed polar location of holo-subunit inclusion bodies in *E. coli* cells. In another example,

R-PE apo-subunits were genetically fused to cytoplasmic and periplasmic versions of *E. coli* maltose binding protein (MBP). Fluorescent proteins formed after attachment of PEB to MBP-subunit fusions *in vitro* and *in vivo* contained PEB as the sole chromophore, were soluble, and displayed high orange fluorescence. Fluorescence microscopy showed that fusions are located either throughout cells or at cell poles. In addition, cells containing fluorescent holo-subunits or MBP-subunit fusions were up to ten times brighter than control cells as measured by flow cytometry. Results show that the fluorescent proteins formed after non-enzymatic attachment of PEB to R-PE subunit fusions could be used as reporters of gene expression and protein localization in cells as well as fluorescence labels in flow cytometry.

Finally, we demonstrated a high-throughput method able to record emission fluorescence spectra of individual cells containing fluorescent proteins. Upon excitation with a 488 nm argon-ion laser many bacterial cells were imaged by a 20X microscope objective while they moved through a capillary tube. Fluorescence was dispersed by a transmission diffraction grating, and an intensified charge-coupled device (ICCD) camera simultaneously recorded the zero and the first orders of the fluorescence from each cell. Single-cell fluorescence spectra were reconstructed from the distance between zero-order and first-order maxima as well as the length and the pixel intensity distribution of the first-order images. By using this approach, the emission spectrum of *E. coli* cells expressing green fluorescent protein (GFP) was reconstructed. Also, fluorescence spectra of *E. coli* cells expressing apo-subunits of R-PE were recorded after incubation of the cells with PEB. The fluorescence spectra are in good agreement with results obtained on the same cells using a fluorescence spectrometer and a fluorescence microscope. When spectra are to be acquired, this approach could have a higher throughput, better sensitivity, and better spectral resolution compared to spectral flow cytometry.

CHAPTER 1. GENERAL INTRODUCTION

Dissertation Organization

This dissertation begins with a general introduction. The following chapters are presented as three complete scientific manuscripts followed by cited literature, tables and figures. General conclusions summarize the work and provide some prospective for future research.

Single-Cell Analysis

The cell is the basic structural and functional unit of each living organism. In the hierarchy of biological organization the cell is the simplest form of matter that can live.¹ Diverse forms of life, for example bacteria², exist as the single-cell organisms. More complex organisms contain many kinds of specialized cells that are cooperatively connected in tissue and organs. Even if arranged into higher levels of organization, cells still could be singled out and analyzed.

Cells can be studied at the level of a population or individually.³ Information of how cells respond to their environment, interact with each other, or undergo complex processes of differentiation and gene expression can be obtained by averaging data from a population of cells.⁴ Individual cells in a population however may differ widely from each other in terms of their genetic composition, physiology, biochemistry or behavior. The heterogeneity in a cell population is taken into account if cells are examined at the single-cell level.^{3,4} Single-cell analysis is also a method of choice if the limited number of cells is available.³ The choice between population and single-cell studies depends on the addressed research questions. The best approach to explore cells would be the combination of results from both population and single-cell studies, if possible.³

Many bioanalytical tools and techniques have contributed to the great insights that we have today in the structure and chemistry of the cell.^{5,6} Light microscope is indispensable tool for cell analysis since its discovery by van Leeuwenhoek in the 17th century. Improvements in light microscopy techniques and discoveries of specific probes for labeling of cellular compartments make light microscopy the method of choice for single-cell imaging

and spectroscopy.⁷⁻¹¹ Electron and scanning probe microscopes have enabled imaging of cells in great details thanks to their nanometer-scale resolutions and extremely high magnifications.¹ Flow cytometers sort cells and detect fluorescent tags bound to proteins, carbohydrates, lipids and nucleic acids.^{12, 13} DNA extraction and polymerase chain reaction (PCR) are used for genotyping of single-cells, as well as in biotechnology.^{3, 13} Electrochemistry monitors chemical reactions and transport of metabolites in cells providing both temporal and spatial information.⁵ Separation methods including capillary electrophoresis (CE)^{14,15}, liquid chromatography^{5,16}, and microfluidic technologies¹⁷ can both analyze and sort cells. Mass spectrometry (MS) is used to analyze individual cells due to its universality and high sensitivity.^{5, 18}

New challenges in deciphering the mechanisms of cellular functions are ahead. Scientists including analytical chemists try to answer questions of post genomic era related to proteomics, metabolomics and system biology.¹⁹ Many of these questions hide the answers at the molecular level. Since the number of copies of a molecule in a cell is limited sensitive bioanalytical techniques are prerequisite.³ Development and application of microscopes that will simultaneously follow and localize specific molecules in a cell at the high spatial resolution is one way to solve many of unknowns of cellular life and function.²⁰

Single-Molecule Detection

Single-molecule detection (SMD) is the ultimate level in both sensitivity and selectivity of an analytical technique. Exploring single-molecules at surfaces is possible by electron or atomic force microscopes. On the other hand, advances in sensitive optical technologies during last fifteen years led to detection and spectroscopic characterization of single-molecules by light microscopy. SMD is performed on molecules both on surfaces and in condensed matter.^{21, 22} Results are usually reported for many molecules, one by one, which allows construction of frequency histograms for the actual distribution of measured parameters.²¹ The distribution of results contains more information than the average value from the ensemble experiment, although it is beneficial to compare both approaches.

Optical SMD has become a laboratory tool that provides information on physical and chemical characteristics of molecules that are obviously hidden in ensemble experiments.²³ For example, diffusion coefficients, photobleaching rates or chemical activities of single protein or DNA molecules can be measured in free solution.^{24, 25} Processes of adsorption at the surfaces, enzymatic reactions and separation of single-molecules have been demonstrated.²⁵⁻²⁹ Sequencing of DNA molecules can also be done at the single-molecule level.³⁰ High-throughput SMD techniques can analyze thousands of molecules each second.^{28, 31, 32} In addition, single molecules can be detected and followed in cells.³³⁻³⁶ This provides a possibility to screen for DNA, RNA or protein molecules within single-cell for disease markers.³⁷

For detecting single molecules it is necessary to have sufficient signal to record the event (high sensitivity), but also to have the ability to recognize the target molecule in its environment (high selectivity). Several technical considerations made detection of single-molecule possible.^{21, 22, 38} Since many photons should be detected, the simplest way of SMD is to monitor molecular fluorescence. Fluorescence of the molecule can be cycled thousands of times before photobleaching of a fluorophore occurs. Fluorophores with high absorption coefficients, high quantum yields and high photostability are desirable.³⁹ Another approach to improve signal in SMD is to get multiple products from the same molecules, for example by the reaction catalyzed by the single-molecule of an enzyme.²⁶ Although detection of a single fluorophore is possible, multiple labeling of a molecule improves sensitivity of SMD. The highest sensitivity is achieved if above considerations are combined.

To increase selectivity of SMD all sources of background noise should be suppressed. Use of appropriate excitation and emission filters and time-gated detectors can suppress stray light of the bulk medium containing molecules of interest. Since impurities might contribute to the detected signal, media should be ultra pure. Miniaturization of the observed volume helps to increase both effective concentration of the molecule (sensitivity) and to isolate molecules from similar molecules in the medium (selectivity). This could be achieved in several ways including hydrodynamic focusing in a sheath flow or a capillary, confocal microscopy and evanescent wave excitation.^{37, 40} In addition to the above considerations,

both SMD and single-cell analysis require the high-resolution microscopy and spectroscopy to yield the maximal amount of information from the interrogated system.

***High-Resolution and High-Contrast Light Microscopy and Spectroscopy
for Imaging of Cells and Molecules***

Important characteristics of light microscopy techniques include magnification, contrast and resolution.⁴¹ The highest useful magnification of a light microscope is approximately one thousand times the objective numerical aperture (NA).⁴² For oil immersion objective with NA of 1.4 useful magnification is around 1400 times. Magnification above this (empty magnification) makes an image bigger but does not resolve any additional details. Two details in an image will not be resolved by light microscopy if they are separated by distance smaller than approximately the half of the wavelength of light. As Abbe found one hundred and thirty years ago the highest resolution of the light microscope is limited by the diffraction limit of light. For 100x oil immersion objective (NA = 1.4) and oil immersion condenser (NA = 1.4) diffraction limit for green light and lateral (x-y) resolution of the microscope is ~ 200 nm. Fortunately, improvements in high-resolution and high-contrast light microscopy techniques have enabled detection of cellular structures and single-molecules that are even smaller than diffraction limit of light.

Fluorescence microscopy

Fluorescence imaging is highly specific and sensitive. If the background has negligible fluorescence, images of high contrast are produced that are suitable for automated image analysis. Fluorescence microscopy has advanced its applications because of the rapid development of new technologies for fluorescence imaging and suitable fluorescence probes.⁴³⁻⁴⁵ Visualization of cellular structures, for example organelles and cytoskeleton, and tracking metabolic processes is selectively and specifically achieved by fluorescence microscopy. It is also the method of choice for tracking single molecules in solution or even in a single cell.³³⁻³⁶

Epi-fluorescence microscopy

Epi-fluorescence is still the most widely used mode of fluorescence imaging. In this technique light from a high-intensity lamp is transmitted through the excitation filter and reflected by the dichroic mirror through the objective onto the sample.^{7, 41} Sample fluorescence is collected by the same objective and transmitted through dichroic mirror and emission filter onto the microscope detector, usually a charge coupled device (CCD). Special fluorescent filter sets and objectives are readily available. In general the most intense fluorescence images are collected with the objectives of the higher NA and lower magnification (I_{fl} proportional to $NA_{\text{obj}}^4 / M_{\text{obj}}^2$).⁴¹ On the other side, objectives of the high magnification and shallow depth of field work best for optical sectioning. Optical sectioning is the ability of an optical microscope to image thin planes of the object without physically sectioning it.⁴¹ Cells are sectioned by change of objective focus, slices are recorded and stored in the computer memory, and complete 3-D structure of cell is reconstructed by imaging software. Single cells and single molecules can routinely be analyzed and detected by an epi-fluorescence microscope. In addition cellular and single-molecule processes can be followed in time (time lapse microscopy) adding temporal dimension to the spatial information.⁷ Other fluorescence imaging modes have even improved the widespread use of fluorescence microscopes.

Confocal fluorescence microscopy

Confocal microscopes use lasers for excitation instead of imaging a complete field of view like in epi-fluorescence. They build an image using either a spinning disk or rapidly rotating mirrors to scan the specimen by a high NA objective, which pinpoints light in a diffraction-limited spot.⁴¹ After fluorescence signal is collected through dichroic mirror and emission filter by the photo multiplier tube (PMT), the scanning mechanism moves the spot in a raster scan. When one section of the specimen has been scanned, a stepping motor moves the stage in z direction, and scanning is repeated. Ultimately, 3-D representation of an object is achieved. The advantage of using a confocal microscope over epi-fluorescence microscope

is the ability of getting thinner and cleaner sections of cells. If 100 x objectives with NA of 1.4 are used vertical (axial) resolution of the confocal microscope is around 200 nm, compared to a value of ~ 600 nm for epi-fluorescence and other light microscopy modes. Such a superior axial resolution is due to a confocal pinhole that is responsible for rejecting out of focus fluorescent light. Confocal microscopes have enabled scientists to see how many cellular structures look like in three dimensions for the first time. Confocal microscope has also proved to be efficient for SMD.⁴⁰ In addition, multiphoton confocal systems have enabled use of longer excitation wavelengths that penetrate deeper into cells and reduce photobleaching.⁷

Total Internal Reflection Fluorescence Microscopy (TIRFM)

Total internal reflection is a phenomenon of complete reflection of the incident beam of light at the interface of two media for angles exceeding the critical angle of light (angle at which transmitted light is parallel to the boundary of two media). Although the beam is totally reflected radiation does penetrate a small distance (~100 nm) into a medium of lower refraction index, what making a so called evanescent wave.⁴⁵ In TIRFM the evanescent wave made by a laser directed through a prism is used for excitation of the thin layer in which molecules or cells are located.⁷ Since many cellular processes occur in specific areas of the cells, like in membranes, TIRFM is very useful for investigation of these processes.^{33, 34, 46} It is also the method of choice for SMD in the free solution^{24, 26, 27} or in gels^{47, 48}. Use of variable-angle excitation further improves data set obtained by SMD.⁴⁹

Fluorescence Resonance Energy Transfer (FRET)

FRET occurs when two chromophores are in close proximity to each other so that emission spectrum of the donor chromophore overlaps with the excitation spectrum of the acceptor chromophore.⁴³ Because intensity of energy transfer is inversely proportional to the sixth power of the distance between the donor and the acceptor, FRET allows measurement

of protein-protein interactions in a single-cell.^{7, 43} Several important FRET pairs include fluorescent proteins.⁵⁰

Specialized fluorescence techniques for studying dynamics of fluorescent proteins

Novel fluorescence imaging techniques have been used to examine localization and kinetic behavior of fluorescent proteins.^{51, 52} These techniques were influenced by developments in both time-lapse microscopy and fluorescent protein probes. Kinetic properties of the molecules like diffusion coefficients or mobile fractions of a protein are measured. Information whether the protein is immobilized to the scaffold, free to diffuse or undergoing constant exchange between compartments can be obtained.

In fluorescence recovery after photobleaching (FRAP) an area of the cell is photobleached with a high-intensity laser pulse and the movement of unbleached molecules into bleached area is recorded by time-lapse microscopy. Fluorescence loss in photobleaching (FLIP) is performed by repeatedly photobleaching fluorescence in one area of the cell, while the image of the whole cell is collected. Cells and molecules can be imaged in very small area by fluorescence correlation microscopy (FCS). The fluctuations in properties of molecules moving through the focal volume are analyzed.⁵¹

Another approach to study protein changes in the cell is to use destabilized fluorescent proteins. For example, fluorescent timer protein drFP583 changes its green fluorescence into red fluorescence after several hours. The age of a molecule fused to a timer protein can be determined by the measured ratio of green to red fluorescence over time. Also, protein lifetimes and turnover rates can be analyzed by using photoactivable fluorescent proteins. These proteins increase their low fluorescence at the imaging wavelengths after irradiation at a different wavelength. This results in the highlighting of distinct pool of molecules in a cell or in a solution. Three proteins, namely PA-GFP, kaede and KFP1 display ≥ 30 – fold increases in fluorescence after photoactivation.^{51, 52}

Transmitted Light Microscopy Techniques

Imaging living cells with transmitted light is used to provide information on cell structure, position and motility. It is often combined with fluorescence microscopy and very useful especially if cells change their shapes as in exocytosis, apoptosis and mitosis.⁷

Bright-field (BF) microscopy

Bright-field microscopy is the oldest microscopy mode in which a sample is evenly illuminated through a condenser and the image is acquired by the objective. This is still the cheapest mode available on every microscope. Because it lacks the contrast, BF works the best for stained samples.⁴¹ Several contrasting techniques have been developed on a BF microscope with addition of specific optical components.

Differential Interference Contrast (DIC) microscopy

DIC microscopy was introduced in 1969 by Allen, David and Nomarski. It achieved an immediate success because it could produce high-contrast images with fine structural details of unstained specimens.⁵³ In the case of the high NA objectives (NA = 1.4) and evenly illuminated condenser (NA = 1.4) diffraction limited resolution of light is achieved. DIC contrast depends on gradients in optical path ($OP = n \times d$, where n is index of refraction and d is the specimen thickness). Because of that, DIC produces exceptionally clear optical sections of cells and other relatively thick, transparent specimens.^{41, 53}

A DIC microscope is a dual beam interferometer, which uses a brightfield polarizing microscope.^{41, 53} In the polarizing microscope the polarizer is inserted in the light path beneath the condenser and the analyzer is inserted above the objective. A prism beam splitter is inserted between polarizer and condenser. This prism splits the light coming from the polarizer into two divergent polarized light waves. Condenser converts these divergent beams into two wavefronts that pass through the specimen separated from each other in the wedge direction (termed “shear direction”) by the distance that is less than the resolution limit of the

microscope. These two wavefronts are recombined by the objective lens and another prism that is in front of the analyzer. Depending on the optical path differences of two rays the interference can be partly destructive and show up as a dark spot in the image.

The contrast of the DIC image depends on the “compensation” or “bias retardation” (Δ_c) between two wavefronts along the microscope axis.⁵³ If the objective prism is aligned perfectly with the condenser prism ($\Delta_c = 0$) background light is extinguished, and the edges of the object appear like in darkfield microscopy. When one wavefront is retarded relative to each other background brightens. One edge of the object becomes brighter than the background while the other edge of the object becomes darker than the background, what produces the “shadow-cast” appearance of the DIC images. Compensators are devices that can add or subtract bias retardation between two orthogonal beams. In some microscopes bias retardation is achieved by sliding the prism in the shear direction. Other microscopes use deSenarmont compensator. This compensator uses the quarter-wave retardation waveplate mounted on a rotatable polarizer or analyzer. The combination of the quarter waveplate and rotation of polars induces the bias retardation.

DIC as well as the other contrasting techniques have benefited greatly from the advances in sensitive video detectors.⁵⁴ When viewed by the eye or recorded by photography fine structural details near the limit of resolution are often invisible because they have too little contrast. In 1981 Allen et al discovered that electronic contrast enhancement capabilities of video cameras could make visible tiny structures, such as 25-nm diameter microtubules.⁵⁵ A new method called video-enhanced DIC (VE-DIC) was introduced and used widely for imaging of cells and single-microtubules. Since digital cameras and image processing software have advanced greatly since early 1980s, this method is implemented today with a high-resolution DIC microscope and a CCD camera. Excellent high-resolution DIC images and movies that represent processes inside living cells as well as motor protein assays are presented in the literature.⁵³⁻⁵⁷

Darkfield (DF) microscopy

In DF microscopy specimen is imaged by a hollow cone of light so that just photons scattered, reflected or diffracted from the specimen are collected by an objective.⁴¹ These photons have a possibility of entering the collecting angle of the objective and form the bright image of the specimen on the dark background. The prerequisite for achieving DF imaging is that condenser numerical aperture is higher than numerical aperture of the objective. Low magnification DF microscopy can be performed by inserting a central stop into the front focal plane of the condenser. High-resolution and high-magnification DF uses a special condenser and objective with an iris diaphragm used to control NA of the objective. High intensity illumination will increase the intensity of the scattered light from the specimen. Since light could be scattered by impurities on slide extremely clean cover glasses, slides and solutions are necessary in DF microscopy. Cells and cellular structures are readily imaged by DF microscopy. With the high-resolution DF tiny features such as bacterial flagellum ($d = 20 \text{ nm}$) and microtubules ($d = 25 \text{ nm}$) could be visualized.

Phase contrast

This method was described by Frits Zernike in 1934. It not only earned him the Nobel Prize for physics in 1953 but also revolutionized basic biomedical research on unstained cells.⁴¹ Phase contrast works for the select range of specimens: those that create an optical path difference of only 1/8th of a wavelength of light.⁴¹ Fortunately, this category includes many biological specimens ranging from bacteria and microtubules, to general histological and cytological preparations. Small differences exist between thicknesses and refractive indices of the cell and surrounding medium. As a result a light wave that has passed through a cell lags behind the light that has only passed through the surrounding medium. This lag is called the phase shift. The eye cannot see phase shift in the microscope image, but it can distinguish between different intensities. To translate phase difference into grey values two additional components are inserted into the microscope. A ring called phase stop is placed in front of condenser for illumination of the specimen so that the image of the phase stop is

created on the objective pupil. A phase ring is built in the objective which does two things: it attenuates the bright light coming from the phase stop of the condenser and it adds a constant phase shift to this light. If the specimen contains cells, they prevent the light from reaching the phase ring of the objective. Light passing through cells will not be attenuated and retarded, and will form an image over fully attenuated direct rays.

Improving the resolution of light microscopy

Besides improvement in contrast achieved by implementation of video technology, researchers have developed light microscopy techniques that are able to image beyond the diffraction limit of light.⁵⁸ All these techniques try to increase resolution by altering the assumptions on uniform illumination and imaging with a single objective proposed by Abbe.

The technique called structured illumination microscopy has demonstrated ability to improve the lateral resolution from 200 to 100 nm, and the axial resolution from 600 to 300 nm. This technique varies the intensity of illumination across the sample at a known spatial frequency. Moire fringes are produced that can be coarse enough to be measured even if the sample frequencies are beyond the normal resolution limit. The highest spatial frequencies that can be recovered from the image are twice as high as in standard microscopy. The method was successfully applied for imaging microtubules within the fruit fly centrosome.

Another technique called I⁵M has demonstrated an improvement in axial optical resolution from 600 nm to about 90 nm. Axial resolution is improved by imaging of the specimen by two objectives both at the opposite side of the sample. The resolution enhancement is analogous to how the resolution of the microscope increases with the increase of numerical aperture. Illumination from both sides of the sample generates a nonuniform intensity pattern. Two images can optically interfere making an enhancement in resolution.

According to inventors, a method called nonlinear structured illumination theoretically has unlimited resolution. In traditional light microscopy the assumption that response of the sample to the illumination is linear holds true. If the intensity of excitation light is high enough to saturate dye molecules, emission rate of a fluorophore is no longer a linear

function of the illumination. The non-linear response generates harmonics with much higher frequency illumination patterns than physically possible when the response is linear. These frequencies produce moire fringes with the spatial frequencies of the sample, theoretically resulting in infinitely high resolution.

An approach called super lens was able to achieve the resolution of 60 nm.⁵⁹ Instead of imaging light coming from the object, this technique images the evanescent field coming from the object with a 35 nm-thick silver film as a lens. The silver film resonates with the evanescent waves from the object, and transfer waves to the other side with increased amplitude. A photoresistor on another side of the silver super-lens records an image.

All of above objective based imaging methods show great promise for light microscopy imaging of cells and molecules on a new size scale with a high-resolution. In addition, developments in near-field scanning optical microscopy (NSOM)^{60, 61} and atomic force microscopy (AFM)⁴¹ provide additional tools for cell biology and single-molecule detection beyond the diffraction limit.

Recording and analysis of images and spectra

CCD cameras are often used as detectors in microscopy and spectroscopy.^{62, 63} CCD is an array of photodiodes that acquires a complete image or a spectrum at once. Each photodiode (pixel) is responsible for detection of light coming from an area of the sample. After the CCD chip is exposed charge accumulated in each photodiode is shifted into a register, digitized and displayed on the computer screen.

Several performance requirements are very important for use of CCDs in imaging applications.^{64, 65} The sensitivity of the camera is determined by its quantum efficiency as well as the readout noise. For example, back-illuminated CCDs have quantum efficiency greater than 90 % and readout noise of few electrons per second. In addition, dark current is efficiently reduced by cooling the camera. Speed of the CCD cameras is important for recording of dynamic events in cells and SMD. CCDs that record movies at speeds even higher than the video rate (30 frames/s) are available. Dynamic range of the CCD is defined

as its ability to capture both dim and bright signals. Cameras with 8, 12 or 16-bit dynamic range are available. Linearity of the CCD is important in quantitative applications.

It is important to match the pixel size with the resolution of a microscope.⁶⁶ Now CCD cameras are available with as small pixels as $4.65\ \mu\text{m} \times 4.65\ \mu\text{m}$. In order to see two features of the specimen separately in the image they should be separated by two pixels. For features separated at diffraction limit of light (200nm) at 100 X magnification, pixel size should be in the minimum $10\ \mu\text{m} \times 10\ \mu\text{m}$. CCDs are usually interfaced with computers that enable high-speed collection of data. Images and movies are processed, archived after digitization and displayed on the computer screen. Contrast enhancement that originally required complicated hardware is now easily performed by sophisticated imaging software.

Photomultiplier tubes are detectors that are used in many applications including confocal microscopy and flow cytometry.^{11, 41} Photomultiplier tubes contain a photosensitive cathode that interacts with light, dynodes that multiply electrons ejected from the cathode, and the collection anode.⁴⁵ Because of the high gains of PMTs they are very useful for low-light-level detection. The most important characteristics of PMTs include sensitivity, spectral response, gain and linearity.

Spectral imaging

In addition to recording spatial and temporal changes microscopy provides a fifth dimension that includes measuring spectral response of the sample. Spectral imaging is a powerful method for measuring the full spectrum of light at every pixel of a two dimensional image. This method is a combination of spectral dispersion, CCD imaging, light microscopy and analysis software. The spectral imaging optical head attaches to the CCD port of a microscope.⁶⁷ Light is projected from the microscope port into the optical head. Spectral dispersion is achieved by interferometer (in SpectraCube method)⁶⁷ or diffraction grating⁶⁸. CCD array collects for all pixels simultaneously the light intensity required to measure or calculate the spectrum at each point of the image. A real image of the sample is produced by CCD while spectral information is collected and displayed by the software.

Spectral imaging has been continuously useful in the area of remote sensing to provide important insights about planets, including Earth.⁶⁷ For example changes in chlorophyll absorption spectra can give information on the effects of soil composition on trees. Combining spectroscopy and imaging is particularly useful in investigations of fluorescent probes in cells or in the free solution. Automated image microscopy is able to analyze large number of cells. However, the throughput of the system is limited to the microscopist's skills and software capabilities. As described below, a way to improve throughput of spectral imaging is to measure spectral information from cells and molecules in the flow.

High-Throughput Spectral Analysis of Single-Molecules and Single-Cells

Development of high-throughput methods will benefit the use of single-cell analysis and SMD in biomedical and clinical research. Several methods have proven their ability for daily use in high-throughput analysis of clinical samples. Spectral information is a factor of discrimination used in these methods.

Flow Cytometry

Flow cytometry is a method for measuring the fluorescence and light scattering of individual cells in large numbers.^{12,69} Cells are usually labeled with a fluorescent dye, although natively fluorescent compounds could be detected as well. From the fluorescent signal the content of the dye in the cell could be measured. Scattered light gives information on the cell size, shape and structure.

The optical scheme of a flow cytometer resembles that of the epi-fluorescence microscope. The cells are carried by laminar flow of water or buffer in a single file ("sheath flow") through a focused light beam whose wavelength matches the wavelength of the dye used for cell labeling.^{69,70} Although fluorescence lamps and filters could be used for cell illumination, lasers are used more often because they provide higher excitation intensity. When passing through the focus each cell emits a pulse of fluorescence and scattered light that are detected by PMTs. Fluorescence is usually split by dichroic mirrors and filters into

several color components, so that separate detectors can analyze multiple labeled cells simultaneously. Light scattered to small and large angles is also measured by separate detectors so that cells could be distinguished based on their size as well as structure. Modern flow cytometers can measure above cell parameters for thousands of cells per seconds. That is why they have found large clinical applications especially for analysis of mammal cells. In addition, modern flow cytometers have the ability to sort cells with desired properties, so called fluorescence activated cell sorting (FACS).^{13, 70}

Several research groups demonstrated measuring of single-cell fluorescence spectra by a flow cytometer.^{71, 72} The maximum throughput of these instruments was limited at measuring spectra of up to 50 cells/s. Although a spectral flow cytometer is commercially available⁷³, due to moderate throughput it did not find widespread use. In the majority of flow cytometry experiments spectral imaging information are discarded, so that the discrimination of cells based on the minor differences in their fluorescence spectra is not possible.

High-throughput single-molecule and single-cell spectroscopy

This is a spectral imaging method in which emission fluorescence spectra of many molecules and cells are recorded as they move on a chip or in a capillary tube.^{11, 31, 32} A laser is used for excitation of molecules and cells, either directly or through the evanescent wave. Fluorescence is collected by an objective and dispersed through a diffraction grating. CCD camera records both cell image (zero-order spectrum) and first-order fluorescence emission spectrum. If grating spacing and distance between CCD chip and grating are known, fluorescence emission spectrum can be reconstructed by measuring the distance between maxima of zero-order image and first-order spectrum. The system shows the promise for imaging and spectrum acquisition of thousands of molecules or cells simultaneously.

Screenings of DNA and protein molecules as well as their chemical reactions have been done by this method.³² Emission fluorescence spectra of individual bacterial cells that contain fluorescent proteins have been determined as well.¹¹ Spectra of cells containing genetically expressed GFP were measured. In another example spectra of fluorescent proteins formed by attachment of phycoerythrobilin (PEB) chromophore to genetically expressed

R-PE apo-subunits were measured¹¹. Excellent agreement between spectra measured by high-throughput single-cell spectroscopy and regular fluorescence spectroscopy were found after isolation of fluorescent proteins from cells.¹¹

Fluorescent Proteins

Protein fluorescence can be intrinsic (native or autofluorescence) or extrinsic (due to attached fluorescence labels).⁴³ Native fluorescence of proteins originates mainly from aromatic amino acids phenylalanine, tyrosine and tryptophan. These amino acids show a characteristic protein absorption and excitation band at 280 nm, and are responsible for protein fluorescence that peaks at 340 nm. The majority of the known proteins contains these amino acids and can be analyzed in near ultra violet (UV) region of electromagnetic spectrum. Fluorescence of some proteins is due to bound prosthetic groups such as hydrated form of nicotinamide adenine dinucleotide (NADH), flavine adenine dinucleotide (FAD), flavine mononucleotide (FMN), pyridoxal phosphate, chlorophyll or heme.⁴³ For example, NADH shows excitation fluorescence maxima at 360 nm, and emission fluorescence maximum around 450 nm, while flavin proteins could be excited with blue light and fluoresce between 520 and 560 nm. Although their fluorescence enters the visible region of electromagnetic spectrum, these proteins are not convenient as fluorescence probes of cell structure because they are common source of autofluorescence in many organisms.⁷⁴ Fortunately several classes of proteins with exceptional fluorescent properties (e.g., high absorption coefficients and quantum yields) fluoresce at visible wavelengths and have found widespread use in single-cell analysis and single-molecule detection.

Phycobiliproteins

Phycobiliproteins are highly fluorescent proteins found as components of photosynthetic apparatus in cyanobacteria, red algae and cryptomonads.^{75,76} They are organized in protein complexes called phycobilisomes. Phycobilisomes are responsible for the absorption of light and efficient energy transfer in 470 to 650 nm region, between the

blue and far-red absorption peaks of chlorophyll a. Phycobiliproteins are globular proteins divided in three groups: phycoerythrins, phycocyanins and allophycocyanins. They are all composed of two subunits (α and β), while the third subunit (γ), a linker peptide, is found in phycoerythrins. The structure of R-phycoerythrin (R-PE) and B-phycoerythrin (B-PE) can be described as $(\alpha\beta)_6\gamma$, while phycocyanin (PC) and allophycocyanin (APC) have the structure $(\alpha\beta)_3$.

Phycobiliprotein fluorescence is due to phycobilin chromophores and their interactions within polypeptide chains.⁷⁵ Phycobilins are open-chain tetrapyrrole groups that are covalently bound to cysteines by thioether bonds. The most representative phycobilins are phycoerythrobilin (PEB), phycourobilin (PUB), phycocynobilin (PCB), and phycobiliviolin (PXB). Each phycobiliprotein displays different spectral properties depending on the type and number of bound bilins. For example, thirty four PUB and PEB molecules are found in single molecule of R-PE. Such a high concentration of chromophores contributes to exceptionally high absorption coefficients of phycoerythrins ($\sim 2 \times 10^{-6} \text{ cm}^{-1}\text{M}^{-1}$) and quantum yields that approach to 1 (0.82 for R-PE and 0.98 for B-PE).^{43, 75} Hence, it is not surprising that phycoerythrins are molecules that were used in numerous single-molecule experiments.⁷⁷⁻⁷⁹

In addition, phycobiliproteins have other properties that make them extremely useful for labeling of cells.⁷⁵ They are highly water-soluble, stable over the wide pH range (from 5 to 9), and readily conjugated to other biomolecules without alteration of their spectral properties. That is why they are indispensable fluorescent labels in immunocytochemistry and flow cytometry assays. Phycobiliproteins are isolated from cyanobacteria or algae and purified by liquid chromatography.⁸⁰ Also, recombinant phycobiliproteins can be synthesized with variety of tags in cyanobacteria.⁸¹ Tagged apo-proteins are inserted in the cyanobacterial cells at the site of chromophore attachment.

Phycobiliprotein subunits are also highly fluorescent.^{10, 82} Subunits can be isolated from phycobiliproteins by chromatography or electrophoresis under denaturing conditions and renatured for further use. Another way to get fluorescent subunits of phycobiliproteins is non-enzymatic attachment of phycobilin chromophores to genetically expressed apo-subunits.⁸³⁻⁸⁷ Incubation of apo-subunits from cyanobacteria with a specific phycobilin *in*

vitro yields adducts that usually contain several isomeric phycobilins. Attachment of PEB to R-PE apo-subunits expressed in *E. coli* happens although subunits are located in inclusion bodies.^{11,88} Interestingly, when apo-subunits are fused to maltose binding protein (MBP) both *in vitro* and *in vivo* attachment of PEB yields to a single PEB-containing fluorescent product.⁸⁸ For the first time non-enzymatic phycobilin attachment to a phycobiliprotein apo-subunit happens without isomerization into other bilins. Further experiments will show if this is an inherent property of properly folded R-PE apo-subunits.

Complete biosynthesis of a phycobiliprotein subunit in a heterologous host is also possible.^{89,90} The enzymes that make PCB and PXC from cellular heme and attach these chromophores to apo-subunits of phycobiliproteins were elucidated. These discoveries led to the expression of holo-alpha subunits of C-PC and phycoerythrocyanin (PEC) in *E. coli* without need for exogenous supply of the PCB and PXC chromophores.^{89,90} Elucidation of biosynthetic and attachment pathways for other phycobilin chromophores would obviously contribute to the new recombinant phycobiliproteins.

Green Fluorescent Protein (GFP)

Cloning and expression of GFP from jellyfish *A. victoria* in different types of cells and organisms have revolutionized research in cellular and molecular biology. GFP was originally discovered by Shimomura in 1962.⁹¹ It took researchers thirty years to realize that GFP can make a breakthrough in cell analysis because its fluorescence is genetically encoded with no need for supply of a fluorescent substrate exogenously. The gene encoding GFP was cloned in 1992.⁹² Fully functional GFP was successfully expressed in heterologous host two years later clearly envisioning the potential of the GFP for a marker of gene expression and protein localization in the cell.⁹³ Soon after GFP fusions were constructed and used to localize proteins in cells.⁹⁴ So called “green revolution” started and it is still going on.⁹⁵ More than ten thousand papers has been published during the last ten years on application of GFP mainly for analysis of cells, but also for single-molecule detection.

The reason for such a success is the fact that GFP approached the closest to the requirements for an ideal fluorescent protein tag. According to Cabantous et al⁹⁶, an ideal

protein tag would be genetically encoded, would work both *in vitro* and *in vivo*, would provide a sensitive analytical signal, and would not require external chemical reagents or substrates. The fluorophore of GFP is p-hydroxybenzylideneimidazolinone.⁹⁷ In the wild-type GFP this chromophore is formed by cyclization of serine, tyrosine and glycine (residues 65-67 of wild-type GFP) in the presence of the oxygen. Chromophore is shielded in the β -barrel structure that contains eleven β sheets. Wild-type GFP has a main excitation maximum in the near UV region of the EM spectrum (395 nm) and a minor excitation spectrum at 475 nm. The blue excitation is still sufficient to excite the green emission that peaks at 511 nm. Changes in the amino-acid sequence of GFP resulted in the design of its variants with improved brightness.⁹⁸ GFP variants that can be excited and fluorescent at various wavelengths are obtained by mutagenesis (e.g., cyan fluorescent protein, blue fluorescent protein and yellow fluorescent protein).^{97,98} GFP proteins sensitive to pH changes have been used to visualize secretion and synaptic transmission in cells.⁹⁹ Also, a split GFP was developed that found extreme importance in investigation of protein-protein interactions.^{96,100} In this system, GFP fragments are expressed at different dynamic structures of cells and fluorescence is reconstituted when fragments come into proximity to each other.

Although GFP is widely used in the analysis of cells, there are some constraints in working with GFP and its variants, mainly due to their interactions with the system under investigation, slow maturation, and required spectroscopic properties.^{101,102} Some of disadvantages are related to relatively high molecular weight of the protein (~27 kDa), inappropriate folding and aggregation, or insufficient signal in some experiments. Because of that the search for fluorescent proteins that will complement GFP is very intensive.¹⁰²⁻¹⁰⁵ New proteins from GFP-family were discovered in corals (*Anthozoa*).¹⁰³ The most known of them is red fluorescent protein DsRED. Its fluorescence is very bright and at the wavelengths that avoid cellular autofluorescence. However, DsRED is heterodimeric protein, with relatively slow maturation what could disturb the investigated system.¹⁰¹ Another red fluorescent protein from corals eqFP611 shows the largest Stokes shift from the all non-modified proteins from GFP-family.¹⁰⁴ Kaede protein shows a remarkable property of the UV-induced green-to-red conversion enabling a new technique for regional optical marking.¹⁰⁵ The search for the new native GFP-like fluorescent proteins continues.

Phytofluors

Phytofluors are a relatively new class of fluorescent protein probes.^{43, 107} These intensively orange fluorescent proteins are formed spontaneously upon incubation of recombinant plant phytochrome apo-proteins with PEB.¹⁰⁷ Phytochromes are homodimeric biliprotein photoreceptors from plants containing the open-chain tetrapyrrole chromophore phytychromobilin (P ϕ B). Native phytochromes are low fluorescent in the red region of electromagnetic spectrum. However when the P ϕ B is replaced with PEB fluorescent adducts are formed that have large absorption coefficients, quantum yields above 0.7 and excellent photostability over wide range of pH.¹⁰⁷ Phytofluors also have high anisotropy what makes them suitable for fluorescence anisotropy measurements. They were successfully reconstituted *in vivo* (in plant *Arabidopsis thaliana*), and *in situ* (in yeast *Saccharomyces cerevisiae*). Since these fluorescent proteins are formed spontaneously, fluorescent phytochromes can become useful probes of gene expression. The major drawback is the need for the exogenous supply of the PEB chromophore. This could be overcome, however, with the discovery of the mechanism of cell mediated formation and attachment of PEB.

Covalent and non-covalent labeling of proteins

Proteins can be labeled with various fluorophores.^{43, 44} Labeling of proteins is usually conducted by the fluorophore attachment to the primary amino or thiol groups.¹⁰⁸ Covalent labeling of proteins is important for studying of cellular structure and environment. An important benefit of using small fluorophores such as fluorescein or rhodamine is minimization of steric problems that can interfere with the protein function. However, the chemistry of chromophore binding to the protein is not trivial and often lacks specificity.¹⁰⁹ Another important factor that should be considered for labeling of protein in cells is cell membrane permeability.

Recently, two techniques have been discovered for labeling of proteins with small organic molecules. First, a genetically engineered tetracysteine sequence was labeled with bi-arsenic group bound to fluorescein (FlAsh). Therefore, a protein of interest can be genetically

fused to a short peptide containing the tetracysteine sequence, and this fusion expressed in the cells. The FIAsh label is cell permeable and non-fluorescent, showing fluorescence only after binding to the tetracysteine sequence. Derivatives of FIAsh are also made with altered fluorescent properties. Another synthetic probe that binds to the tetracysteine motif was used to image conformational changes of proteins.¹¹⁰ The second technique uses the enzymatic activity of human O⁶-alkylguanine- DNA alkyltransferase (hAGT). This enzyme shows increased activity to benzylguanine containing fluorescein (BGFL). If a fusion protein is made containing hAGT, specific labeling with fluorescein is achieved. Other approaches include binding of fluorescent heptanes to the antibodies, or binding of biotin labeled with a fluorophore to avidin. An excellent source describing protein fluorescent probes and mechanism of their binding is the Molecular Probes catalog.⁴³

Proteins can be labeled non-covalently with ligands that are in equilibrium between bound and unbound form.¹⁰⁸ Ligands that have been used to probe protein binding sites often fluoresce significantly only when bound. In most cases where non-covalently bound ligand is used as fluorescent probe, the ligand is anionic. For example, ligand auramine O binds to the active site of alcohol dehydrogenase. Many ligands are synthesized with quantum dots, crystalline fluorescent nanoparticles. Quantum dots have great advantages over organic fluorophores because of their broad excitation spectra as well as narrow and symmetrical emission spectra that can be tuned with the particle size and composition.¹¹¹ The major drawback of quantum dots is their low biocompatibility. Yet quantum dots as well as gold nanoparticles have found interesting applications in cellular imaging of proteins and peptides.¹¹²⁻¹¹⁴

Isolation and characterization of fluorescent proteins

Techniques for purification and exploring proteins are well developed and described in biochemistry textbooks.¹¹⁵ Isolation of fluorescent proteins from cells starts with the rupture of membranes and thorough lysis of cell by physical or chemical means.^{88, 107} Proteins are separated from the pool of other cellular substances on the basis of their size and/or charge, usually by chromatography, electrophoresis, or by precipitation with ammonium sulfate and

centrifugation. Isolation of fluorescent proteins could be easier if they have pronounced color.¹¹ But precautions should be taken about photobleaching of fluorophores. If proteins of high purity are required HPLC, affinity chromatography, gel electrophoresis or capillary electrophoresis can be used. The most important properties of fluorescent proteins are excitation and emission spectra, absorptivities and quantum yields. These characteristics are measured by absorption and fluorescence spectrometers or spectrometric detectors.⁸⁸ Structural properties of fluorescent proteins related to amino-acid sequence and tertiary structure could be determined by combination of HPLC and electro-spray ionization mass spectrometry (ESI-MS). Three-dimensional structure of proteins is achieved by X-ray diffraction or NMR.¹¹⁵ Since the structure of the protein is related to its function, all of the above structural methods in combination with mutagenesis techniques may help improve the spectral properties of fluorescence proteins.

Localization and Expression of Proteins in Escherichia coli (E. coli)

E. coli is a prokaryotic microbial organism belonging to the bacterial family *Enterobacteriaceae* (enteric bacteria).² It is considered by many scientists as the best studied and most completely characterized organism.¹¹⁶ *E. coli* is the host cell for most of the research in molecular biology, microbiology and biotechnology. The bacterial cell, which was once considered as a “bag of enzymes”, is now known to contain variety of molecules located in the specific subcellular compartments revealing more similarities between prokaryotes and eukaryotes than imagined previously.¹⁰¹

Structure of E. coli cell

E. coli is a Gram-negative bacterium found in the colon and large intestine of most animals. Wild-type *E. coli* can grow both aerobically and anaerobically, and it does not have special growth factors requirements. Laboratory *E. coli* strains require solid or liquid medium containing all nutrients required for bacterial growth. Cells divide through binary fission. *E. coli* cell is a rod-shaped bacterium, measuring approximately 2 μm in length and 0.8 μm in

width.¹¹⁶ Main components of the cell include: cytoplasm, inner and outer cell membranes, periplasm, cell wall, flagella and pili. The cytoplasm contains the chromosomal DNA, RNA, ribosomes or polyribosomes, inclusion bodies or storage granules, small organic molecules, and proteins. Chromosome interacts with nuclear proteins and condenses into a body called nucleoid.

The outer cell membrane consists of a lipid bilayer structure composed of lipopolysaharide and phospholipids.^{2, 116} The other major component of this membrane include proteins, mainly porins. Porins are passive diffusion channels that allow hydrophilic molecules like nutrients to pass through. The width of the outer membrane is about 10-15 nm. The cell wall contains peptidoglycan that is covalently bound to the outer membrane, and it gives the cell its characteristic shape and prevents the cell from being osmotically lysed. Peptidoglycan layer is a very thin monolayer. The inner membrane is composed of lipid bilayer about 8 nm thick consisting of ~ 40% phospholipids and ~ 60 % proteins. The inner membrane in combination with outer membrane serves as an osmotic barrier, a nutrient specific transporter, a lipid synthesizer, peptidoglycan and protein synthesizer, electron-transport system, a place for chromosomal segregation, and a site for chemical sensing. The periplasmic space is the space between the inner and the outer membrane. It is about 10 nm thick and occupies between 10 and 20% of the volume of an *E. coli* cell. It houses proteins essential for nutrient binding, peptidoglycan synthesis, degradative enzymes (proteases and endonucleases), detoxifying enzymes (beta-lactamase), electron-transport systems and chemotaxis and chemosensing proteins.

Flagella are rigid screw-like appendages that are anchored to the outer membrane. They rotate in a propeller-like fashion to facilitate bacterial movement. They are 10-20 μm long and approximately 25nm wide. Flagella are motor systems consisting of up to 50 different proteins that spontaneously assemble to form nano-scale rotors, stators and power (ATP) supply. They are scattered uniformly around *E. coli* cell. Fimbriae or pili are thin appendages that are approximately 6.5 nm in diameter and between 200 nm and 2 μm in length. A cell may have between 100 and 300 pili or fimbriae. These are also protein structures. Fimbriae are responsible for surface attachment, while pili mediate attachment to other bacteria.

Localization of proteins in E. coli

As described above, proteins play numerous structural and functional roles in the *E. coli* cell. Various bioanalytical techniques have been used to explore bacterial structure through protein localization.² Obviously, microscopy is the method of choice to determine location of a protein in *E. coli* cell. Since bacteria are very small in size, high-resolution and high-contrast techniques are requirement for localization of proteins in *E. coli*.

Much of our knowledge about bacterial structure was inferred from electron microscopy data.^{117, 118} EM has superior resolution what makes it method of choice for the investigation of detailed cellular structure. However, procedures for cell staining such as immunogold labeling are demanding and time consuming. In addition EM on live cells is not possible due to requirement for sample imaging in vacuum. A great alternative for EM is the use of immunofluorescence microscopy (IFM).¹¹⁹ The IFM is based on highly-specific fluorescence microscopy detection of a protein that is targeted with a fluorescent probe conjugated to an antibody raised against protein of interest. It has been effectively used to target proteins in specific cellular compartments. As in the case of immunogold labeling it takes time to raise antibodies especially against proteins present in low abundance.¹⁰¹

Another excellent approach for the localization of proteins in *E. coli* is the use of fluorescent proteins.^{101, 120} Gene-fusions using proteins from GFP-family can be constructed relatively easy. Since the GFP chromophore is formed spontaneously, neither invasive sample preparation nor substrate addition is required. GFP has been successfully used to localize proteins in variety of cellular processes such as cell division and septation¹²¹, chromosome segregation and replication¹²², sporulation¹⁰¹, development¹⁰¹, signal transduction and protein export^{120, 123}. Still, GFP is not without its limitations.¹⁰¹ For example, GFP does not give sufficient signal under all conditions under which *E. coli* cells normally grow. Since the GFP chromophore requires some time for maturation, short-lived bacterial proteins cannot be suitably labeled. Also, GFP is a relatively large molecule that can alter the function and location of the target protein.

Proteins involved in chromosome segregation can be localized by combination of fluorescent protein labels and fluorescence *in situ* hybridization (FISH). Transmission light

microscopy techniques (DIC, phase contrast, darkfield) also provide additional information of cell morphology and localization of proteins in inclusion bodies.^{88, 124} All described approaches have their advantages and drawbacks, so that the choice of imaging method depends on the localization and the nature of a protein in the cell. Use of imaging methods in combination can help to validate conclusions about protein localization.¹⁰¹ Development of novel microscopy techniques and fluorescent proteins will provide additional possibilities for efficient protein localization.

Expression of proteins in E. coli

Recombinant proteins have very important applications in biochemical, bioanalytical and structural studies of proteins, as well as in immunization, biotechnology and therapeutic use.^{2, 125} *E. coli* is a frequently used host for expression of recombinant proteins since it facilitates protein expression with relative simplicity, inexpensive and fast high-density cultivation, well known genetics, and compatible molecular tools.¹²⁵

Production of a recombinant protein in *E. coli* involves cloning of the gene encoding the protein into an expression vector under the control of an inducible promoter.¹²⁶ Efficient expression of the recombinant gene depends on variety of factors such as optimal transcription and translation, correct protein folding and optimal growth of cells. There is no optimal expression system that works with all recombinant proteins. High-level of synthesis has to be optimized in the case of each protein by empirical variations of expression parameters.

The main purpose of recombinant protein expression is often to obtain a high-degree of soluble and fully functional protein.¹²² This is not always accepted by the metabolic system of *E. coli* cell and in some situation cellular stress response is encountered. Another response that happens in recombinant cells is the accumulation of target proteins into insoluble aggregates called inclusion bodies.¹²⁴ Inclusion bodies are aggregated proteins that are generally misfolded and thus biologically inactive.¹²⁵ Aggregation of recombinant proteins in bacterial cells results from high-concentrations of folding intermediates or from insufficient processing by molecular chaperones. Refolding of recombinant protein from inclusion bodies

is possible. However, resolubilization process could lead to poor recovery yield and affect the integrity of refolded protein.

Modifying the expression strategy to achieve the production of soluble protein might be a desirable way to improve recombinant protein production.¹²⁵ Modification can be achieved without further engineering of the target protein by testing various strains, media, or temperatures. Also, molecular chaperones and tRNA-expressing plasmids can be included during expression. Another approach is to engineer the target protein by fusion protein technology (affinity tagging of proteins), or by screening for and selection of soluble variants. Affinity tags provide easier purification of recombinant proteins from *E. coli*. They also improve yield, prevent proteolysis, and increase solubility of recombinant proteins *in vivo*. The most potent solubility enhancing proteins include *E. coli* maltose binding protein (MBP), hexa-histidine tag, *E. coli* N-utilizing substance (NUSa), inteine, thioredoxin, calmodulin binding protein, and glutathione-S-transferase (GST). High-throughput screening and selection of more soluble variants of a protein can be achieved through a number of different approaches. If the structure of a protein is available its solubility can be enhanced by rational site directed mutagenesis. A more general way is to find more soluble variants by directed evolution.¹²⁷ Libraries generated in this context include random point mutants, deletions and fragments. The generated mutants are screened for solubility either by the function of the protein of interest (if it is known) or by more general screens. One way of general screening includes formation of fusion reporters.¹²⁸ For example, fluorescence of *E. coli* cells expressing a target gene fused to the GFP is related to the solubility of the target gene expressed alone. Hence, protein folding for a certain protein in *E. coli* can be improved by searching for fluorescing mutants.

Sometimes expression of proteins in *E. coli* might require translocation of a recombinant protein from reducing environment of cell cytoplasm to oxidizing environment of the periplasmic space.¹²⁶ Reasons for translocation of proteins include: formation of disulfide bonds, decreased protein degradation and number of other proteins compared to cytoplasm, and easy purification of protein by osmotic shock. There are two systems involved in the translocation of proteins through the inner membrane, the Sec and the Tat (twin-arginine-transport) pathway. With both systems, proteins to be relocated contain a signal sequence at

their N-terminus, which has a length of 15-30 amino acid residues. For translocation of a recombinant protein through the inner membrane, any signal sequence can be fused to the protein of interest. Several other proteins SecA, SecB and SecYEG, molecular chaperones, and a signal recognition particle (SRP) are included in protein translocation during Sec pathway. SRP is a protein-RNA complex consisting of the Ffh protein and 4.5S RNA. To become exported by the Sec pathway, proteins have to be maintained in an export-competent state. This can be achieved either simultaneously with translation (process aided by SRP) or posttranslationally (folding is prevented by molecular chaperones). In contrast, Tat pathway accepts only folded proteins and details of the secretion process are not elusive.¹²⁶

Expression of proteins in *E. coli* yields useful recombinant proteins that contain as building blocks not only twenty common amino acids but also unnatural amino acids with specific properties. If unnatural amino acids are supplied with nutrients, *E. coli* strains can express proteins containing amino acids p-benzoyl-L-phenylalanine and amino acid p-acetyl-L-phenylalanine.^{129, 130} These amino acids respectively have excellent photocrosslinking properties and good suitability for attachment of fluorophores. In addition, *E. coli* was engineered that could make the unnatural amino acid p-aminophenylalanine in its own without the need for unnatural amino acid supply.¹³¹ Bacteria with a 21 amino acid genetic code, or other organisms with altered genetic code, provide the possibility to examine evolutionary consequences and functional improvements of proteins due to incorporation of new amino acids.¹³¹

Our Goal

Development of novel fluorescent proteins and improvements in light microscopy methods will answer many questions in both basic and applied sciences. Our goal is to develop new approaches in single-cell analysis and single-molecule detection through implementation of novel fluorescent protein probes and improvements of available analytical techniques. We deal with subunits of highly fluorescent protein R-PE with the desire to isolate and characterize these subunits as well as to check their suitability for SMD. With the help of genetic engineering we want to express and reconstitute in a single bacterial cell fluorescent

subunits that will hopefully retain most of the excellent spectroscopic properties of R-PE. We employ high-resolution and high-contrast imaging techniques for localization of proteins in the free solution and in *E. coli* cells. Also, we want to demonstrate a spectral imaging method, which will record in high-throughput manner fluorescence spectra of bacterial cells containing fluorescent proteins. We hope that fluorescent proteins based on R-PE subunits and described imaging methods will be used to solve research enigmas in biology, chemistry, physics, and medicine.

REFERENCES

1. N. A. Campbell, *Biology*, The Benjamin/Cummings Publishing Company, New York, **1996**, p. 110.
2. P. Singleton, *Bacteria in Biology, Biotechnology and Medicine*, John Wiley & Sons, New York, **1999**, p. 1.
3. K. Cottingham, *Anal. Chem.* **2004**, 76, 235A.
4. B. F. Brehm-Stecher and E. A. Johnson, *Microbiol. Mol. Biol. Rev.* **2004**, 68, 538.
5. D. M. Cannon, Jr., N. Winograd, and A. G. Ewing, *Annu. Rev. Biophys. Biomol. Struct.* **2000**, 29, 239.
6. L. Ruth, *Anal. Chem.* **2001**, 73, 159A.
7. D. J. Stephens and V. J. Allan, *Science*, **2003**, 300, 82.
8. E. S. Yeung, *Anal. Chem.* **1999**, 71, 522A.
9. C. A. Aspinwall and E. S. Yeung, *Anal. Bioanal. Chem.* **2005**, 381, 660.
10. D. Isailovic, I. Sultana, G. J. Phillips, and E. S. Yeung, **2005**, manuscript in preparation.
11. D. Isailovic, H-W. Li, G. J. Phillips, and E. S. Yeung, *Appl. Spectrosc.* **2005**, 59, 221.
12. H. M. Davey and D. B. Kell, *Microbiol. Rev.* **1996**, 60, 641.
13. F. L. Battye, A. Light and D. M. Tarlinton, *J. Immunol. Methods* **2000**, 243, 25.
14. E. S. Yeung, *J. Chromatogr. A* **1999**, 830, 243.
15. S. N. Krylov, D. A. Starke, E. A. Arriaga, Z. Zhang, N. W. C. Chan, M. M. Palcic, and N. J. Dovichi, *Anal. Chem.* **2000**, 72, 872.
16. R. T. Kennedy and J. W. Jorgenson, *Anal. Chem.* **1989**, 61, 436.

17. M. A. McClain, C. T. Culbertson, S. C. Jacobson, and J. M. Ramsey *Anal. Chem.* **2001**, 73, 5334.
18. E. N. Fung and E. S. Yeung, *Anal. Chem.* **1998**, 70, 3206.
19. K. Cottingham, *Anal. Chem.* **2005**, 77, 197A.
20. R. Y. Tsien, *Nature Rev. Mol. Cell Bio.* **2003**, 4, SS16.
21. W. E. Moerner and M. Orrit, *Science*, **1999**, 283, 1670.
22. S. Weiss, *Science*, **1999**, 283, 1676.
23. H. Neuweiler and M. Sauer, *Anal. Chem.*, **2005**, 77, 179A.
24. X-H. Xu and E. S. Yeung, *Science*, **1997**, 275, 1106.
25. Q. Xue and E. S. Yeung, *Nature*, **1995**, 373, 681.
26. X-H. Xu and E. S. Yeung, *Science*, **1998**, 281, 1650.
27. H-W. Li, H-Y. Park, M. D. Porter and E.S. Yeung, *Anal. Chem.* **2005**, 77, 3256.
28. M. R. Shortreed, H. Li, W-H. Huang, and E.S. Yeung, *Anal. Chem.* **2000**, 72, 2879.
29. A. Bensimon, A. Simon, A. Chiffaudel, V. Croquette, F. Heslot, and D. Bensimon, *Science* **1994**, 265, 2096.
30. R. A. Keller, W. P. Ambrose, P. M. Goodwin, J. H. Jett, J. C. Martin, and M. Wu, *Appl. Spectrosc.* **1996**, 50, 12.
31. E. S. Yeung, *The Chemical Record* **2001**, 1, 123.
32. Y. Ma, M. R. Shortreed, and E. S. Yeung, *Anal. Chem.* **2000**, 72, 4640.
33. Y. Sako and T. Yanagida, *Nature Rev. Mol. Cell Bio.* **2003**, 4, SS1.
34. W. E. Moerner, *Trends Anal. Chem.* **2003**, 22, 544.
35. M. Goulian and S. M. Simon, *Biophys. J.* **2000**, 79, 2188.
36. T. Kues, R. Peters, and U. Kubitscheck, *Biophys. J.* **2001**, 80, 2954.
37. H. Li, G. Xue and E. S. Yeung, *Anal. Chem.* **2001**, 73, 1537.
38. E. S. Yeung, *1997 Yearbook of Science and Technology*, **1996**, McGraw-Hill, New York, p. 433.
39. K. A. Willets, O. Ostroverkhova, M. He, R. J. Twieg and W. E. Moerner, *J. Am. Chem. Soc.* **2003**, 125, 1174.
40. S. Nie, D. T. Chiu, and R. N. Zare, *Science*, **1994**, 266, 1018.

41. B. Foster, *Optimizing Light Microscopy for Biological and Clinical Laboratories*, Kendall/Hunt Publishing Company, Dubuque, IA, **1997**.
42. J. G. Delly, *Photography through the Microscope*, Eastman Kodak Company, Rochester, NY, **1988**, p. 14.
43. J. R. Lakowicz, *Principles of Fluorescence Spectroscopy*, Kluwer Academic/Plenum Publisher, New York, **1999**.
44. R. P. Haugland (Editor) *The handbook a Guide to Fluorescent Probes and Labeling Technologies*, Invitrogen Molecular Probes, Eugene, OR, **2005**.
45. J. D. Ingle, Jr. and S. R. Crouch, *Spectrochemical Analysis*, Prentice Hall, Englewood Cliffs, NJ, **1988**, p. 433.
46. J. T. Jones, J. W. Myers, J. E. Ferrel, Jr., and T. Meyer, *Nat. Biotechnol.* **2004**, 22, 306.
47. R. M. Dickson, D. J. Norris, Y-L. Tzeng, and W. E. Moerner, *Science*, **1996**, 274, 966.
48. R. M. Dickson, A. B. Cubitt, R. Y. Tsien, and W. E. Moerner, *Nature*, **1999**, 388, 355.
49. Y. He, H-W. Lee and E. S. Yeung, *J. Phys. Chem. B*, **2005**, 109, 8820.
50. A. G. Harpur, F. S. Wouters, and P. I. H. Bastiaens, *Nat. Biotechnol.* **2001**, 19, 167.
51. J. Lippincott-Schwartz and G. H. Patterson, *Science*, **2003**, 300, 87.
52. J. Lippincott-Schwartz, N. Altan-Bonnet, and G. H. Patterson, *Nat. Biotechnol.* **2003**, 5, S7.
53. E. D. Salmon and P. Tran, *Methods Cell. Biol.* **1995**, 56,153.
54. S. Inoue and K. R. Spring, *Video Microscopy The Fundamentals*, Plenum Press, New York, NY, **1997**.
55. R. D. Allen, *Ann. Rev. Biophys. Biophys. Chem.* **1985**, 14, 265.
56. S. Inoue, *Appl. Optics* **1987**, 26, 3219.
57. C. L. Rieder and A. Khodjakov, *Science*, **2003**, 300, 91.
58. R. Gaughan, *Photonics Showcase*, **2004**, March 2004, 17.
59. N. Fang, H. Lee, C. Sun, X. Zhang, *Science*, **2005**, 308, 534.
60. A. Lewis, H. Taha, A. Strinkovski, A. Manevitch, A. Khatchatouriants, R. Dekhter, and E. Ammann, *Nat. Biotechnol.* **2003**, 21, 1378.
61. F. de Lange, A. Cambi, R. Huijbens, B. de Bakker, W. Rensen, M. Garcia-Parajo, N. van Hulst, and C. G. Figdor, *J. Cell Sci.* **2001**, 114, 4153.

62. J. V. Sweedler, R. B. Bilhorn, P. M. Epperson, G. R. Sims, and M Bonner Denton, *Anal. Chem.* **1988**, 60, 282A.
63. P. M. Epperson, J. V. Sweedler, R. B. Bilhorn, G. R. Sims, and M Bonner Denton, *Anal. Chem.* **1988**, 60, 327A.
64. R.Guntupalli and J. Grant *Photonics Spectra*, **2004**, April 2004, p. 63.
65. X. F. Wang and B. Herman (editors), *Fluorescence Imaging Spectroscopy and Microscopy*, John Willey & Sons, New York , **1996**, p. 93.
66. E. D. Salmon, S. L. Shaw, J. Waters, C. M. Waterman-Storer, P. S. Maddox, E. Yeh and K. Bloom, *Methods. Cell Bio.* **1995**, 56,153.
67. X. F. Wang and B. Herman (editors), *Fluorescence Imaging Spectroscopy and Microscopy*, John Willey & Sons, New York , **1996**, p. 87.
68. M. B. Sinclair, J. A.Timlin, D. M. Haaland, and M. Werner-Washburne, *Applied Optics*, **2004**, 43, 2079.
69. D. Lloyd (editor), *Flow Cytometry in Microbiology*, Springer-Verlag, London, **1993**.
70. G. V. Chapman, *J. Immunol. Methods* **2000**, 243, 3.
71. M. R. Gaucci, G. Vesey, J. Narai, D. Veal, K. L. Williams, and J. A. Piper, *Cytometry* **1996**, 25, 388.
72. D. A. Veal, D. Deere, B. Ferrari, J. Piper, and P. V. Attfield, *J. Immunol. Methods* **2000**, 243, 191.
73. T. W. Petersen, S. F. Ibrahim, A. H. Diercks, and G. van den Engh, *Cytometry*, **2004**, 60A, 173.
74. N. Billinton and A. W. Knight, *Anal. Biochem.* **2001**, 291, 175.
75. A.N. Glazer, L. Stryer, *Trends Biochem. Soc.* **1984**, 9, 423.
76. K.E. Apt, J.L. Collier, and A.R. Grossman, *J. Mol. Biol.* **1995**, 248, 79.
77. D. C. Nguyen, R. A. Keller, J. H. Jett, and J. C. Martin, *Anal. Chem.* **1987**, 59, 2158.
78. K. Peck, L. Stryer, A.N. Glazer, and R.A. Mathies, *Proc. Natl. Acad. Sci. (U.S.A.)* **1989**, 86, 4087.
79. S.H. Kang and E.S. Yeung, *Anal. Chem.* **2002**, 74, 6334.
80. *Fluorescent Labels for Antibodies and Molecular Probes*,
<http://www.hmds.org.uk/fluorochrome.html>, **2002**, accessed last time on June 27, 2005.

81. Y. A. Cai, J. T. Murphy, G. J. Wedemayer, and A. N. Glazer, *Anal. Biochem.* **2001**, 290, 186.
82. B. Zickendraht-Wendelstadt, J. Friedrich, W. Rudiger, *Photochem. Photobiol.* **1980**, 31, 367.
83. D. M. Arciero, D. A. Brajant, and A. N. Glazer, *J. Biol. Chem.* **1988**, 263, 18343.
84. D. M. Arciero, J. L. Dallas, and A. N. Glazer, *J. Biol. Chem.* **1988**, 263, 18350.
85. D. M. Arciero, J. L. Dallas, and A. N. Glazer, *J. Biol. Chem.* **1988**, 263, 18358.
86. C. D. Fairchild and A. N. Glazer, *J. Biol. Chem.* **1994**, 269, 28988.
87. M. Storf, A. Parbel, M. Meyer, B. Strohmamm, H. Scheer, G-M. Deng, M. Zheng, M. Zhou, and K-H. Zhao, *Biochemistry* **2001**, 40, 12444.
88. D. Isailovic, H-W. Li, and E.S. Yeung, *J. Chromat. A* **2004**, 1051, 119
89. A. J. Tooley, Y. A. Cai, and A. N. Glazer, *Proc. Natl. Acad. Sci. (U.S.A.)* **2001**, 98, 10560.
90. A. J. Tooley, and A. N. Glazer *J. Bacteriol.* **2002**, 184, 4666.
91. O. Shimomura, F. H. Johnson, and Y. Saiga, *J. Cell. Comp. Physiol.* **1962**, 59, 223.
92. D. C. Prasher, V. K. Eckenrode, W. W. Ward, F.G. Prendergast and M. J. Cormier, *Gene*, **1992**, 111, 229.
93. M. Chalfie, Y. Tu, G. Euskirchen, W. W. Ward, and D. C. Prasher, *Science*, **1994**, 263, 802.
94. S. X. Wang and T. Hazelrigg, *Nature*, **1994**, 369, 400.
95. T. Stearns, *Curr. Biol.* **1995**, 5, 262.
96. S. Cabantous, T. C. Terwilliger and G. S. Waldo *Nat. Biotechnol.* **2005**, 23, 102.
97. R. Y. Tsien, *Annu. Rev. Biochem.* **1998**, 67, 509.
98. R. Heim and R. Y. Tsien, *Curr. Biol.* **1996**, 6, 178.
99. G. Miesenbock, D. A. De Angelis, and J. E. Rothman, *Nature*, **1998**, 394, 192.
100. T. Ozawa, M. Takeuchi, A. Kaihara, M. Sato, and Y. Umezawa, *Anal. Chem.* **2001**, 73, 5886.
101. G. J. Phillips, *FEMS Microbiol. Lett.* **2001**, 204, 9.
102. A. Miyawaki, A. Sawano, and T. Kogure, *Nat. Cell Biol.* **2003**, 5, S1.

103. J. Zhang, R. E. Campbell, A. Y. Thing, and R. Y. Tsien, *Nat. Rev. Mol. Cell Biol.* **2002**, 3, 906.
104. Y.A. Labas, N.G. Gurskaya, Y.G. Yanushevich, A.F. Fradkov, K.A. Lukyanov, S.A. Lukyanov, M.V. Matz, *Proc. Natl. Acad. Sci. (U.S.A.)* **2002**, 99, 4256.
105. J. Wiedenmann, A. Schenk, C. Rocker, A. Girod, K-D. Spindler, and G. Ulrich Nienhaus, *Proc. Natl. Acad. Sci. (U.S.A.)* **2002**, 99, 11646.
106. R. Ando, H. Hama, M. Yamamoto-Hino, H. Mizuno, and A. Miyawaki, *Proc. Natl. Acad. Sci. (U.S.A.)* **2003**, 99, 12651.
107. J. T. Murphy and J. C. Lagarias, *Curr. Biol.* **1997**, 7, 870.
108. G. Mocz, *Intrinsic Fluorescence of Proteins and Peptides*, <http://dwb.unl.edu/Teacher/NSF/C08/C08Links/pps99.cryst.bbk.ac.uk/projects/gmocz/fluoor.htm>, **1999**, accessed last time on June 27, 2005.
109. C. Edwards (editor) *Environmental Monitoring of Bacteria*, Humana Press, Totowa, NJ, **1999**, p. 243.
110. J. Nakanishi, T. Nakajima, M. Sato, T. Ozawa, K. Tohda, and Y. Umezawa, *Anal. Chem.* **2001**, 73, 2920
111. C. J. Murphy and J. L. Coffe Appl. Spectrosc. **2002**, 56, 16A
112. L. Zhu, S. Ang, W-T. Liu, *Appl. Env. Microbiol.* **2004**, 70, 597
113. L. Cognet, C. Tardin, D. Boyer, D. Choquet, P. Tamarat, and B. Lounis, *Proc. Natl. Acad. Sci. (U.S.A.)*, **2003**, 100, 11350
114. A. G. Tkachenko, H. Xie, D. Coleman, W. Glomm, J. Ryn, M. F. Anderson, S. Franzen and D. L. Feldheim *J. Am. Chem. Soc.* **2003**, 125, 4700
115. L. Stryer, *Biochemistry*, W. H. Freeman and Company, New York, **1988**.
116. B. Habibi-Nazhad, *About E. coli*, http://redpoll.pharmacy.ualberta.ca/CCDB/intron_new.html, **2004**, accessed last time on June 27, 2005.
117. L. Shapiro and R. Losick, *Science*, **1997**, 276, 712.
118. J. R. Maddock and L. Shapiro, *Science*, **1993**, 259, 1717.
119. L. C. Javois (editor) *Methods Mol. Biol.* Humana Press, Totowa, New Jersey, **1994**.

120. B. J. Feilmeier, G. Iseminger, D. Schroeder, H. Webber, and G. J. Phillips, *J. Bacteriol.* **2000**, 182, 4068.
121. X. Ma, D. W. Ehrhardt, and W. Margolin *Proc. Natl. Acad. Sci. (U.S.A.)* **1996**, 93, 12998.
122. D. J. Sherrat, I. F. Lau and F-X. Barre, *Curr. Opin. Micobiol.* **2001**, 4, 653.
123. J. D. Thomas, R. A. Daniel, J. Errington, and C. Robinson, *Mol. Microbiol.* **2001**, 39, 47.
124. J. F. Kane and D. L. Hartley, *Trends Biotechnol.* **1988**, 4, 95.
125. H. P. Sorensen and K. K. Mortensen, *Micro. Cell Factories* **2005**, 4, 1.
126. W. Schumann and L. C. S. Fereira, *Gen. Molec. Biol.* **2004**, 27, 442.
127. E. T. Farinas, T. Bulter and F. H. Arnold, *Curr. Opin. Biotechnol.* **2001**, 12, 545.
128. G. S. Waldo, B. M. Standish, J. Berendzen, and T. C. Terwilliger, *Nat. Biotechnol.* **1999**, 17, 691.
129. J. W. Chin, A. B. Martin, D. S. King, L. Wang and P. G. Shultz, *Proc. Natl. Acad. Sci. (U.S.A.)* **2002**, 99, 11020.
130. L. Wang, Z. Zhang, A. Brock and P. G. Shultz, *Proc. Natl. Acad. Sci. (U.S.A.)* **2002**, 99, 11020.
131. R. A. Mehl, J. C. Anderson, S. W. Santoro, L. Wang A. B. Martin, D. S. King, D. M. Horn, and P. G. Shultz, *J. Am. Chem. Soc.* **2003**, 125, 935.

**CHAPTER 2. ISOLATION AND CHARACTERIZATION
OF R-PHYCOERYTHRIN SUBUNITS AND ENZYMATIC DIGESTS**

A paper published in Journal of Chromatography A*

Dragan Isailovic, Hung-Wing Li and Edward S. Yeung

ABSTRACT

Subunits and enzymatic digests of the highly fluorescent phycobiliprotein R-phycoerythrin (R-PE) were analyzed by several separation and detection techniques including HPLC, sodium dodecyl sulfate–polyacrylamide gel electrophoresis (SDS–PAGE), CE, and HPLC–electrospray ionization (ESI) MS. R-PE subunits were isolated by HPLC and detected as single molecules by total internal reflection fluorescence microscopy. The results show efficient absorption and fluorescence of the R-PE subunits and digest peptides, originating from the incorporation of phycoerythrobilin and phycourobilin chromophores in them. In addition, HPLC-ESI-MS and SDS–PAGE were optimized to determine the molecular masses of phycobiliprotein subunits and the chromophore-containing peptides, as well as the amino acid sequences of the latter. Favorable spectroscopic and structural properties of R-PE subunits and enzymatic digests, even under denaturing conditions, make these molecules suitable for use as fluorescence labels for biomolecules.

Keywords: Total internal reflection fluorescence microscopy; Detection, LC; Phycoerythrin; Phycobiliproteins; Proteins

*Reprinted with permission from Journal of Chromatography A, 1051 (2004) 119-130

1. Introduction

Research on fluorescent proteins has been intensive, especially after the expression of green fluorescent protein (GFP) from jellyfish *A. victoria* in different types of cells [1]. Recently, new fluorescent proteins from the GFP family were discovered in corals [2]. Phycobiliproteins are found in cyanobacteria and several groups of eucaryotic algae (red algae, cryptomonads and glaucophytes) [3]. These organisms contain phycobilisomes, phycobiliprotein complexes that have an important role in the photosynthesis. Although they cannot be cloned directly due to complexity of their structures, phycobiliproteins remain as very useful fluorescent probes due to their excellent spectroscopic properties [4, 5].

Phycobiliproteins consist of three groups: allophycocyanins, phycocyanins and phycoerythrins [3]. They are all composed of two subunits (α and β), while the third subunit (γ), a linker peptide, is found in phycoerythrins. The structure of R-phycoerythrin (R-PE) and B-phycoerythrin (BPE) can be described as $(\alpha\beta)_6\gamma$, while phycocyanin (PC) and allophycocyanin (APC) have the structure $(\alpha\beta)_3$ [4]. Each subunit contains one or more phycobilin chromophores (phycobilins) bound to specific cysteines in the polypeptide chains by thioether bonds. The outstanding absorption and fluorescence properties of phycobiliproteins in the visible region originate from phycobilins and their interactions within polypeptide chains [4,5]. Eight different phycobilins were found in phycobiliproteins [6]. The most representative phycobilins are phycoerythrobilin (PEB), phycourobilin (PUB), phycocyanobilin (PCB) and phycobiliviolin (PXB) (Fig. 1). PEB is found in C-phycoerythrin (C-PE), R-PE, B-PE and PC, PUB is found in R-PE and B-PE, PCB is found in PC, APC, phycoerythrocyanin (PEC) and phycoerythrins, while PXB is found in PEC [3,7]. The number of phycobilins and the phycobiliprotein structure depend on the species of origin, but some phycobilin-binding sites were conserved during phycobiliprotein evolution [3,7].

R-PE from red algae *G. coulteri* has the structure $(\alpha\beta)_6\gamma$ and molecular mass (M_r) of ~240,000 [8]. Two γ subunits differing in amino-acid sequences were found in this protein. The α subunit ($M_r \approx 17,000$) contains two PEB chromophores; the β subunit ($M_r \approx 18,000$) contains two PEB and one PUB chromophore, while the γ subunits (M_r values $\approx 30,000$) contain three PUBs and one PEB chromophore [8]. Two or three γ subunits and different

chromophore contents were found in R-PE from other red algal species [9,10]. The absorption spectrum of R-PE shows maxima at 496 and 565 nm due to the presence of PUB and PEB chromophores, respectively. This was confirmed by spectral characterization of R-PE chromophores and peptide digests [8,11,12]. The single fluorescence maximum of R-PE at 580 nm is a consequence of fluorescence resonance energy transfer (FRET) from PUB to PEB chromophore [13].

Phycobiliproteins conjugated to antibodies are used in numerous fluorescence assays [4, 5]. Due to their stability, high absorption coefficients and high quantum yields, B-PE and R-PE have been detected as single-molecules [14–16] and imaged by total internal reflection fluorescence microscopy (TIRFM) on a fused-silica prism [16]. Also, R-PE has been tracked by fluorescence video microscopy in the cytoplasm and nucleoplasm of a single mammalian cell [17].

Sequences of many phycobiliprotein apo-subunits have been obtained by sequencing cyanobacterial and algal genomes [7]. However, characterization of phycobiliprotein subunits and their enzymatic digests is necessary to elucidate phycobiliprotein composition and chromophore content. HPLC, gel filtration, ion-exchange chromatography and sodium dodecyl sulfate–polyacrylamide gel electrophoresis (SDS–PAGE) have been used for the analysis of phycobiliprotein subunits and enzymatic digests. A universal-reversed-phase (RP)-HPLC gradient consisting of 0.1% trifluoroacetic acid (TFA) in water and 0.1% TFA in 2:1 (v/v) acetonitrile:isopropanol on a C4 column was used to separate and characterize subunits of diverse phycobiliproteins [18]. Fast performance LC (FPLC) and SDS–PAGE were used to separate γ subunits of R-PE from red algae *C. corymbosum* and *A. sparsum* [9]. α and β subunits of C-PE from cyanobacteria *Pseudanabaena* W 1173 were separated by gel filtration and ultracentrifugation, and their absorption coefficients and quantum yields were determined [19]. SDS–PAGE followed by Coomassie staining and HPLC was used for the separation of C-PE and APC subunits isolated from cyanobacteria *S. platensis* [20]. B-PE isolated from the unicellular red algae *P. cruentum* was characterized by SDS–PAGE and by RP-HPLC, using 0.1% TFA in water and 0.1% TFA in acetonitrile on a C4 column [21]. Recently, RP-HPLC–electrospray ionization (ESI) MS, using also 0.1% TFA in water and

0.1% TFA in acetonitrile on C4 column, was used to analyze C-PC and APC subunits from phycobilisomes of cyanobacteria *Synechocystis* 6803 [22,23].

Separation and purification of phycobiliprotein enzymatic digest peptides were performed by gel filtration, ion exchange chromatography and HPLC, to sequence them and to find the phycobilin-binding sites in B-PE and R-PE [8,24,25]. Secondary-ion mass spectrometry was used to determine molecular masses and to confirm the sequences of chromophore-containing peptides [26,27].

Although CE with laser-induced fluorescence (LIF) was used to study phycobiliproteins [28], there have been no reports on using CE for the separation of R-PE subunits and enzymatic digests. One specific way to detect phycobilin-bound proteins and peptides in gels is SDS-PAGE in the presence of zinc acetate [29]. After excitation by UV light, orange fluorescence of phycobiliprotein-zinc complexes in gels or membranes is detected. This method is comparable in sensitivity to commonly used Coomassie gel staining.

In this research, HPLC, SDS-PAGE and CZE with absorption and fluorescence detections were used to analyze R-PE subunits and enzymatic digests. The goal was to isolate these polypeptides, determine their spectroscopic properties and evaluate their suitability for single-molecule detection. In addition, we develop HPLC-ESI-MS and SDS-PAGE methods to determine the molecular weights of phycobiliprotein subunits and peptide digests, as well as the amino acid sequences of the chromophore-containing peptides.

2. Experimental

2.1. Chemicals

Phycobiliproteins (R-PE, B-PE and APC) were purchased as solutions in phosphate buffer ($C = 4$ mg/ml, pH = 7.4) from Molecular Probes (Eugene, OR, USA). R-PE was from red algae *P. tenera*, B-PE was from red algae *P. cruentum*, and APC was from cyanobacteria *A. variabilis*. HPLC grade acetonitrile, dimethyl sulfoxide (DMSO), 88% formic acid, methanol, mercury (II) chloride and urea were from Fisher Scientific (Pittsburgh, PA, USA). TFA, Tris base, sodium phosphate, ammonium hydrogen carbonate, pepsin and trypsin were

from Sigma (St. Louis, MO, USA). Milli-Q nano-pure water and Sep-Pak cartridges were from Waters–Millipore (Milford, Boston, MA, USA). SDS–PAGE chemicals were from Bio-Rad (Richmond, CA, USA).

2.2. Sample preparation

Protein solutions were centrifuged in the microcentrifuge at 5000 rpm for 10 min. The supernatant was discarded and the pellet was dissolved in water just before the experiments. For pepsin digestion of R-PE, 30 μ l of R-PE ($C = 1$ mg/ml) was centrifuged as above. Then 9 μ l of pepsin solution ($C = 2$ mg/ml) and 90 μ l of 0.025M HCl was added. The mixture was heated at 37 °C for 4 h. The procedure for trypsin digestion was adopted from reference [8]. Twenty-five μ l of R-PE ($C = 1$ mg/ml) was centrifuged as above. Seventy-five μ l of 0.025 M HCl was added. One μ l of trypsin ($C = 1$ mg/ml) and 1 mg of NH_4HCO_3 were added and the mixture was heated at 37 °C for 2 h. Then, a new 1 μ l aliquot of trypsin solution was added and incubation continued at 37 °C for two more hours. PEB was a generous gift of Max Storf (University of Munich, Germany). An urobilin product, presumably PUB, was isolated from B-PE using a modified procedure for PEB isolation [30]. 2 mg of B-PE was refluxed in 100 ml of HgCl_2 solution in methanol ($C = 2$ mg/ml) at 45 °C for 16 h. After centrifugation at 17,000 $\times g$ for 20 min, 200 μ l of 2-mercaptoethanol was added, and the solution was centrifuged again as above. The methanol solution was evaporated under vacuum and the remaining supernatant was cleaned by solid phase extraction through a C18 Sep-Pak cartridge.

2.3. HPLC separations with absorption and fluorescence detection

A Shimadzu Class VP HPLC system (Shimadzu Scientific Instruments, Columbia, MD, USA) was used for HPLC separations on an analytical C4 column (250mm \times 4.6 mm, Vydac, Hesperia, CA, USA). The instrument was equipped with both photodiode array (PDA) UV–vis and spectrofluorimetric detectors. For subunit separations, 10 μ l of R-PE solution ($C = 4$ mg/ml) was injected on the column previously equilibrated with 75% of phase A (0.1% TFA

in water) and 25% of phase B (0.1% TFA in acetonitrile). The flow rate was 0.8 ml/min. A gradient from reference [21] was used. Later it was found that following gradient gives baseline separation as well: 0–40 min 75% of B, 40–45 min 95% of B, and 45–50 min 25% of B. The PDA detector was set with both deuterium and tungsten lamps on to monitor the absorbance of the eluent from 190 to 800 nm. For subunit absorption coefficient determination, four R-PE solutions with concentration of 1, 2, 3 and 4 mg/ml were prepared and run in a sequence using the above gradient.

For fluorescence detection, the excitation wavelength was set at 496 nm and the emission wavelength was set at 580 nm. To measure excitation and emission spectra of the subunits on-line, pumps were stopped during the rising edge of the absorbance and fluorescence peaks, and a wavelength scan was acquired. Subunits were collected manually as they elute out of the column for subsequent fluorescence measurements.

For separations of pepsin and trypsin digests, 20 μ l of digests were injected on the C4 column equilibrated with 95% of phase A and 5% of phase B. Separations were done according to the following gradient: 0–15 min 20% B, 15–45 min 35% B, 45–55 min 45% B and 55–65 min 95% B. The eluent was monitored as in the case of the subunits.

2.4. Fluorescence and absorption spectrometry

A luminescence spectrometer LS50B (Perkin-Elmer, Beakonsfield, UK) was used to measure fluorescence spectra of the collected subunits and chromophores in increments of 0.5 nm. Widths of the excitation and emission slits were set at 10 nm. Absorbance spectra of chromophores were measured by an 8452A diode-array spectrophotometer (Hewlett Packard, Palo Alto, CA, USA) in increments of 2 nm.

2.5. TIRFM

Subunits collected after HPLC separation were diluted one thousand times by phosphate buffer (pH = 9). Five μ l of a subunit solution was set on a 22 mm square cover slip (Corning, New York, NY, USA) and put on a fused-silica prism (Melles Griot, Irvine, CA, USA). A

Coherent, Innova 90 (Santa Clara, CA, USA) 488-nm argon-ion laser was used to excite R-PE subunits. Fluorescence was collected by a 40X immersion-oil Plan-Neofluor objective, NA = 1.3 (Carl Zeiss, Thornwood, NY, USA) through type FF immersion oil (Cargille, Cedar Grove, NJ, USA) with a refractive index of $n = 1.48$. Fluorescence images were taken by a cascade intensified charge-coupled device (ICCD, Roper Scientific, Trenton, NJ, USA) with a pixel size of $7.5 \mu\text{m} \times 7.5 \mu\text{m}$. The camera chip was kept at -35°C by thermoelectric cooling. A 488-nm holographic notch filter (Kaiser Optical System, Ann Arbor, MI, USA) with an optical density of > 6 was placed between the objective and ICCD camera to prevent stray light from reaching the ICCD. The exposure times for the ICCD camera and the laser shutter were synchronized by a shutter driver/timer, Uniblitz ST132 (Vincent Associates, Rochester, NY, USA). The digitization resolution of the camera was 16 bit. The digital-analog converter (DAC) setting was 3689. The data rate was 2 Hz (0.5 s/frame). The exposure time for each frame was 20 ms. The frame transfer of the ICCD camera was operated in the external synchronization mode. A sequence of frames was acquired for each sample via V++ software (Roper Scientific). All frames were analyzed off-line.

2.6. CE separations with absorption and fluorescence detection

A Beckman PACE/MDQ CE instrument (Beckman Coulter, Carlsbad, CA, USA) equipped with a UV-vis PDA detector and a 488-nm argon-ion laser-induced fluorescence (LIF) detectors was used for separation and detection on $75 \mu\text{m}$ i.d. fused-silica capillaries (Polymicro, Phoenix, AZ, USA). Samples were injected hydrodynamically using pressure of 3447 Pa for 5 s. A voltage of 25 kV was applied on the 60 cm long capillary. For absorbance measurements, the PDA detected signal from 190 to 600 nm. For LIF detection, a 488-nm notch filter and a 580-nm band-pass emission filter were used. Separation of the subunits was accomplished in 50mM phosphate buffer containing 4.5 M urea (pH = 2) within 90 min. Trypsin digest was separated in 0.1M phosphate buffer (pH = 2.5) in 60 min. After pretreatment of the capillary with 0.1M NaOH for 5 min, pepsin digest was separated in 0.1M Tris buffer (pH = 7.6) for 15 min.

2.7. SDS–PAGE analysis

SDS–PAGE equipment was from Bio-Rad. Ten μl of phycobiliproteins ($C = 4 \text{ mg/ml}$) was centrifuged at 5000 rpm for 10 min. Forty μl of water, 47.5 μl of Laemli sample buffer and 2.5 μl of 2-mercaptoethanol were added and the mixture was heated for 10 min at 95 °C. Thirty μl of the mixture and 5 μl of molecular mass standards were loaded on the 12% polyacrylamide (PA) Tris–HCl gel and were separated using a current of 30 mA. After separation, the gel was washed three times for 5 min each in water, and scanned by a fluorescence imager Typhoon 8600 (Amersham Pharmacia Biotech, Piscataway, NJ, USA) using a 532-nm laser for excitation, 580BP30 filter for emission, and a detector voltage of 600 V. After fluorescence detection, the gel was stained with Bio-safe Coomassie blue for 1 h and washed in water for 30 min.

2.8. HPLC/ESI-MS experiments

A Shimadzu LCMS-2010 instrument equipped with a dual-channel UV–vis detector was used for the HPLC–ESI-MS experiments. 3.7% (v/v) formic acid in water (A) and 3.7% (v/v) formic acid in acetonitrile (B) were used as solvents. Separations were performed on a Vydac C4 HPLC column (250mm x 2.1 mm) using a flow rate of 0.1 ml/min. Mass spectra were collected in the positive-ion mode using the LCMS Solution Main Program. The following values were set in the tuning file: CDL temperature 250 °C, nitrogen gas flow 4.5 l/min, block temperature 200 °C, probe voltage 4.5 kV, CDL voltage 25V, Q array voltage 30.0 V/25.0 V/55.0V, and Q array RF 150.00. The dual UV–vis detector was set to monitor absorption of subunits and chromophore-containing peptides at their respective absorption maxima (496 and 555 nm in the case of R-PE and B-PE subunits, 650 nm for APC subunits, and 496 and 550 nm for R-PE digest peptides). Molecular mass of subunits and chromophore-containing peptides were determined using LCMS Profile Post Run program.

In the case of subunits separation, 15 μl of phycobiliproteins ($C = 4 \text{ mg/ml}$) was loaded on the column after equilibrating with 75% of phase A and 25% of phase B. The gradient used for the separation of R-PE and B-PE subunits and their mixture was: 0–40 min 75% B,

40–45 min 95% B and 45–50 min 25% B. For separation of APC subunits and their mixture with R-PE and B-PE subunits the following gradient was used: 0–60 min 75% B, 60–70 min 95% B, and 70–80 min 25% B. The scan range of the MS detector was 850–1650 m/z with a scan interval of 5 s, scan speed of 500 and detector gain of 1.5 kV.

For separations of R-PE digests, 20 μ l of pepsin or trypsin R-PE digest was injected on the column after equilibrating with 5% B. The scan range of MS detector was 300–1800 m/z with a scan interval of 5 s, scan speed of 500 and detector gain of 1.5 kV. For pepsin digest, the gradient used was 0–15 min 20% B, 15–75 min 30% B, 75–90 min 95% B, and 90–100 min 5% B. For trypsin digest separation the following gradient was used: 0–15 min 20% B, 15–40 min 30% B, 40–55 min 60% B, 55–80 min 95% B, and 80–90 min 5% B. The measured M_r values of subunits and peptides were compared with their respective MWs found in the Swiss-Prot and TrEMBL protein database [7] and calculated by the program PAWS (ProteoMetrics, New York, NY, USA).

3. Results and discussion

3.1. Isolation and spectroscopic characterization of R-PE subunits

R-PE subunits were baseline separated by HPLC (Fig. 2). The elution profile looks similar as in earlier HPLC separations of R-PE and B-PE subunits [18, 20]. Assignment of subunits was achieved from their absorption spectra (inset of Fig. 2 and Table 1). The α subunit ($t_R = 24.8$ min) shows an absorption maximum at 555 nm due to the presence of PEB chromophore, while the β subunit ($t_R = 30.4$ min) and γ subunits ($t_R = 17.0$ min and $t_R = 18.2$ min) show maxima at both 496 and 555 nm due to the presence of both PUB and PEB chromophores [4,8,18]. Chromophore content of R-PE subunits is characteristic for R-PE from *P. tenera* and several other species [7]. As in the work of Bermejo et al on HPLC separation of B-PE subunits [21], HPLC separation of R-PE subunits was semi-preparative. Subunits were manually collected for further analysis (fluorescence spectroscopy and fluorescence microscopy).

Subunit absorption coefficients were determined from the calibration curve of on-line subunit absorbance versus subunit concentration. Slight adsorption of the subunits on the column stationary phase occurred (approximately 5% of the amount injected on the column). Because of that, a correction was introduced for subunit absorbance. Values of $\sim 10,000 \text{ cm}^{-1} \text{ M}^{-1}$ were found for absorption coefficients of α subunit (at 555 nm) and β subunit (both at 555 and 496 nm). R-PE subunits were diluted in the detection cell of the HPLC UV-vis PDA detector, so that exact values of absorption coefficients at pH of 2 should be higher than determined values. Because the subunits were denatured in the mobile phase, absorption coefficients of “native” R-PE subunits should be much larger than $10,000 \text{ cm}^{-1} \text{ M}^{-1}$. Absorption coefficients of C-PE α and β subunits were determined to be 151,300 and $266,200 \text{ cm}^{-1} \text{ M}^{-1}$ at their respective absorption maxima (566 and 557 nm) in phosphate buffer at pH = 7 [19]. Since the structure and chromophore content of C-PE [31] is similar as structure of R-PE it is reasonable to expect approximately the same absorption coefficients of R-PE subunits.

Despite the low pH used for separation, all subunits show high fluorescence (Fig. 2, lower chromatogram). Excitation and emission spectra of R-PE subunits were recorded by spectrofluorometric HPLC detector and fluorescence spectrometer (Fig. 3), and the fluorescence maxima are listed in Table 1. Excitation spectra of subunits show maxima at approximately the same wavelengths as their respective absorbance spectra. The α subunit emission spectrum has a single emission maximum at 564 nm, while β and γ subunits show emission maxima both at 504 and ~ 565 nm. Peaks at 505 and 565 nm are due to fluorescence of covalently bound PUB and PEB chromophores respectively, as confirmed by the absorption and fluorescence spectra of free chromophores (Table 1). The absorption and fluorescence maxima of PEB chromophore show hypsochromic effect when bound to the polypeptide chain due to decreased conjugation of the double bonds.

The quantum yields of subunits could be determined by the fluorescence spectrometer using the method of Parker and Rees [32]. If the fluorescence spectra of two compounds are measured with the same instrument at the same excitation wavelength, the ratio of fluorescence intensities is given by the ratio of the spectral areas. For this measurement to be used with an HPLC detector it is necessary to have a standard compound with known

quantum yield at the pH value used for separation. Unfortunately, there were no such standards. Quantum yields of 0.51 and 0.56 were found for C-PE α and β subunits at pH = 7 based on measurements in the fluorescence spectrometer [19].

It was interesting to try to separate R-PE subunits by capillary zone electrophoresis (CZE). CZE separations followed by LIF detection showed several fluorescent peaks (Fig. 4). Fluorescent subunits show also absorbances at 496 and 555 nm (data not shown), but the CE PDA detector could not reconstruct the absorption spectra of the subunits. So, the assignment of these peaks to specific subunits was not possible. Considering the amount of sample injected, the high fluorescence of R-PE subunits is obvious. CE subunit separation times were relatively long and the reproducibility was inferior. From the amino acid sequences of R-PE subunits from *P. tenera* [7], we calculated the *pI* values to be 5.40 and 6.23 for α and β subunits, respectively. So, subunits are positively charged at the pH used for CE separation and adsorption on the negatively charged capillary wall is significant. Adsorption could be prevented and separation improved if coated capillaries were used.

3.2. Separation and spectroscopic characterization of R-PE enzymatic digests

RP-HPLC separation of trypsin and pepsin digests (Fig. 5) was achieved on a C4 column. Separations on the C4 column were more efficient than separations on C8 and C18 columns due to the hydrophobicity of phycobilin-containing peptides. Peptides having retention times from 20 to 25 min show absorption maxima at 496 nm (left inset of Fig. 5), and correspond to PUB-containing peptides. Peptides eluting from 25 to 34 min correspond to PEB-containing peptides and have absorption maxima at 550 nm (right inset of Fig. 5). Both PEB peptides (Fig. 5, lower) and PUB containing peptides are fluorescent because of the chromophore. R-PE pepsin and trypsin digests were also separated by CZE. Fig. 6 shows the CZE separation of R-PE pepsin digest followed by LIF detection. Fluorescence of PEB-containing peptides is evident and the separation reproducibility was very good.

3.3. Single-molecule detection of R-PE subunits by TIRFM

Single-molecule experiments confirm that R-PE subunits are highly efficient in absorption and in fluorescence. After isolation by HPLC, R-PE subunits were seen as individual molecules in the phosphate buffer (pH = 9) by TIRFM (Fig. 7). From the amount of R-PE on the column, it was calculated that the concentrations of imaged subunits were around 1 nM. If the thickness of the excitation zone in TIRFM is 200 nm and the size of the imaging window (200 pixels x 200 pixels) is 2.25 mm², the number of molecules present in the volume of 4.5 x 10⁻⁴ mm³ after magnification with 40X objective should be around 200. We observed 198, 498 and 297 molecules for α , β and γ subunits, respectively. The β and γ subunits are brighter than the α subunit (Table 2) due to more efficient excitation of β and γ subunits at 488 nm. This wavelength is also close to the excitation maximum of the PUB chromophore. If R-PE subunits are imaged in the HPLC mobile phase (pH \approx 2.0), they aggregated and became permanently adsorbed on the glass surface (shown for the α subunit in Fig. 7). Subunits are positively charged at low pH and are attracted to the negatively charged silica prism, confirming the adsorption effect seen during CZE separation. Same type of correlations between adsorption of proteins in TIRFM and during CZE was noticed for R-PE molecules [16].

3.4. SDS-PAGE analysis of phycobiliprotein subunits

To gain further insights into the properties and structures of R-PE subunits and enzymatic digests, SDS-PAGE and HPLC-ESI-MS were employed. Coomassie-stained gel after SDS-PAGE analysis (Fig. 8, left) shows one band corresponding to overlapped α and β subunits ($M_r \approx 20,000$) and two low-intensity bands corresponding to two different gamma subunits ($M_r \approx 30,000$). SDS-PAGE analysis followed by fluorescence detection also showed two other bands with M_r values between 40,000 and 50,000 (Fig. 8, right). These bands could correspond to either non-denatured subunit aggregates or the structurally different gamma subunits. SDS-PAGE was used for separation of B-PE and APC as well. For separation of B-PE subunits, the bands look similar to those for the R-PE subunits due to structural

similarities of B-PE and R-PE. Improved resolution of the subunits from these proteins could probably be achieved if higher percentage PA gels are used. α and β subunits of B-PE from *P. cruentum* were separated by SDS-PAGE on 16.5% polyacrylamide gel [21]. In the case of APC two bands with respective M_r values of approximately 16,000 and 18,000 (Fig. 8) are seen in both Coomassie and fluorescence detection. These bands correspond to APC α and β subunits respectively. The fluorescence gel imager has been successfully used for imaging phycobiliproteins after native PAGE [33]. Here we show that this instrument can also be used for the detection of phycobiliprotein subunits on the denaturing gel. This method is more sensitive but is less selective for the detection of bilin-bound proteins than UV-excited fluorescence of zinc-phycobiliprotein complexes [29]. The method could also be used to detect phycobilin-bound peptides in gels or on membranes.

3.5. HPLC-ESI-MS analysis of phycobiliprotein subunits

HPLC-ESI-MS separation of R-PE subunits was achieved (Fig. 9). An unusually high content of formic acid was used during the separation to match the pH of the mobile phase when 0.1% of TFA was used. Formic acid (HCOOH) is used in LC-ESI-MS to replace TFA because it makes weaker complexes with the ions of interest than TFA and improves the ion signal [34]. While usually up to 1% (v/v) of formic acid was used for HPLC-ESI-MS separations [34,35], we used 3.7% (v/v) formic acid in both water and acetonitrile. HPLC separation of α and β subunits is achieved efficiently, while separation of γ subunits is even better than in the case when 0.1% TFA was used in the mobile phase. Up to four peaks corresponding to R-PE gamma subunits could be seen (Fig. 9). Mass spectra of α , β and one of γ subunits ($t_R = 17.5$ min) show multiply charged ions (insets in Fig. 9). Subunits' M_r values were calculated from these mass spectra (Table 1). To check if HPLC-ESI-MS could be used for the analysis of other phycobiliproteins, B-PE and APC subunits were separated (Fig. 10). The measured M_r values of B-PE α and β subunits are 18,977 and 20,327, respectively (Fig. 11). Three values (17,928, 17,824 and 16,763) were obtained from ESI mass spectrum of the APC α subunit (Fig. 11), probably due to cluster formation with formic

acid molecules or slight changes in the structure of this subunit at low pH. The nominal M_r of the APC β subunit is 17,846. R-PE, B-PE and APC subunits were separated from their respective mixtures, what could make this HPLC–ESI-MS method useful for analysis of phycobilisomes of algae or cyanobacteria [22,23]. Also, M_r values of the subunits provide the possibility to determine the number of the chromophores on a subunit if the sequence of an apo-subunit is known. The measured M_r values are in excellent agreement with M_r values of the phycobiliprotein subunits from *P. tenera*, *P. cruentum* and *A. variabilis* found in Swiss-Prot and TrEMBL protein database (Table 3 and [7]). These values are more accurate than M_r values of R-PE subunits found by SDS–PAGE (Section 3.4).

3.6. HPLC–ESI-MS analysis of R-PE enzymatic digests

In the case of trypsin and pepsin digests, separations were efficient as well. Molecular weights of several PEB containing peptides were determined (Fig. 12). Trypsin cuts amino-acid chains on the C terminus of lysine and arginine. Pepsin is relatively non-specific but preferentially cleaves the peptide bonds of hydrophobic amino acids. Triply charged ions found on peptides from trypsin digest originate from positive charges on the N terminus of the peptide, the N terminus of arginine, and the positively charged PEB chromophore. Doubly charged ions from pepsin digest originate from the positively charged peptide N terminus and the positively charged PEB chromophore. Sequences of several chromophore-containing peptides were deduced from sequences around the chromophore-binding sites in R-PE from *P. tenera* [7]. It is known that PEB is bound to cysteine residues 82 and 139 of the alpha subunit and to cysteine residues 82 and 158 of the beta subunit. PUB is bound to cysteines 50 and 61 of the beta subunit by two thioether bonds [7]. There is excellent agreement between the measured peptide M_r values and peptide M_r values calculated from sequences of α and β subunits of R-PE from *P. tenera* (Table 4). There are several chromophore-containing peptides whose M_r values were not determined because they are larger than the m/z limit of the present MS quadrupole detector (2000 m/z). Sequences of these peptides could be found if MS–MS capabilities of the instrument are employed. That

will make this method comparable in performance to amino acid sequencing of phycobilin-containing peptides [8].

3.7. Conclusion and future prospects

HPLC, CZE and SDS-PAGE separations followed by absorbance, fluorescence and MS detections were used for spectroscopic and structural characterization of R-PE subunits and enzymatic digests. The same methodology could be employed in the analysis of other phycobiliproteins and fluorescent proteins in general. Along with their high absorbance, R-PE subunits and chromophore-containing peptides are highly fluorescent even under denaturing conditions and at the low pH conditions used in above separations.

M_r values of R-PE subunits are smaller than the M_r of the widely used GFP while the values for their absorption coefficients are comparable. As shown here, one way to obtain these highly fluorescent molecules is semi-preparative chromatography. In vitro binding of chromophores for genetically expressed subunits [36] or solid-phase synthesized peptides are other pathways to obtain highly fluorescent RPE peptides and subunits. It would be of the great interest to establish the biosynthesis pathway for these subunits, as was done for the alpha subunits of C-PC and PEC [37, 38]. Phycobiliprotein subunits could be conjugated to different bioactive moieties as antibodies, histidine tags, streptavidin or biotin [39]. Although they are less bright than R-PE itself we show here that R-PE subunits can be detected down to the single-molecule level. They would interfere less with the system under interrogation (for example cells or surfaces) than R-PE because of the absence of interactions associated with quaternary structure and because of the smaller size compared to R-PE. Hence, R-PE subunits and chromophore-containing peptides have good potential for use as fluorescence probes in single-molecule detection and single-cell analysis.

Acknowledgements

We thank Max Storf for the generous gift of PEB. Shimadzu Scientific Instruments and Joe Burnett provided us with the Shimadzu Class VP HPLC system. Jake C. Lagarias, Craig

Aspinwall, Chanan Slusznay and Robert Classon helped with various parts of this research. E.S.Y. thanks the Robert Allen Wright Endowment for Excellence for support. The Ames Laboratory is operated for the US Department of Energy by Iowa State University under Contract W-7405-Eng-82. This work was supported by Director of Science, Office of Basic Energy Sciences, Division of Chemical Sciences.

References

- [1] M. Chalfie, Y. Tu, G. Euskirchen, W.W. Ward, D.C. Prasher, *Science* 263 (1994) 802.
- [2] Y.A. Labas, N.G. Gurskaya, Y.G. Yanushevich, A.F. Fradkov, K.A. Lukyanov, S.A. Lukyanov, M.V. Matz, *Proc. Natl. Acad. Sci. (U.S.A.)* 99 (2002) 4256.
- [3] K.E. Apt, J.L. Collier, A.R. Grossman, *J. Mol. Biol.* 248 (1995) 79.
- [4] A.N. Glazer, L. Stryker, *Trends Biochem. Soc.* 9 (1984) 423.
- [5] R.P. Haugland (Ed.), *Handbook of Fluorescent Probes and Research Products, Molecular Probes*, Eugene, OR, 2002.
- [6] M. Storf, A. Parbel, M. Meyer, B. Strohmann, H. Scheer, M. Deng, M. Zheng, M. Zhou, K. Zhao, *Biochemistry* 40 (2001) 12444.
- [7] <http://us.expasy.org/cgi-bin/sprot-search-de?R-phycoerythrin>, on July 18, 2005.
- [8] A.V. Klotz, A.N. Glazer, *J. Biol. Chem.* 260 (1985) 4856.
- [9] K.E. Apt, S. Metzner, A.R. Grossman, *J. Phycol.* 37 (2001) 64.
- [10] I.N. Stadnichuk, A.V. Knokhlachev, Y.V. Tikhonova, *J. Photochem. Photobiol. B: Biol.* 18 (1993) 169.
- [11] P. O'Carra, R.F. Murphy, S.D. Killilea, *Biochem. J.* 187 (1980) 303.
- [12] S.D. Killilea, P. O'Carra, *Biochem. J.* 226 (1985) 723.
- [13] T. Jiang, J. Zhang, D. Liang, *Proteins: Struct. Funct. Gen.* 34 (1999) 224.
- [14] D.C. Nguyen, R.A. Keller, J.H. Jett, J.C. Martin, *Anal. Chem.* 59 (1987) 2158.
- [15] K. Peck, L. Stryer, A.N. Glazer, R.A. Mathies, *Proc. Natl. Acad. Sci. (U.S.A.)* 86 (1989) 4087.
- [16] S.H. Kang, E.S. Yeung, *Anal. Chem.* 74 (2002) 6334.
- [17] M. Goulian, S.M. Simon, *Biophys. J.* 79 (2000) 2188.

- [18] R.V. Swanson, A.N. Glazer, *Anal. Biochem.* 188 (1990) 295.
- [19] B. Zickendraht-Wendelstadt, J. Friedrich, W. Rudiger, *Photochem. Photobiol.* 31 (1980) 367.
- [20] R. Bermejo, E.M. Talavera, J.M. Alvarez-Pez, J.C. Orte, *J. Chromatogr. A* 778 (1997) 441.
- [21] R. Bermejo, E.N. Talavera, J.M. Alvarez-Pez, *J. Chromatogr. A* 917 (2001) 135.
- [22] L. Zolla, M. Bianchetti, *J. Chromatogr. A* 912 (2001) 269.
- [23] L. Zolla, M. Bianchetti, S. Rinalducci, *Eur. J. Biochem.* 269 (2002) 1534.
- [24] D.J. Lundell, A.N. Glazer, R.J. DeLange, D.M. Brown, *J. Biol. Chem.* 259 (1984) 5472.
- [25] R.W. Schoenleber, D.J. Lundell, A.N. Glazer, H. Rapoport, *J. Biol. Chem.* 259 (1984) 5481.
- [26] R.W. Schoenleber, D.J. Lundell, A.N. Glazer, H. Rapoport, *J. Biol. Chem.* 259 (1984) 5485.
- [27] J.O. Nagy, J.E. Bishop, A.V. Klotz, A.N. Glazer, *J. Biol. Chem.* 260 (1985) 4864.
- [28] P.J. Viskari, C.L. Colyer, *J. Chromatogr. A* 972 (2001) 269.
- [29] T.R. Berkelman, J.C. Lagarias, *Anal. Biochem.* 156 (1986) 194.
- [30] J.T. Murphy, J.C. Lagarias, *Curr. Biol.* 7 (1997) 870.
- [31] <http://us.expasy.org/cgi-bin/sprot-search-de?C-phycoerythrin>, on July 18, 2005.
- [32] C.A. Parker, W.T. Rees, *Analyst* 85 (1960) 587.
- [33] *Fluorescence Imaging: Principles and Methods, Technical Manual*, Amersham Pharmacia Biotech, Inc., Piscataway, NJ, 2000.
- [34] R.B. Cole (Ed.), *Electrospray Ionization Mass Spectrometry: Fundamentals, Instrumentation, and Applications*, Wiley, New York, 1997, p. 325.
- [35] *High Performance Liquid Chromatograph Mass Spectrometer LCMS-2010, System User's Guide*, Shimadzu Corporation Analytical Instruments Division, Kyoto, Japan, pp. 4–6.
- [36] C.D. Fairchild, A.N. Glazer, *J. Biol. Chem.* 269 (1994) 28988.
- [37] A.J. Tooley, Y.A. Cai, A.N. Glazer, *Proc. Natl. Acad. Sci. (U.S.A.)* 98 (2001) 10560.
- [38] A.J. Tooley, A.N. Glazer, *J. Bacteriol.* 184 (2002) 4666.
- [39] Y.A. Cai, J.T. Murphy, G.J. Wedemayer, A.N. Glazer, *Anal. Biochem.* 290 (2001) 186.

Table 1. Spectroscopic characteristics and molecular weights of R-PE subunits compared to spectroscopic characteristics and molecular weights of R-PE and its chromophores.

	$\lambda^{max}_{abs} (nm)$	$\lambda^{max}_{ex} (nm)$	$\lambda^{max}_{em} (nm)$	<i>MW (Da)</i>
<i>R-PE</i>	496, 565	496, 565	575	240000
<i>PUB</i>	494	494	505	590.72
<i>PEB</i>	592	592	626	586.69
<i>α subunit</i>	555	544	564	18888
<i>β subunit</i>	496, 555	496, 557	504, 565	20304
<i>γ subunits</i>	496,555	496, 557	504, 565	30168

Molecular mass of R-PE was taken from the literature [5]. Molecular masses of phycobilins were calculated from their molecular formulas. Molecular weight of one of the γ subunits was determined.

Table 2. Signal-to-background ratios in single-molecule experiments.

Subunit	Signal (s)	Background (bg)	Background deviation (d)	(s-bg)/d
R-PE α	15,000	8,600	1,307	4.90
R-PE β	30,000	9,900	1,498	13.42
R-PE γ	20,000	10,770	1,622	5.69

Table 3. Comparison of measured (by HPLC/ESI-MS) and calculated M_r values of phycobiliprotein subunits.

Subunit	R-PE α	R-PE β	B-PE α	B-PE β	APC β
Species of Origin	<i>P. tenera</i>		<i>P. cruentum</i>		<i>A. variabilis</i>
Measured M_r (Da)	18,888	20,304	18,977	20,327	17,847
Calculated M_r (Da)	18,839	20,201	18,990	20,332	17,779

M_r values were calculated from amino acid sequences, phycobilin content, and posttranslational modifications of respective phycobiliprotein subunits found in Swiss-Prot and TrEMBL protein database [7].

Table 4. Sequences of several PEB-containing peptides derived from HPLC/ESI-MS data and Swiss-Prot and TrEMBL protein database [7].

Digest	Retention time (min)	Measured molecular mass (Da)	Calculated molecular mass (Da)	Amino acid sequence
Pepsin digest	38.8	807.324	806.99	PEB-CV
	47.8	820.243	820.99	PEB-CL
	43.0	892.088	892.09	PEB-ACL
Trypsin digest	28.0	1027.322	1027.19	PEB-CYR
	34.8	1173.474	1173.49	PEB-LCVPR
	37.0	1250.406	1250.49	PEB-MAACLR

The molecular mass of PEB chromophore is 586.69 Da. M_r values of peptides were calculated using program PAWS.

FIGURE CAPTIONS

- Figure 1. Structures of four representative phycobilins: phycoerythrobilin (PEB), phycourobilin (PUB), phycocyanobilin (PCB), and phycobiliviolin (PXB).
- Figure 2. HPLC separation of R-PE subunits. Chromatograms were simultaneously recorded by UV-vis PDA detector (top) and spectrofluorometric detector (bottom). Peaks were assigned according to the subunit absorbance spectra (inset). Dotted line represents the HPLC gradient in percentage of acetonitrile with 0.1 %TFA [21].
- Figure 3. (A) Normalized excitation and emission fluorescence spectra of R-PE α subunit recorded by the HPLC spectrofluorometric detector. (B) Normalized excitation and emission fluorescence spectra of R-PE β subunit recorded in a fluorescence spectrometer. The γ subunit fluorescence spectra are same as the β subunit spectra.
- Figure 4. CZE separation of R-PE subunits.
- Figure 5. HPLC separation of chromophore-containing peptides. Chromatograms were simultaneously recorded by UV-vis PDA detector (top) and a spectrofluorometric detector (bottom). Dotted line represents the HPLC gradient in percentage of acetonitrile with 0.1 %TFA (for gradient details see Section 2.3.)
- Figure 6. CZE separation of R-PE pepsin digest.
- Figure 7. Images of R-PE subunits taken by TIRFM. Each spot represents a single molecule.

- Figure 8. SDS-PAGE separation of R-PE, B-PE and APC subunits followed by Coomassie staining (left) and fluorescence detection (right). Da = Dalton.
- Figure 9. HPLC/ESI-MS analysis of R-PE subunits. Dotted line represents the HPLC gradient in percentage of acetonitrile with 3.7 % HCOOH (for gradient details see Section 2.8.). Insets show the mass spectra of α , β and one of γ subunits ($t_R = 17.5$ min).
- Figure 10. HPLC/ESI-MS analysis of B-PE and APC subunits. Dotted line represents the HPLC gradient in percentage of acetonitrile with 3.7 % HCOOH (for gradient details see Section 2.8.)
- Figure 11. (A) Mass spectra and molecular weights of B-PE α and β subunits. (B) Mass spectra and molecular weights of APC α and β subunits. M_r of one out of three determined values for APC α subunit is shown.
- Figure 12. HPLC-ESI-MS analysis of R-PE trypsin digest. Dotted line represents the HPLC gradient in percentage of acetonitrile with 3.7 % HCOOH (for gradient details see Section 2.8.)

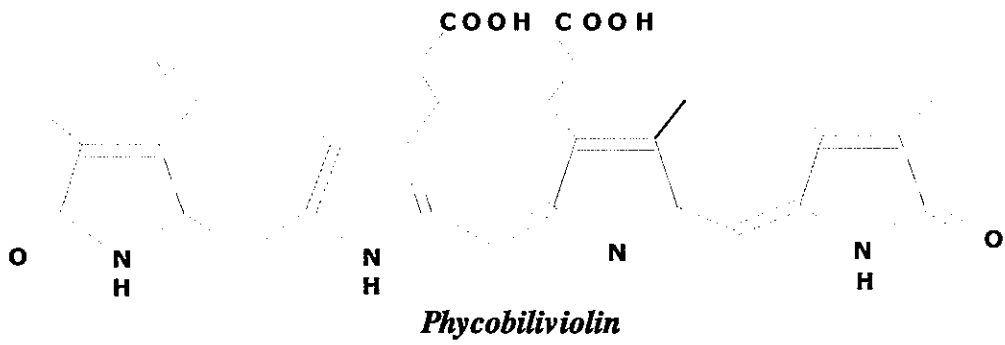
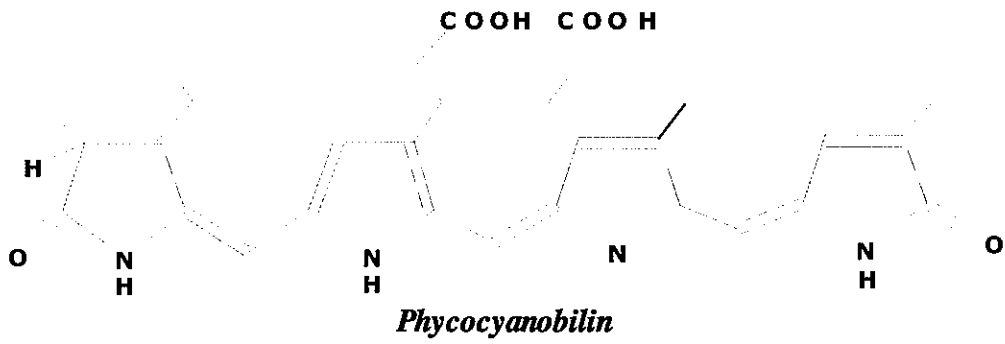
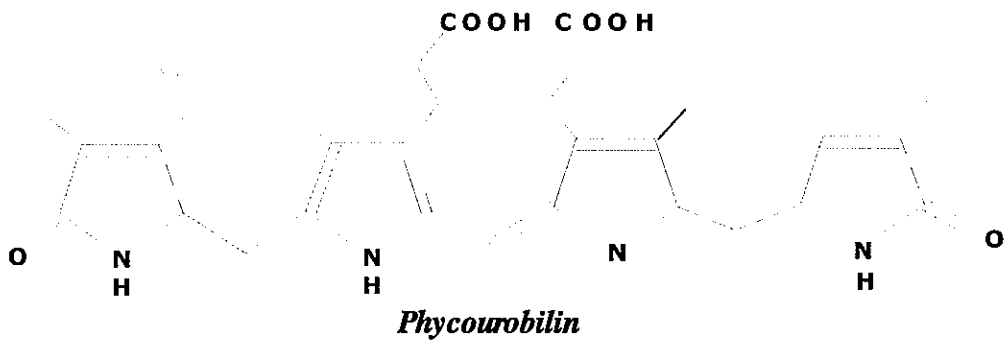
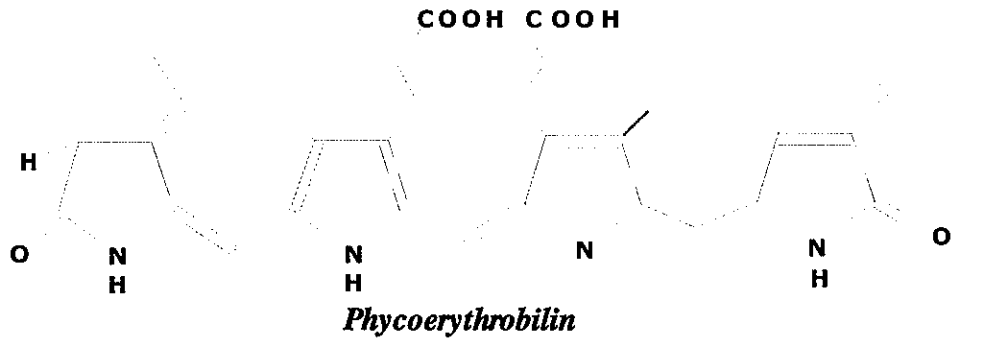


Figure 1.

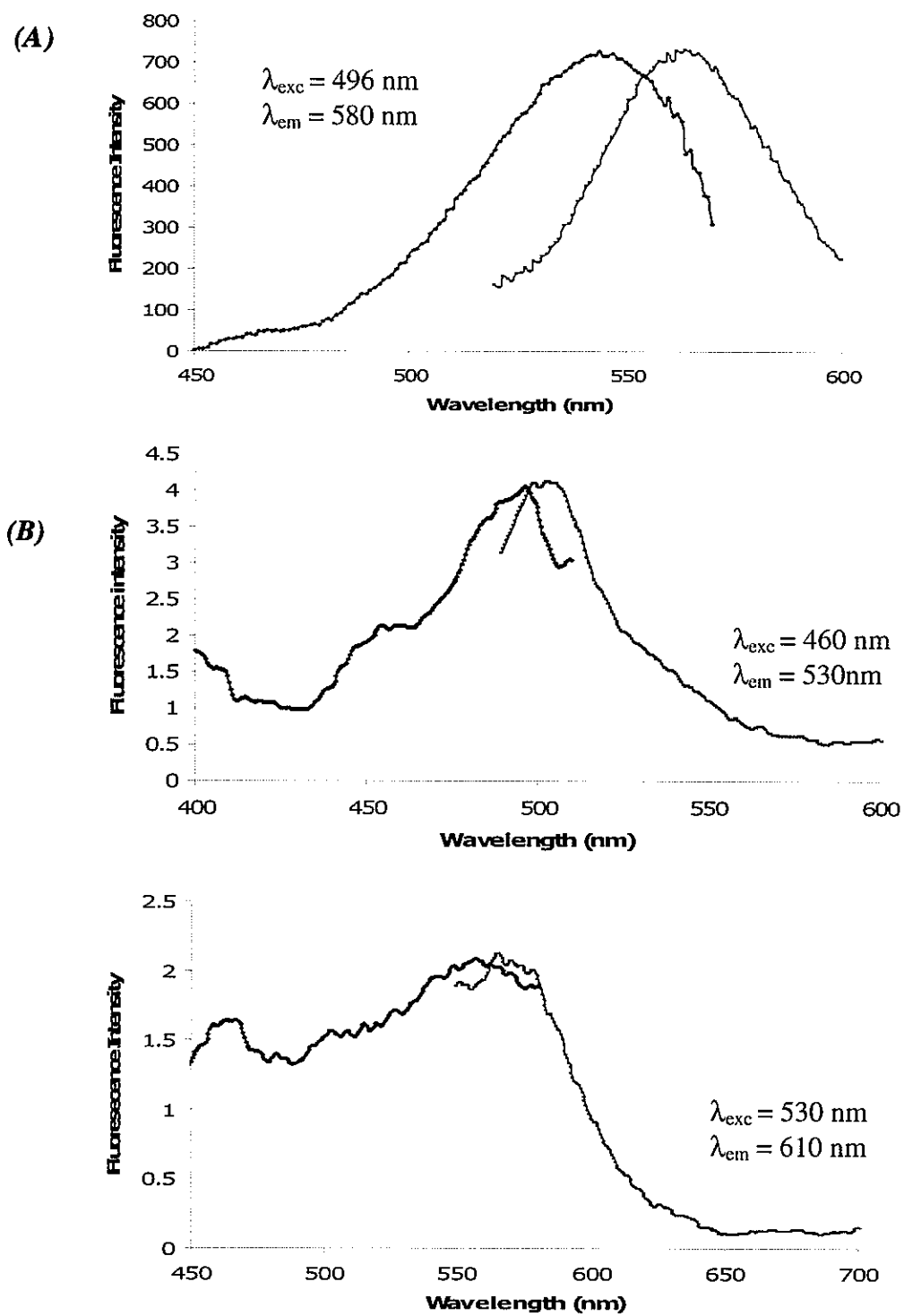


Figure 3.

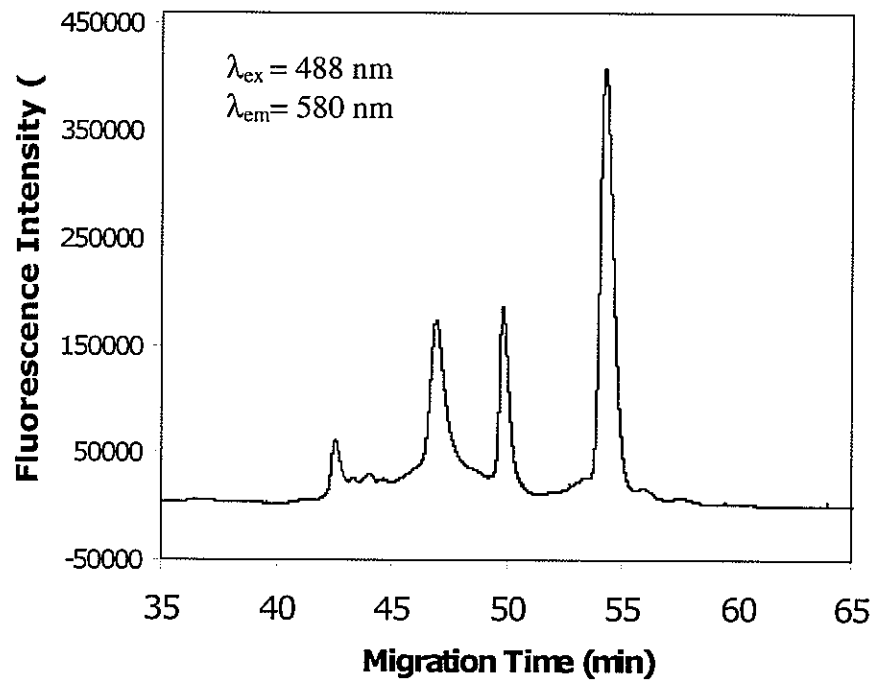


Figure 4.

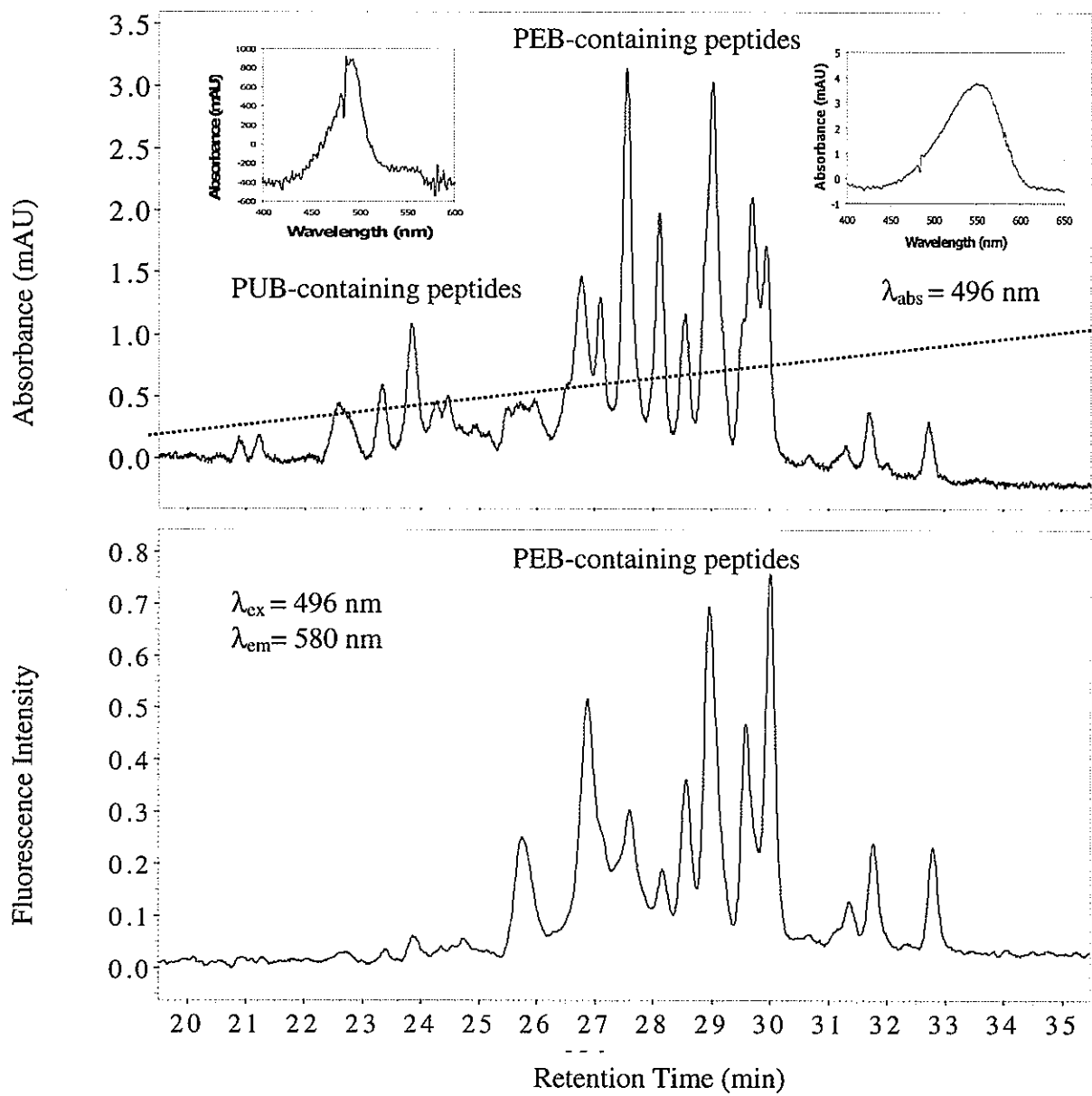


Figure 5.

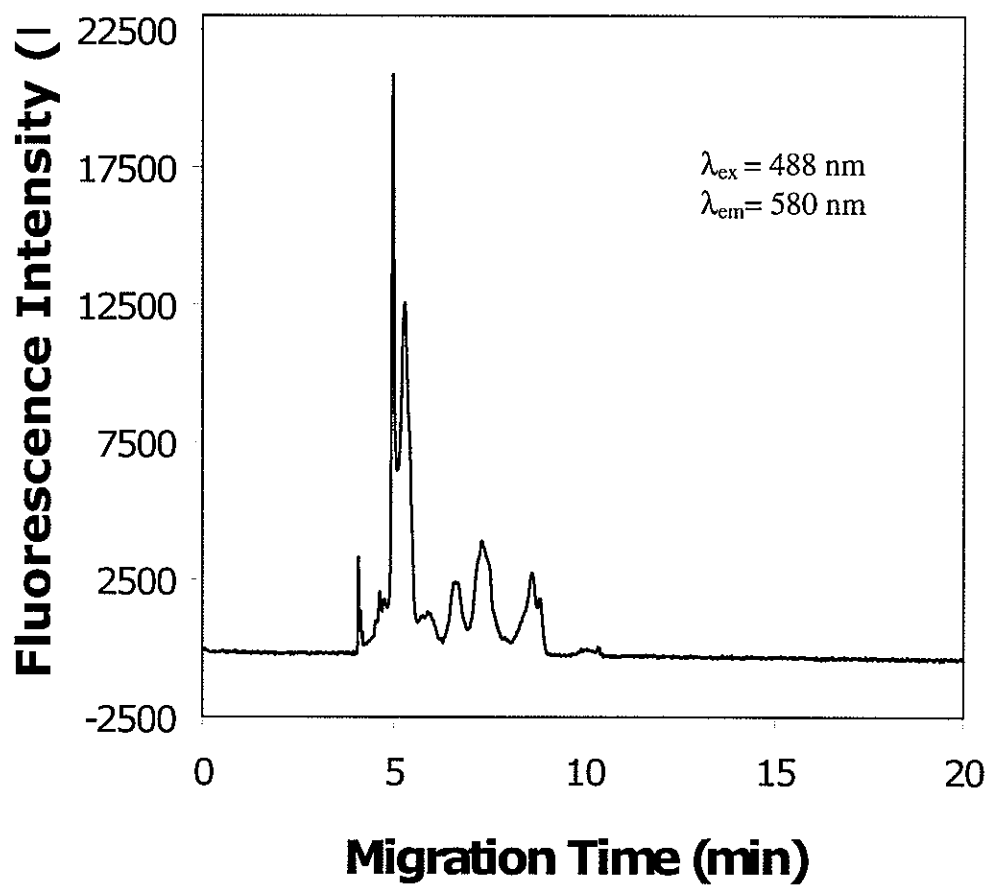


Figure 6.



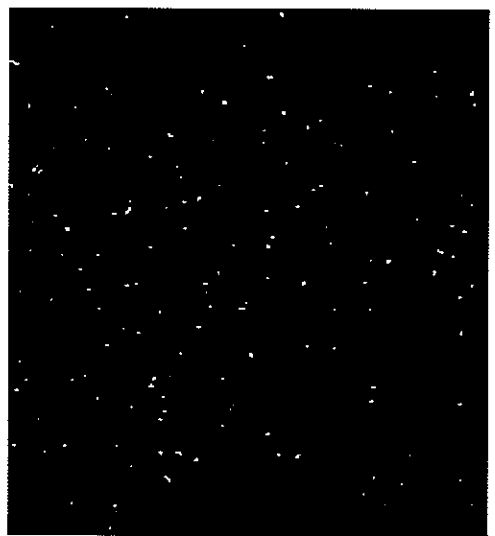
Alpha subunit at pH 9.0



Alpha subunit at pH 2.0



Beta subunit at pH 9.0



Gamma subunit at pH 9.0

Figure 7.

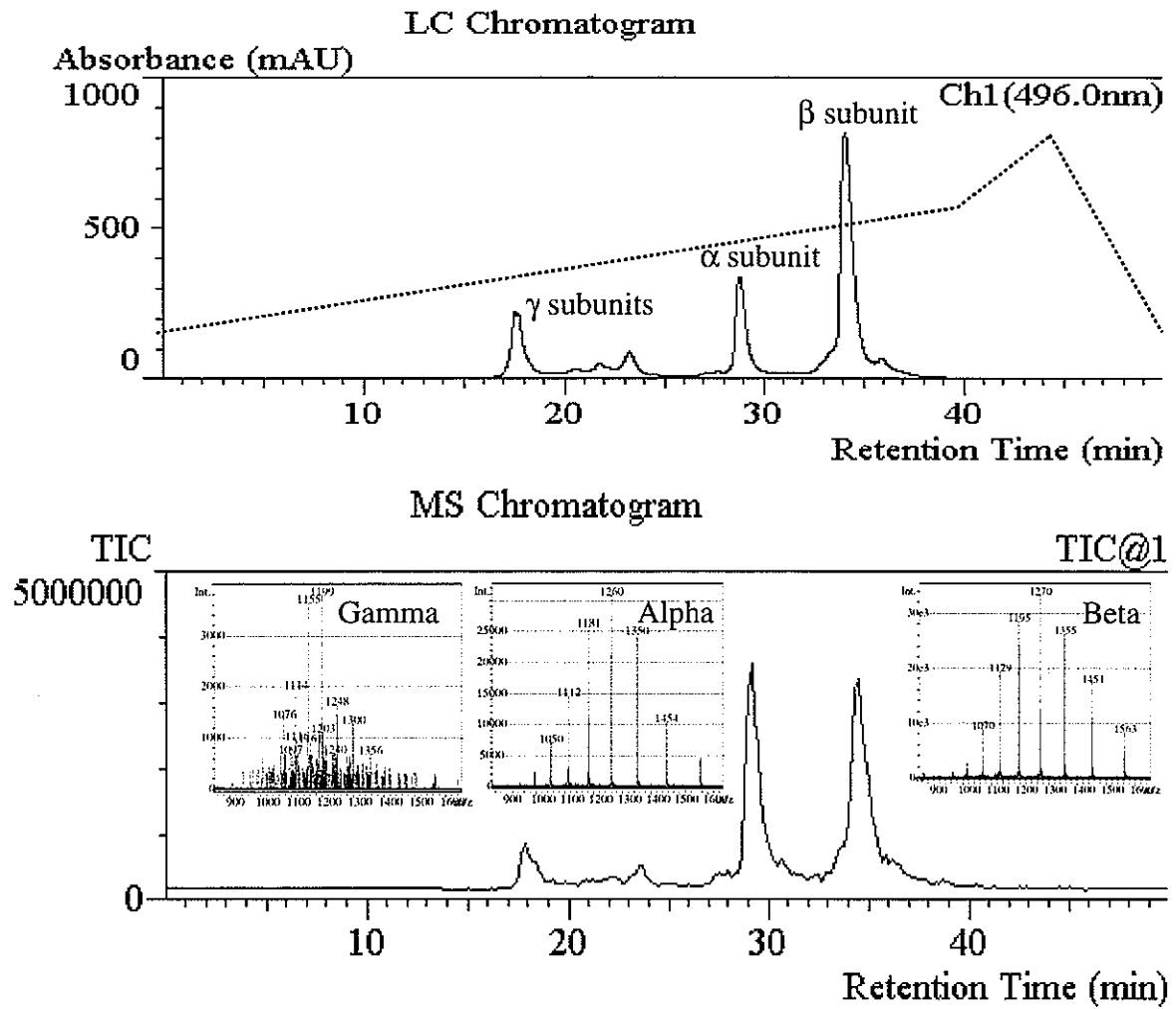


Figure 9.

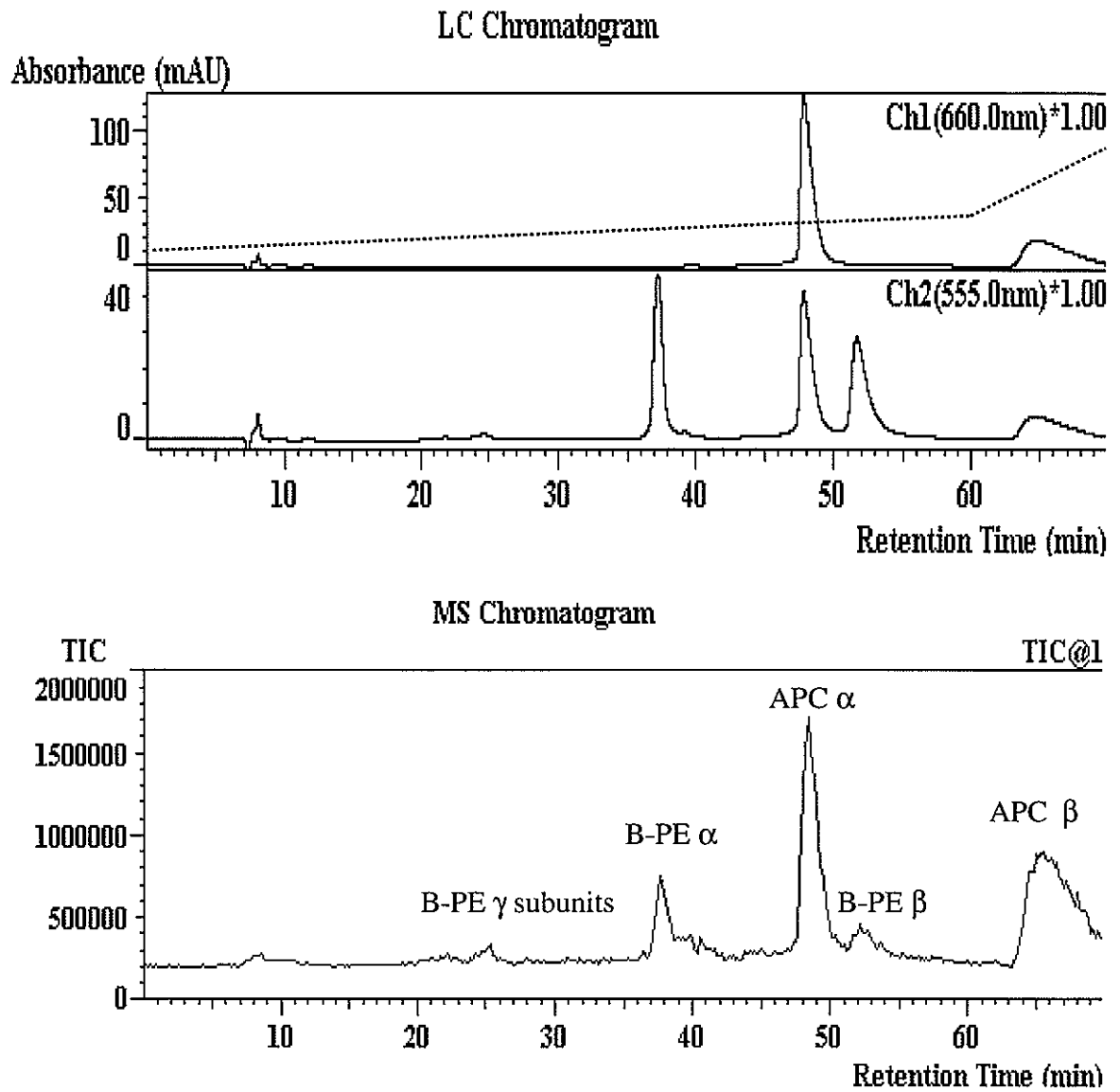


Figure 10.

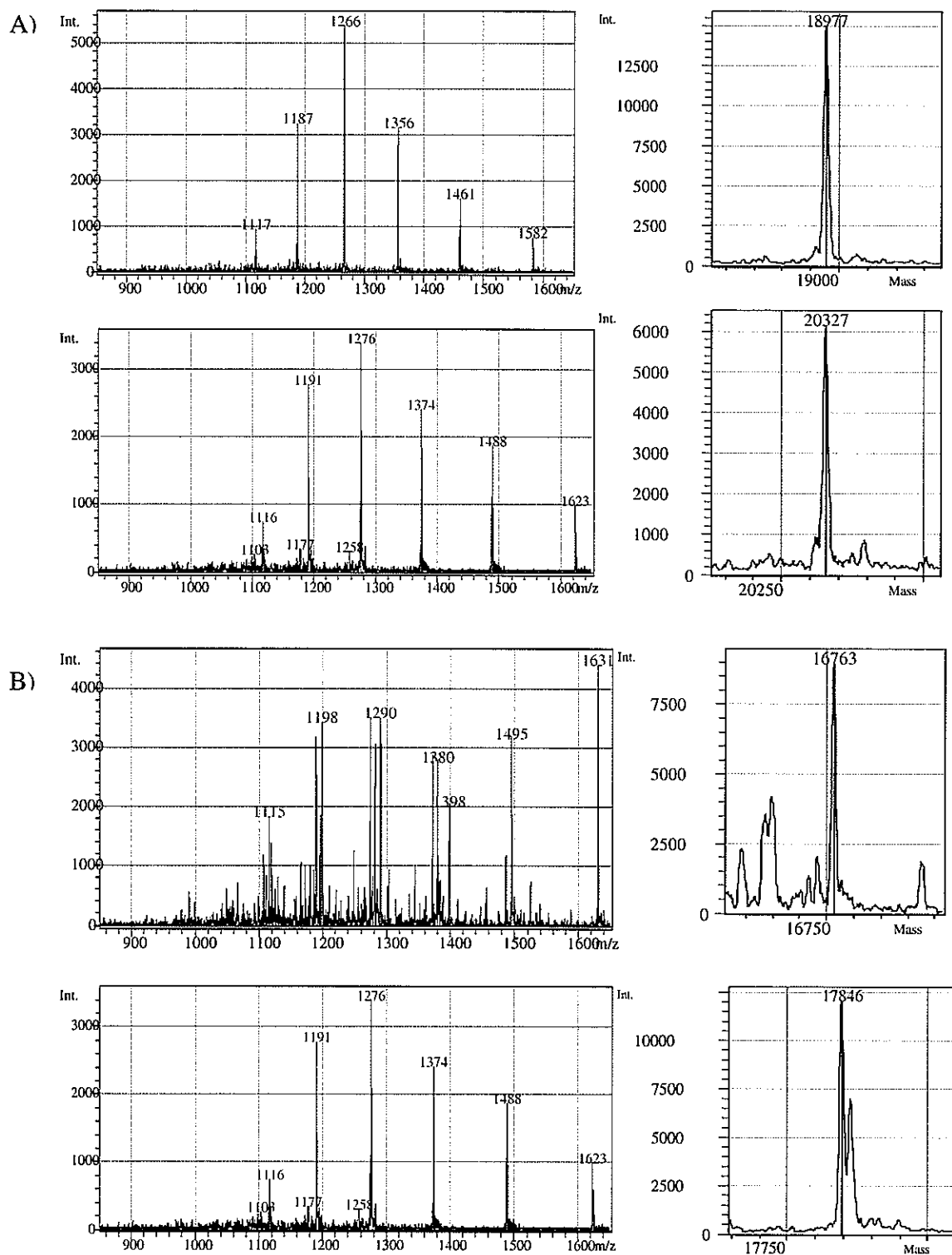


Figure 11.

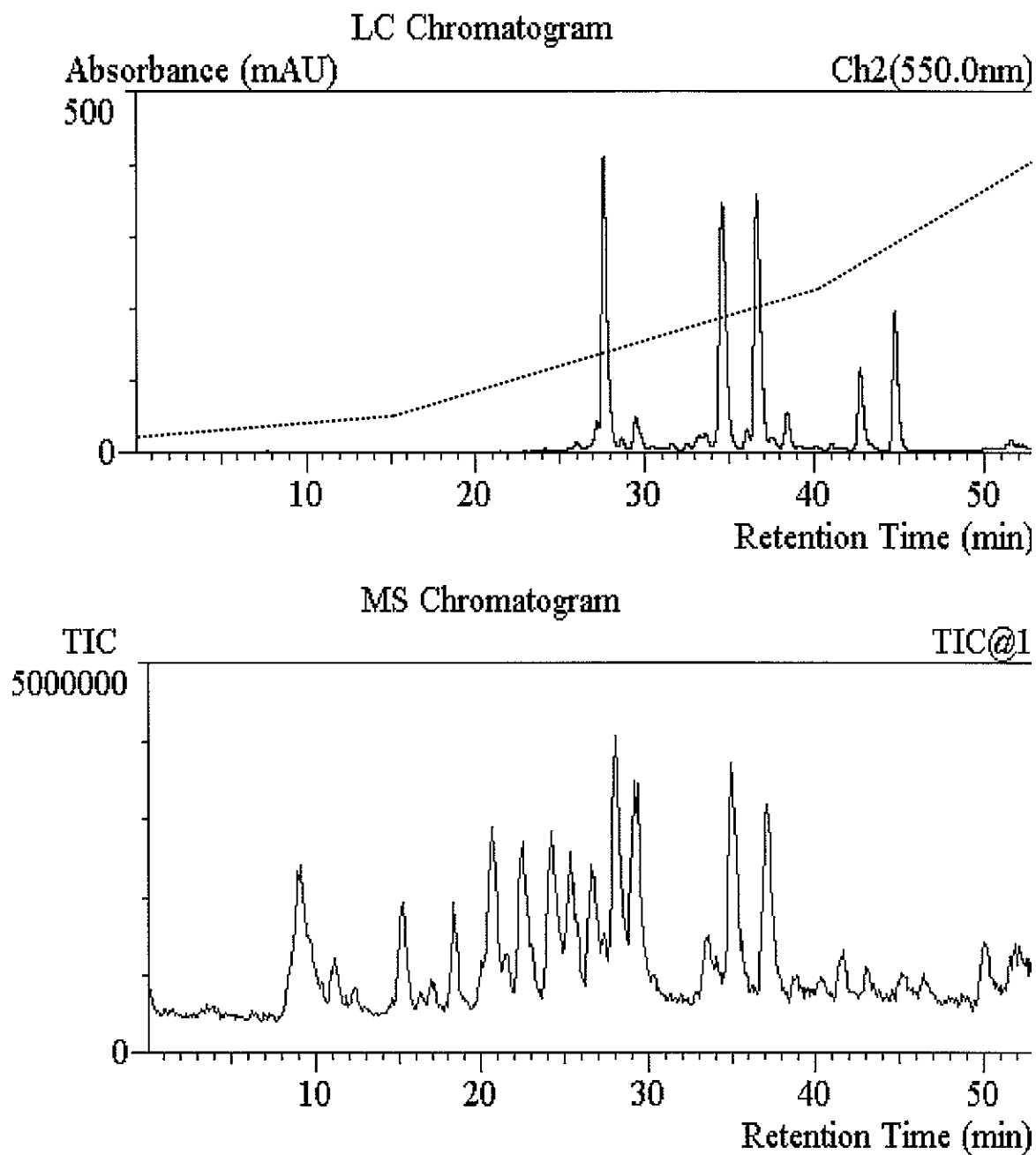


Figure 12.

**CHAPTER 3. FORMATION OF FLUORESCENT PROTEINS BY
NON-ENZYMATIC ATTACHMENT OF PHYCOERYTHROBILIN
TO R-PHYCOERYTHRIN ALPHA AND BETA APO-SUBUNITS
IN VITRO AND IN VIVO (IN ESCHERICHIA COLI)**

A paper prepared for submission to Journal of Biological Chemistry*

Dragan Isailovic, Ishrat Sultana, Gregory J. Phillips, and Edward S. Yeung

SUMMARY

Subunits of phycobiliprotein R-phycoerythrin (R-PE) are highly fluorescent due to phycoerythrobilin (PEB) and phycourobilin (PUB) chromophores that are covalently bound to specific cysteine residues. We explored the possibility for formation of fluorescent subunits by incubation of recombinant R-PE apo-subunits with exogenously supplied PEB. Alpha and beta apo-subunit genes of R-PE from red algae *Polysiphonia boldii* (*P. boldii*) were cloned in plasmids pET-21d (+). His-tagged apo-alpha and apo-beta R-PE subunits were expressed in *Escherichia coli* (*E. coli*) strain BL21(DE3). Although expressed apo-subunits formed inclusion bodies, fluorescent holo-subunits were constituted after incubation of *E. coli* cells with PEB. Holo-subunits contained both PEB and urobilin (UB) chromophores as confirmed by their spectroscopic characterization. Fluorescence and differential interference contrast (DIC) microscopy showed polar location of holo-subunit inclusion bodies in *E. coli* cells. Cells containing fluorescent holo-subunits were several times brighter than control cells as found by fluorescence microscopy and flow cytometry. Addition of PEB to cells did not show cytotoxic effects in contrast to expression of proteins in inclusion bodies. In an attempt to improve solubility, R-PE apo-subunits were fused to cytoplasmic and periplasmic variants of maltose binding protein (MBP) and incubated with

PEB both *in vitro* and *in vivo*. Highly fluorescent soluble fusion proteins were formed containing PEB as the sole chromophore. MBP-R-PE subunit fusions were localized by fluorescence microscopy either throughout the *E. coli* cells or at cell poles. Flow cytometry showed that cells containing fluorescent MBP-fusions were up to ten times brighter than control cells. Results indicate that fluorescent proteins formed by attachment of PEB to expressed apo-subunits of phycobiliproteins could be used as fluorescent probes for analysis of cells by microscopy and flow cytometry. A unique property of these fluorescent reporters is that they work both for properly folded (soluble) subunits and for subunits aggregated in inclusion bodies.

Introduction

Fluorescent proteins with useful spectroscopic properties in the visible region of the spectrum are widely used for analysis of cells and molecules in numerous fluorescence assays (1). Green fluorescent protein (GFP) and its variants have made a significant impact on cell biology as *in vivo* reporters of protein localization and gene expression (1, 2). Novel and improved fluorescent protein probes will increase the repertoire of available fluorescent labels, and contribute to new discoveries about cell structure and function (3).

Phycobiliproteins, including R-phycoerythrin (R-PE), are highly fluorescent proteins with absorption coefficients and quantum yields that are superior compared to other fluorescent proteins (1, 4). These proteins are found in nature as components of the photosynthetic apparatus in cyanobacteria, red algae and cryptomonads. They have proven valuable fluorescent probes in flow cytometry and immunofluorescence microscopy (4, 5). Subunits of phycobiliproteins are also highly fluorescent (6, 7). The fluorescence of phycobiliproteins and their subunits results from covalently bound phycobin chromophores. Phycobilins are tetrapyrrole compounds bound to specific cysteines of phycobiliproteins by either single or double thioether bonds (1, 4). For example, subunits of R-PE, whose structure has been described as $(\alpha\beta)_6\gamma$, are highly fluorescent due to covalently bound phycoerythrobilin (PEB) and phycourobilin (PUB) chromophores (1, 4, 7).

Recombinant proteins that retain the excellent fluorescence properties of phycobiliproteins are highly desirable fluorescent probes (8-10). Although phycobilin

chromophores are not genetically encoded such as the chromophore of GFP, there are ways to form phycobilin chromophores and attach them to apo-subunits of phycobiliproteins *in vivo*. The first approach is based on the use of enzymes that will form and attach phycobilin chromophores to recombinant apo-subunits (8). Phycobilin 3Z-phycoerythrin (3Z-PCB) is formed from heme through two enzymatic reactions that are mediated by heme oxygenase and PCB ferredoxin reductase, and include biliverdin IX α as an intermediate product (11-14). 3Z-PCB is further isomerized to native chromophore of C-phycoerythrin (C-PC) 3E-PCB, and attached to apo-subunits of C-PC by heterodimeric cpcE + cpcF lyase/isomerase (8, 15). Also, 3Z-PCB can be isomerized to phycobiliviolin (PXB), which is the native chromophore of protein phycoerythrocyanin (PEC), and further attached to PEC apo-subunits by enzyme PecE + PecF lyase/isomerase (9). Expression of these enzymes in *E. coli* along with apo-alpha subunits of C-PC and PEC lead respectively to complete biosynthesis of fluorescent holo-alpha subunits of C-PC and PEC *in vivo* (8, 9). Another enzymatic approach included expression of fusion proteins between C-phycoerythrin apo-subunits and specific tags in cyanobacterium *Anabaena* sp. PCC7120 (10). Chromophore attachment happened *in vivo* and yielded fluorescent proteins that were readily purified and usable as fluorescence labels. Both of these enzymatic approaches yielded fluorescent recombinant phycobiliprotein subunits *in vivo*.

Non-enzymatic (autocatalytic) attachment of phycobilins to genetically expressed apo-subunits of phycobiliproteins is also possible since phycobilins can be isolated and purified from phycobiliproteins after reflux in methanol (14, 15). Attachment of phycobilins to recombinant apo-phycobiliproteins from cyanobacteria has been investigated only *in vitro*. This process yielded fluorescent isomeric products with distinct spectral characteristics, and did not show specificity of enzymatic binding *in vivo* (14). PCB binds *in vitro* to expressed apo-subunits ($\alpha\beta$ monomer) of C-PC and forms phycobilin mesobiliverdin (MBV) (16, 17). PEB also binds for $\alpha\beta$ monomer of C-PC and forms not only PEB adduct but also transforms during attachment into 15, 16-dihydrobiliverdin (DBV) (18). Products of *in vitro* attachment of PEB to apo-alpha subunit of C-phycoerythrin (C-PE) include covalently bound PEB, DBV and urobilin (UB) (19). After prolonged sonication of apo-subunits located in inclusion

bodies incubation of apo-alpha subunit of phycoerythrocyanin with PCB and PEB yielded PCB and PEB adducts, respectively (15).

In contrast to binding of PEB to recombinant phycobiliproteins from cyanobacteria, PEB can bind to plant phytochrome apoproteins both *in vitro* and *in vivo* (in *Arabidopsis thaliana*) without change in the conformation of the chromophore (20). Phytochromes are photoreceptor proteins responsible for light morphogenesis in plants, and originally contain low-fluorescent phytochromobilin chromophore (1). PEB attachment to phytochrome apoproteins yields highly fluorescent products so called phytofluors (20). PEB, which is a low fluorescent compound, showed roughly 500-1500-fold increase in brightness after binding to apophytochrome protein. These results indicate that it will be of great interest to find recombinant apo-phycobiliproteins such as phytochromes that will be able to bind PEB chromophore and form highly fluorescent proteins.

The attachment of phycobilins to recombinant subunits of R-PE has not been explored thus far. A study that would involve non-enzymatic attachment of PEB and/or PUB to apo-subunits of R-PE from red algae would be very beneficial in two reasons. It could support greatly the eventual characterization of enzymes involved in formation and binding of these chromophores to R-PE apo-subunits in red algae. It is believed that mechanisms of PEB and PUB *in vivo* formation and attachment to apo-subunits of phycobiliproteins are enzymatic as supported by discovery of lyases involved in PEB attachment to the apo-alpha subunit of cyanobacterial C-PE (21). Moreover, fluorescent phycobiliproteins formed by external addition of isolated phycobilins to the genetically expressed apo-phycobiliproteins could represent useful fluorescent probes. We tested possibility for formation of fluorescent proteins upon incubation of recombinant apo-subunits of R-PE with PEB chromophore. Starting from the known sequence of the genes encoding alpha and beta apo-subunits of R-PE from red algae *P. boldii* (22), we cloned and expressed these genes in *E. coli*. R-PE apo-subunits were also fused to periplasmic and cytoplasmic versions of *E. coli* maltose binding protein (MBP). After expression of proteins our goal was to check binding specificity of PEB to apo-subunits and apo-subunit fusions both *in vitro* and *in vivo* (in *E. coli*), and characterize and localize potential fluorescent holo-subunit products in cells.

Materials and Methods

Cloning of apo-subunit genes and expression of His-tagged R-PE apo-subunits – Red algae *P. boldii* was grown in ES-enriched seawater medium (UTEX the Culture Collection of Algae, University of Texas, Austin, TX). *P. boldii* DNA was isolated from algae by DNeasy Plant Mini Kit (Qiagen INC., Valencia, CA) using manufacturer protocol. Hot Start Taq DNA Polymerase PCR kit (Qiagen) was used for polymerase chain reaction (PCR). Primers used to amplify alpha subunit gene were: 5'-ATG AAA TCA GTT ATT ACT ACA ACA ATA AGT GC-3' and 5'-GCT TAA AGA GTT AAT TAA GTA ATC TAG TGC-3'. Primers used to amplify beta subunit gene were: 5'-ATG CTT GAC GCA TTT TCT AGA GTT GTA GT-3' and 5'-ACT AAC AGC AGC AAC AAC TCT ATC GCA-3'. PCR was started at 95⁰C during 15 min. Thirty PCR cycles were conducted by using the following program: 95⁰C for 30 s, 55⁰C for 30 sec, and 72⁰C during 1min. In the end, samples were heated at 95⁰C during 10 min, and cooled down at 4 C⁰. PCR products were separated by electrophoresis on 0.8 % agarose gel using a standard procedure. Products were ligated separately in pBAD-TOPO plasmid using pBAD-TOPO TA Expression Kit (Invitrogen, Carlsbad, CA). These plasmids were further transformed in *E. coli* strain DH5 α and LMG194. Plasmids were isolated, and their sequences were confirmed by DNA sequencing (ISU DNA Facility). His-tagged subunits were expressed by L-arabinose according to manufacturer procedure, and analyzed by SDS-PAGE. The expression yielded a small amount of His-tagged subunits detected only by Western blotting using Opti-4CN colorimetric detection kit (Bio-Rad, Richmond, CA). Subunit genes (including His tags) were cut from pBAD-TOPO plasmids by *Sca* I and *Nco* I enzymes, and ligated separately in plasmids pET – 21d (+) (Novagen, Madison, WI). Resulting plasmids were transformed in *E. coli* strain BL21(DE3) (Novagen). Plasmids were isolated, and their sequences confirmed by DNA sequencing (ISU DNA Facility). Apo-subunit expressions were induced by 1mM isopropyl β -D-thiogalactopyranoside (IPTG) according to manufacturer protocol (Novagen). Induction was omitted in control cells. Cells were further incubated with PEB or used for protein isolation according to procedures described below.

Expression of MBP-R-PE subunit fusions – Genes for R-PE alpha and beta apo-subunits were cut from pET plasmids using *Bam*H I and *Sca* I, and ligated separately into pMAL-p2X and pMAL-c2X vectors that contain genes for cytoplasmic and periplasmic versions of MBP, respectively (New England Biolabs, Beverly, MA). Fusion proteins under control of pTAC promoter were expressed after expression induction with IPTG. Cells were further incubated with PEB or used for isolation of fusion proteins according to procedures shown below.

Apo-subunit purification – Either mini Bead Beater and glass beads (BioSpec Products INC, Bartlesville, OK) or guanidinium lysis buffer and an ultrasonic processor (Sonics, Newton, CT) were used for lysis of *E. coli* cells. His-tagged R-PE apo-subunits were isolated from bacterial cells under denaturing conditions using ProBond™ Protein Purification System and the manufacturer protocol (Invitrogen). Subunits were eluted in denaturing elution buffer (8 M Urea, 500 mM NaCl, 20 mM sodium phosphate, pH 4.0). Expressions of subunits were checked by SDS-PAGE on a mini gel (Bio-Rad). Isolations under native conditions using both ProBond Protein Purification System (Invitrogen) and Qiagen “super flow” Ni²⁺-nitrilotriacetic acid agarose (8) were tried as well.

PEB purification - PEB was the generous gift of Dr. Hugo Scheer and Dr. Max Storf (University of Munich, Germany) (15).

Holo-subunit reconstitution in vitro – Apo-subunit solutions in denaturing elution buffer (500 µl) were incubated with 25 µl of 27.0 µM PEB solution in DMSO at room temperature overnight. Incubations of cell lysates in Tris-HCl buffer (pH 8.2) were also used. Holo-subunit presence in samples was checked as described in the following section.

Holo-subunit reconstitution in vivo - *E. coli* cells were washed in PBS buffer and incubated with shaking in 10 ml of the same buffer containing 100 µl of 33.7 µM PEB solution in DMSO at 25^oC overnight. Control cells were treated in the same way. Holo-subunit formation was checked after cell lysis by SDS-PAGE using fluorescence gel imaging (Typhoon, Amersham Pharmacia Biotech, Piscataway, NJ) and Coomassie staining (7). A 532 nm laser and 580 nm band pass filter were used during fluorescence imaging. R-PE (Invitrogen Molecular Probes, Eugene, OR) was loaded on the gel as a standard fluorescent sample. Visible fluorescence of samples was observed and photographed after illumination through the UV transilluminator FOTO/UV 21 (Fotodyne, Hartland, WI).

Holo-subunit purification - His-tagged R-PE holo-subunits were isolated from bacterial cells under denaturing conditions using ProBond Protein Purification System (Invitrogen) according to the manufacturer protocol. Holo-subunits were eluted in denaturing elution buffer. In addition, fluorescent inclusion bodies were isolated using B-PER Bacterial Protein Extraction Reagent (Pierce Biotechnology, Rockford, IL). Inclusion Body Solubilization Reagent (Pierce) was used for solubilization and refolding of inclusion bodies.

Purification of MBP-R-PE subunit fusions – Purification of fusion proteins was done by affinity chromatography on amylose resin and the manufacturer protocol (New England Biolabs). Proteins were eluted in maltose elution buffer (10 mM maltose, 1 mM EDTA, 20 mM NaCl, 20 mM Tris-HCl buffer, pH 7.4).

PEB attachment to MBP-R-PE subunit fusions in vitro –MBP-fusion solutions (500 μ l) in maltose elution buffer were incubated with 25 μ l of 27.0 μ M PEB solution in DMSO at room temperature overnight. Control solution contained 500 μ l of maltose elution buffer and 25 μ l of 27.0 μ M PEB solution in DMSO.

PEB attachment to MBP-R-PE subunit fusions in vivo – The procedure used was the same as described for *in vivo* reconstitution of holo-subunits.

Digital photography – Images of protein solutions and cells containing recombinant proteins were recorded by Nikon COOLPIX 5000 digital camera (Nikon, INC., Tokyo, Japan).

Preparation of microscope slides - Cells were washed three times and appropriately diluted with PBS buffer. Seventy five μ l of the cell suspensions was spread on poly-L-Lysine treated cover glasses and incubated for 45 minutes. Cells were fixed immediately in 4% paraformaldehyde for 30 minutes. Cover slips were washed three times five-minute each in PBS buffer, and mounted on a glass microscope slides using n-propyl gallate mounting medium. The cover slip was sealed around the edges with a nail polish.

Microscopy - DIC and fluorescence imaging of cells containing inclusion bodies was done by Zeiss Axioplan 2 upright microscope (Carl Zeiss, INC., Thornwood, NY). A 100 X PlanFluor immersion oil objective with numerical aperture (NA) of 1.3 was used in both imaging modes. A dry turret condenser (NA = 0.9) was used for DIC microscopy. DAPI, FITC, TRITC and triple DAPI/FITC/TRITC filter sets were used for fluorescence

microscopy. Images were acquired by AxioCam HRc CCD camera with AxioVision software (Carl Zeiss).

DIC and fluorescence imaging of cells containing MBP-R-PE subunit fusions was done by Nikon Eclipse 80i upright microscope. 100X PlanApo oil objective with numerical aperture (NA) of 1.4 was used in both imaging modes. An oil condenser (NA = 1.4) was applied for DIC microscopy. A TRITC filter set was used for fluorescence microscopy. Magnification was optionally increased with 2X zoom lens in front of the CCD camera. Images were acquired by Micromax CCD camera and WinView 32 imaging software (Roper Scientific, Trenton, NJ).

Flow cytometry - *E. coli* cells were washed three times and appropriately diluted with PBS buffer. Cell suspensions were measured for fluorescence on a Guava PCA flow cytometer (Guava Technologies, Hayward, CA) equipped with a single 532 nm diode laser. Fluorescence was detected using PMT1 in conjunction with a 580 nm band-pass filter. An electronic gate was set around *E. coli* cells based on their forward scatter properties. Up to 10,000 gated events per sample were collected and stored in list mode files. Analysis was performed with FlowJo software (Tree Star, Ashland, OR), displaying forward scatter-gated data in single parameter histograms of logarithmic fluorescence.

Cell viability assay - Cell viability test was done by flow cytometer EPICS ALTRA (Beckman Coulter INC, Fullerton, CA). Two sets of samples were prepared. First set contained cells with and without expressed apo-subunits incubated with the PEB. Second set contained cells with and without apo-subunits not incubated with PEB. Cells were stained with dyes propidium iodide (PI) and Syto-9 (Invitrogen Molecular probes). In the case of cells stained with PI fluorescence was excited with 488 nm laser and detected by 580 nm band pass filter. Fluorescence of the cells stained with Syto-9 was excited at 488 nm and detected by a 520 nm band pass filter. In addition cells fixed with 2% paraformaldehyde were stained and analyzed as above.

Fluorescence spectroscopy - A luminescence spectrometer LS50B (Perkin-Elmer, Beaconsfield, UK) was used to measure fluorescence spectra of protein and PEB solutions in increments of 0.5 nm. Widths of the excitation and emission slits were set at 10 nm.

RESULTS

Cloning and expression of R-PE apo-subunits - DNA from red algae *P. boldii* was isolated and used as the PCR template to amplify genes that code alpha and beta apo-subunits of R-PE. The sizes of these genes were close to their predicted length of 492 bp and 531 bp respectively as confirmed by agarose gel electrophoresis (22). Genes cloned in pBAD-TOPO plasmids were transformed in *E. coli* strains DH5 α and LMG194. Expression from cells harboring pBAD-TOPO plasmids yielded a low amount of apo-subunits that were detected only by Western blotting. Much higher amounts of apo-subunits were expressed using the plasmid pET - 21d (+) in BL21(DE3) as shown by SDS-PAGE (Fig. 1A). The higher expression from T7lac promoter was consistent with the higher rate of transcriptional initiation in comparison to the *araBAD* promoter. Sequences of the inserts in the pET plasmids showed no differences to that reported by Roell et al for the apo-beta subunit, while an alanine residue was found in place of threonine at position 124 of the apo-alpha subunit (22). From the predicted amino-acid sequences His-tagged apo-subunits should have molecular weights of approximately 22.3 kDa and 23.2 kDa. The molecular weights of the subunits analyzed by SDS-PAGE were close to these values (Fig. 1A).

Attachment of PEB to R-PE apo-subunits - A very low amount of His-tagged R-PE apo-subunits was isolated under native conditions because they precipitated in the pellet after cell lysis. It was possible to isolate high amount of apo-subunits, however, under denaturing conditions indicating aggregation of subunits in inclusion bodies. After incubation of isolated apo-subunits with PEB *in vitro* very low levels of fluorescent subunits were detected by SDS-PAGE and fluorescence imaging. Deposition of apo-subunits in inclusion bodies and their low solubility under native conditions prevented an assay of PEB binding to R-PE apo-subunits *in vitro*. However, fluorescent holo-subunits were formed *in vivo* upon incubation of cells containing apo-subunits with PEB. Fluorescence of holo-subunits was shown by fluorescence imaging after SDS-PAGE (Fig. 1B, lanes 4 and 6). Control cells that contained pET plasmids showed presence of a very low amount of fluorescent holo-subunits after incubation with PEB (Fig. 1B, lanes 5 and 7). This could be attributed to the autocatalytic induction of the T7lac promoter. Cells that were not incubated with PEB did not show the

presence of fluorescent proteins (Fig. 1B, lanes 2 and 9). The color of *E. coli* cells containing apo-subunits was pink after incubation of cells with PEB chromophore indicating the formation of holo-subunits *in vivo* (Fig. 2A). In addition, intensive orange fluorescence was observed from these cells after exposure to UV irradiation.

Spectroscopic characterization of holo-subunits - The color of holo-subunits isolated from *E. coli* cells was pink as well (Fig. 2B). Chromophore binding did not increase the solubility of inclusion bodies so that holo-subunits were also isolated under denaturing conditions. Fluorescent spectra of R-PE holo-subunits were recorded in cells and after isolation of holo-subunits under denaturing conditions (23). Fluorescence and absorption maxima of holo-subunits are shown in Table 1. They were the same for both alpha and beta holo-subunits. Excitation maximum at 495.0 nm and emission maximum at 506.5 nm show that holo-subunits contain urobilinoid chromophore that could be either UB or PUB (Fig. 3A). Excitation maxima at 542.5 nm and 573.0 nm and emission maxima at 569.5 nm and 581.5 nm correspond to holo-subunits containing PEB (Fig. 3B). Absorption spectrum of isolated holo-subunits showed a maximum at 496.0 nm corresponding to UB and another maximum at 552.0 nm corresponding to PEB. UV induced orange fluorescence of cells might be attributed to an excitation peak of covalently bound PEB at 308 nm. This peak was overlapped in excitation fluorescence spectrum with a more intensive excitation peak of proteins at 280 nm.

Localization of holo-subunits in E. coli - We used DIC and epi-fluorescence microscopy to localize and check fluorescence properties of holo-subunits in *E. coli* cells. Cells with holo-subunits contain inclusion bodies usually on one of their poles, as shown by DIC (Fig. 4A and 5A). Polar location of inclusion bodies is also shown by superposition of native fluorescence of cells and fluorescence from holo-subunits by using the triple DAPI/FITC/TRITC filter cube (Fig. 4B and 5B). These inclusion bodies are intensively orange fluorescent as shown by fluorescence microscopy using a TRITC filter cube (Fig. 4C and 5C). Holo-subunit fluorescence was also detected with filters specific for FITC and phycoerythrins what is in agreement with fluorescence spectra of holo-subunits. Control cells did not show evidence of inclusion bodies when analyzed by DIC and fluorescence microscopy (Fig. 4D-F and Fig. 5D-F). Low fluorescence was noticeable from control cells

with improve of image contrast, but visually the intensity of fluorescence from control cells was much lower than fluorescence of cells containing holo-subunits (Fig. 4 and Fig. 5, panels C and F).

Flow Cytometry - To measure quantitatively the fluorescence ratio between cells containing holo-subunits and control cells flow cytometry was used. Distribution of fluorescence intensities for ten thousand cells showed noticeably higher fluorescence of induced cells (Fig. 6). As shown in Table 2 cells containing holo- α and holo- β subunits were in average 5.2 and 2.6 times brighter than control cells. Control cells showed fluorescence that was on average 1.3 times higher than fluorescence of cells that were not incubated with PEB (data not shown).

In a flow cytometry viability assay, each sample showed increased green fluorescence in the case of cell staining with the dye Syto-9, which labeled both dead and live cells. After staining with PI cells without expressed subunits showed a fraction of live cells and a fraction of dead cells. When these cells were killed by fixation in para-formaldehyde they did not show any fluorescence. Even without fixation in para-formaldehyde, cells expressing apo or holo-subunits failed to show any fluorescence after incubation with PI. From these results we concluded that cells containing apo or holo-subunits overexpressed in inclusion bodies were dead, cells without overexpressed subunits remained alive, while PEB addition was not toxic to cells.

Attachment of PEB to MBP-R-PE apo-subunit fusion proteins in vivo - To increase their solubility, R-PE apo-subunits were fused to cytoplasmic and periplasmic variants of MBP forming fusion proteins with molecular weights of ~ 65 kDa. Expression of fusions between cytoplasmic MBP and R-PE subunits produced high yield of soluble fusion proteins that were isolated by affinity chromatography under native conditions (Fig. 7). Fluorescent fusion proteins were isolated from the cells that were incubated with PEB *in vivo* (Fig. 7B). Isolated fluorescent subunits showed fluorescence excitation maximum at 577.5 nm and emission maximum at 584.0 nm (Fig. 8 and Table 3) indicating formation of PEB-containing fusion proteins. Periplasmic MBP was fused to apo-alpha subunits of R-PE and also yielded highly fluorescent proteins. Cells containing fluorescent fusions were differentiated from control cells by pink color and intense fluorescence under UV illumination (Fig. 9). After induction

E. coli cells with both normal and elongated morphology were observed by DIC microscopy (Fig. 10A). DIC microscopy did not reveal presence of inclusion bodies in normal cells. Fluorescence was located throughout these cells indicating that R-PE subunit fusions with MBP are located in the cell cytoplasm (Fig. 10B). Elongated cells showed fluorescence throughout cells as well as at cell poles revealing presence of both soluble fusion proteins located in cytoplasm and insoluble fusion proteins located in inclusion bodies. These cells were brighter than cells that were regular in shape as shown by fluorescence microscopy (Fig. 10B). The presence of two subpopulations among cells containing periplasmic MBP fusions was also observed by flow cytometry indicating good correlation between single-cell microscopy and population-based flow cytometry analysis (Fig. 11). Flow cytometry also revealed that cells containing periplasmic MBP-alpha subunit fusions are up to 10 times brighter than control cells (Table 4).

Attachment of PEB to MBP-R-PE apo-subunit fusion proteins in vitro - MBP-R-PE subunit fusions also bound PEB chromophore *in vitro* and formed highly fluorescent adducts. Fluorescence spectra of solutions containing PEB showed the excitation maximum around 525 nm, the emission maximum at 579.0 and emission shoulder around 625 nm (Fig. 12A and Table 5). Solutions containing MBP-R-PE subunit fusions and PEB also showed an excitation maximum around 525 nm and another intensive excitation maximum at 574.5 nm (Fig. 12B). Fluorescence emission spectrum of MBP-subunit fusions showed a peak at 585.5 nm and a shoulder around 625 nm (Fig. 12B and Table 5). These results confirmed that attachment of PEB to MBP-R-PE subunit fusions both *in vitro* and *in vivo* yielded fluorescent proteins that contained PEB chromophore with the excitation fluorescence maximum around 575 nm and emission fluorescence maximum around 585 nm. Although the same settings were used for fluorescence spectra measurement, the intensity of emission from MBP-subunit fusions was much higher than in the case of PEB solution (Fig. 12). In addition, the strong orange fluorescence of solutions containing subunit fusions was visualized while the fluorescence of solutions containing PEB was unnoticeable after UV illumination (Fig. 13).

DISCUSSION

Here we report on the cloning and expression of fluorescent proteins that are formed by highly specific attachment of PEB to recombinant apo-subunits of R-PE and their fusions with MBP. Although R-Phycoerythrin is highly fluorescent protein that has proven extremely useful in many bioanalytical applications, the large size of this 240-kDa trimeric protein poses problems, such as steric effects, than restrict its use for labeling of cells and molecules. The cloning and expression of such a complex protein in cells would be very difficult. Our approach to overcome these difficulties is to deal with individual R-PE subunits.

We cloned the apo-subunit genes of R-PE from red algae *P. boldii* into *E. coli*. Expressions of R-PE alpha and beta apo-subunits in *E. coli* lead to the formation of inclusion bodies, insoluble aggregates that are made of partially folded or misfolded proteins (24-26). Inclusion body formation happened as well after expression of C-PE alpha and beta apo-subunits in *E. coli* (19) consistent with the similar structures of C-PE and R-PE alpha and beta apo-subunits. The formation of inclusion bodies often yields nonfunctional proteins and makes a major problem in production of biologically active proteins in *E. coli*. Despite location of apo-subunits in inclusion bodies, fluorescent holo-subunits were surprisingly formed after incubation of *E. coli* cells with PEB *in vivo*. PEB (Fig. 3B), which is a charged and partially hydrophilic compound with MW of 586.68 Da, was able to cross bacterial outer and inner membranes as well as cell wall and bind to R-PE apo-subunits.¹ Several analytical methods including SDS-PAGE, fluorescence spectroscopy, microscopy, and flow cytometry showed that PEB attached very specifically to apo-subunits of R-PE located in inclusion bodies and formed fluorescent holo-subunits.² Non-specific binding of PEB for cellular structures was negligible since fluorescence of cells was only slightly higher than native fluorescence of cells.

Spectroscopic characterization of isolated holo-subunits showed that they contained not only PEB but also its isomer urobilin. Interestingly, incubation of cells containing apo-subunits with an urobilinoid chromophore also yielded holo-subunits containing both PEB and UB chromophores.³ PEB and UB chromophores did not show binding specificity to R-PE apo-subunits characteristic for formation of holo-subunits in red algae since the spectral

properties of holo-subunits are different than spectroscopic properties of subunits from native R-PE. This is likely not only due to misfolding of subunits in inclusion bodies but also because the enzymes that are involved in chromophore attachment in red algae are missing in the *E. coli* expressing system. Isomerization between PEB and UB chromophores might be facilitated by the reducing environment of *E. coli* cytoplasm and by oxygen from air. PEB, UB and DBV adducts were detected after incubation of renatured C-PE alpha subunit with PEB *in vitro* (19). We ruled out the presence of DBV in holo-subunits since its absorption maxima at 308 nm and 562 nm as well as fluorescence excitation and emission maxima at 592 nm and 605 nm (19, 27) were absent from the spectra.

Previously inclusion bodies of cytoplasmic proteins have been observed in the cytoplasm, while inclusion bodies of secreted proteins may be located in the cytoplasm as well as in the periplasm (28, 29). Polar location of R-PE subunit inclusion bodies in bacterial cells was unambiguously confirmed by high-resolution and high-contrast images acquired by DIC and fluorescence microscopy. Inclusion bodies can be imaged with other transmission light microscopy techniques such as phase contrast if they are big in size (24, 30). Otherwise they are observed by transmission electron microscopy (TEM) (28, 29). A fluorescent reporter of inclusion bodies based on attachment of PEB to R-PE apo-subunits could be a less expensive and less time consuming alternative for TEM. Since 70 to 80 % of all recombinant proteins form inclusion bodies (31) such a fluorescent reporter could be a sensitive and selective marker of protein aggregation.

Fluorescent proteins were also formed after attachment of PEB chromophore to fusions of *E. coli* maltose binding protein (MBP) and R-PE apo-subunits *in vitro* and *in vivo*. Both cytoplasmic and periplasmic MBP formed fusions with apo-alpha and apo-beta subunits that were soluble. Attachment of PEB to fusion proteins occurred without isomerization of the PEB chromophore and lead to a significant increase in the brightness of the fluorophore. Fluorescence microscopy revealed that fusion proteins are localized either throughout cells or at cell poles, while expression was accompanied by morphological changes in cells containing high amount of overexpressed proteins. Our future goal is to optimize the expression of periplasmic MBP-subunit fusion so that most of the protein is exported to the periplasmic space of *E. coli*. If this is the case attachment of PEB to periplasmic MBP-

subunit fusions should yield fluorescence signal located mainly in the periplasmic space that hopefully might be localized by optical sectioning of *E. coli* cells. While GFP worked as reporter of protein export in the TAT secretion pathway, it did not work as reporter of protein transport in Sec pathway (32, 33). We hope that R-PE-subunit fusions might work as reporters of protein transport in both pathways. This could help us to answer important biological questions related to secretion and transport of proteins from the cytoplasm into periplasmic space of *E. coli*.

Fluorescent subunits were successfully used in flow cytometry and fluorescence microscopy. They also show promise for use in photodynamic therapy of cancer (34).⁴ Possibilities are open for use of recombinant R-PE apo-subunits as reporters of gene expression and protein localization after incubation of cells with PEB chromophore. Valuable properties of R-PE apo-subunit fluorescent fusions include: broad excitation and emission fluorescence spectra, high fluorescence in the orange region of the electromagnetic spectrum (away from cellular autofluorescence), and functioning both *in vitro* and *in vivo*. The unique property of such a reporter is that it works despite the way R-PE apo-subunits are folded. There is still much room for improvement of fluorescent properties of holo-subunits through mutagenesis, as well as the use of other phycobilins in the attachment. The need for exogenous supply of PEB chromophore could be overcome if the complete biosynthetic pathway for formation and attachment of PEB to apo-subunits of R-PE is expressed. Such a project would yield both to new and improved recombinant phycobiliproteins and reveal details of their biogenesis in nature.

REFERENCES

1. Lakowicz, J. R. (1999) *Principles of Fluorescence Spectroscopy*, 82-86, Kluwer Academic/Plenum Publishers, New York
2. Tsien, R. Y. (1998) *Annu. Rev. Biochem.* **67**, 509-544
3. Zhang, J., Campbell, R. E., Thing, A. Y., and Tsien, R. Y. (2002) *Nat. Rev. Mol. Cell Biol.* **3**, 906-918
4. Glazer, A.N., and Stryer, L. (1984) *Trends Biochem. Soc.* **9**, 423-427

5. Mullins, J. M. (1994) in *Methods Mol. Biol.* (L. C. Javois, Editor), 112-113, Humana Press, Totowa, New Jersey
6. Zickendraht-Wendelstadt, B., Friedrich, J., and Rudiger, W. (1980) *Photochem. Photobiol.* **31**, 367-376
7. Isailovic, D., Li, H-W., and Yeung, E. S. (2004) *J. Chromatogr. A*, **1051**, 119-130
8. Tooley, A. J., Cai, Y. A., and Glazer, A. N. (2001) *Proc. Natl. Acad. Sci. (U.S.A.)* **98**, 10560-10565
9. Tooley, A. J., and Glazer, A. N. (2002) *J. Bacteriol.* **184**, 4666-4671
10. Cai, Y. A., Murphy, J. T., Wedemayer, G. J., and Glazer, A. N. (2001) *Anal. Biochem.* **290**, 186-204
11. Beale, S. E., and Cornejo, J. (1991) *J. Biol. Chem.* **266**, 22328-22332
12. Beale, S. E., and Cornejo, J. (1991) *J. Biol. Chem.* **266**, 22333-22340
13. Beale, S. E., and Cornejo, J. (1991) *J. Biol. Chem.* **266**, 22341-22345
14. Schluchter, M. W., and Glazer, A. N. (1999) In *The Phototrophic Prokaryotes* (Pescheck, G.A., Löffelhardt, W., and Schmetterer, G., Editors), 83-95, Kluwer Academic/ Plenum Publishers, New York
15. Storf, M., Parbel, A., Meyer, M., Strohmam, B., Scheer, H., Deng G-M., Zheng, M., Zhou, M., and Zhao, K-H. (2001) *Biochemistry* **40**, 12444-12456
16. Arciero, D. M., Brajant, D. A., and Glazer, A. N. (1988) *J. Biol. Chem.* **263**, 18343-18349.
17. Arciero, D. M., Dallas, J. L., and Glazer, A. N. (1988) *J. Biol. Chem.* **263**, 18350-18357
18. Arciero, D. M., Dallas, J. L., and Glazer, A. N. (1988) *J. Biol. Chem.* **263**, 18358-1863
19. Fairchild, C. D., and Glazer, A. N. (1994) *J. Biol. Chem.* **269**, 28988-28996
20. Murphy, J. T., and Lagarias J. C. (1997) *Curr. Biol.* **7**, 870-876
21. Kahn, K., Mazel, D., Houmard, J., Tandeau de Marsac, N., and Schaefer, M.R. (1997) *J. Bacteriol.* **179**, 998-1006

22. Roell, M. K., and Morse, D. E. (1993) *Plant Molec. Biol.* **21**, 47-58
23. Isailovic, D., Li, H-W., Phillips, G. J., and Yeung, E. S. (2005) *Appl. Spectrosc.* **59**, 221-226
24. Mitraki, A., and King, J. (1989) *Biotechnology* **7**, 690-697
25. Kane J. F., and Hartly, D. L. (1988) *Trends Biotechnol.* **6**, 95-101
26. Villaverde, A., and Carrió, M.M. (2003) *Biotechnol. Lett.* **25**, 1385-1395
27. Wedemayer, G.J., Kidd, D.G., Wemmer, D.E. and Glazer, A. N. (1992) *J. Biol. Chem.* **267**, 7315-7331
28. Bowden, G. A., Paredes, A. M., and Georgiu, G. (1991) *Biotechnology*, **9**, 725-730
29. Sriubolmas, N., Panbabangred W., Sriurairatana, S., and V. Meevovootisom, (1997) *Appl. Microbiol Biotechnol.* **47**, 373-378.
30. Carrió, M.M., Corchero, J. L., and Villaverde, A. (1998) *FEMS Microbiol. Lett.* **169**, 9-15
31. *2003-2004 Applications, Handbook & Catalog, Pierce Biotechnology INC.* Rockford, IL, pp.162.
32. Thomas, J. D., Daniel, R. A., Errington, J., and Robinson, C. (2001) *Mol. Microbiol.* **39**, 47-53
33. B. J. Feilmeier, G. Iseminger, D. Schroeder, H. Webber, and G. J. Phillips (2000) *J. Bacteriol.* **182**, 4068-4076
34. Huang, B., Wang, G.-C., Zeng, C-K, and Li, Z. (2002) *Cancer Biother. Radio.* **17**, 35-42

FOOTNOTES

*We thank Hugo Scheer and Max Storf for the gift of PEB, Shawn Rigby for work on flow cytometry experiments, Bob Doyle for help with microscopy experiments, and Slavica Isailovic for recording digital photos. E.S.Y. thanks the Robert Allen Wright Endowment for Excellence for support. Ames Laboratory is operated for the US Department of Energy by

Iowa State University under Contract No. W-7405-Eng-82. This work was supported by the Director of Science, Office of Basic Energy Sciences, Division of Chemical Sciences.

¹Chromophore transfer in the bacterial cell is a critical step disturbed by the structure of cell wall and efflux mechanisms present in the cell. Fortunately hydrophilic compounds with MW less than approximately 800 Da are delivered through outer bacterial membrane by protein channels embedded in the membrane (porins). PEB also crossed bacterial cell wall and inner membrane toward its way to the cytoplasm, what might have been helped with a small amount of DMSO. We have tried several other procedures for incubations of cells with PEB, but without improvement in chromophore transfer compared to the described method.

²PEB attachment to apo-subunits in cells immediately after protein expression might be possible due to presence of partially folded intermediates in inclusion bodies. Attachment of PEB to apo-subunits in cells that were frozen was not possible. It seems maturation of inclusion bodies at low temperatures prevent the access of the chromophores to the cysteines responsible for chromophore binding. Previous studies and the fact that chromophore remained attached even after denaturing electrophoresis supports formation of thioether bonds between phycobilins and cysteine residues. Less probable scenario for chromophore binding might be its incorporation into inclusion body by inclusion or binding as a ligand. Determination of chromophore binding sites would give the answers on these uncertainties.

³PUB-like chromophore was isolated from B-phycoerythrin (7). In the case of incubation with this chromophore induced and control cells were washed, suspended in 5 ml of PBS buffer, incubated with 50 μ l of 200 nM PUB solution in DMSO, and shaken overnight at 25^oC. Fluorescence spectra of isolated holo-subunits showed the same maxima as in the case of attachment of PEB to apo-alpha subunits.

⁴Photodynamic therapy relates on treatment of cancer cells by combination of chemical photosensitization and light radiation that are in combination lethal to cells. Photosensitizers should have high absorption properties with multiple peaks in the visible region, be well

absorbed by cells and show low phototoxicity. Huang et al have shown that R-phycoerythrin subunits isolated from red algae can be used as photosensitizer in PDT of carcinoma cells. Since PEB shows low phototoxicity and could be absorbed by cells, holo-subunits formed after attachment of PEB or other phycobilins to genetically expressed apo-subunits in a target organ could be potential candidates for photosensitizers.

FIGURE LEGENDS

Fig. 1. Analysis of His-tagged R-PE apo-subunits and holo-subunits by SDS-PAGE.

A, Detection of proteins by Coomassie staining. B, Detection of proteins by fluorescence imaging (excitation wavelength 532 nm; emission filter 580BP30). Cells were suspended in 50 μ l of 1X SDS-PAGE buffer, 47.5 μ l of Laemli sample buffer and 2.5 μ l of β -mercaptoethanol. Cell suspensions were heated at 95 $^{\circ}$ C for 5 minutes, centrifuged at 10,000 rpm for 1 min and heated again at 95 $^{\circ}$ C for 5 minutes. R-PE (Molecular Probes) sample was prepared as described before (7). 20 μ l of cell lysates, 5 μ l of R-PE, and 5 μ l of MW standards were loaded on the 12 % poly acrylamide gel (Bio-Rad) and separated by using constant current of 30 mA. After protein separation gel was first analyzed by fluorescence imaging and then stained with Bio-safe Coomassie blue (7). Molecular weights of His-tagged apo-subunits are around 23 kDa as found by comparison with molecular weight standards. *Lane 1*, R-PE subunits; *lane 2*, lysate of cells that expressed apo-alpha subunit of R-PE; *lane 3*, prestained MW standards, low range 18-106 kDa (Bio-Rad); *lane 4*, lysate of cells that expressed apo-alpha subunit of R-PE and were incubated with PEB. Holo-alpha subunit was formed. ; *lane 5*, lysate of cells that were not induced for expression of apo-alpha subunit of R-PE but were incubated with PEB; *lane 6*, lysate of cells that expressed apo-beta subunit of R-PE and were incubated with PEB. Holo-beta subunit was formed; *lane 7*, lysate of cells that were not induced for expression of apo-beta subunit of R-PE but were incubated with PEB; *lane 8*, lysate of BL21(DE3) cells. Cells were incubated with PEB, but neither contained plasmids bearing subunit genes nor were treated with IPTG; *lane 9*, lysate of cells that expressed apo-beta subunit of R-PE.

Fig. 2. A, The photograph of *E. coli* cells expressing R-PE apo-subunits and control cells after incubation with PEB chromophore. Vials from left to right contained the following cells incubated with PEB: 1. BL21(DE3) cells that neither contained plasmids bearing subunit genes nor were treated with IPTG, 2. Control cells that were not induced for expression of apo-beta subunit of R-PE, 3. Cells that were induced for expression of apo-beta subunit of R-PE, 4. Control cells that were not induced for expression of apo-alpha subunit of R-PE, and 5. Cells that were induced for expression of apo-alpha subunit of R-PE; B, The photograph of holo- alpha subunit solution isolated in the denaturing buffer (right) compared to the pure denaturing buffer (left). Denaturing buffer contains 8M urea, 500 mM NaCl and 20 mM sodium phosphate buffer, pH 4.0. Pink color of holo-subunits in cells and after isolation in denaturing buffer can be seen.

Fig. 3. Structures of covalently bound PEB and PUB chromophores. Chromophores are bound to specific cysteines of phycobiliproteins by either a single thioether bond or double thioether bonds. A, Singly linked phycourobilin; B, Singly linked phycoerythrobilin.

Fig 4. Subcellular localization of holo-alpha subunit. *E. coli* cells expressing R-PE apo-alpha subunit and control cells were fixed on microscope slides after incubation with PEB. Panels A, D: DIC images of induced and control cells. Panels B, E: Fluorescence images of induced and control cells detected by triple DAPI/FITC/TRITC filter cube. Images show merged native fluorescence and fluorescence from PEB attachment to cell components. Panels C, F: Fluorescence images of induced and control cells recorded by TRITC filter cube. Images in these panels confirm that fluorescent holo-alpha subunit is located in inclusion bodies at the poles of induced *E. coli* cells.

Fig 5. Subcellular localization of holo-beta subunit. *E. coli* cells expressing R-PE apo-beta subunit and control cells were fixed on microscope slides after incubation with PEB. Panels A, D: DIC images of induced and control cells. Panels B, E. Fluorescence images of induced and control cells detected by triple DAPI/FITC/TRITC filter cube. Images show merged native fluorescence and fluorescence from PEB attachment to cell components. Panels C, F:

Fluorescence images of induced and control cells detected by TRITC filter cube. Images in these panels confirm that fluorescent holo-beta subunit is located in inclusion bodies at the poles of induced *E. coli* cells.

Fig. 6. Fluorescence intensities of *E. coli* cells containing holo-subunits and control cells measured by flow cytometry after incubation of cells with PEB. Fluorescence was collected for 10,000 cells by using 532 nm laser for excitation and 580nmBP30 filter for emission. *A*, Fluorescence intensities of cells expressing R-PE apo-alpha subunit and control cells are compared after incubation of cells with PEB. *B*, Fluorescence intensities of cells expressing R-PE apo-beta subunit and control cells are compared after incubation of cells with PEB. Fluorescence intensities are shown on x-axes in the logarithmic scale. Numbers of cells shown on Y-axes were normalized for the purpose of graphical presentation. Results on these graphs combined with results in Table 2 show that cells containing holo-subunits are in average several times brighter than control cells.

Fig. 7. Analysis of fusion proteins between cytoplasmic MBP and R-PE apo-alpha subunit by SDS-PAGE. *A*, Detection of proteins by Coomassie staining. *B*, Detection of proteins by fluorescence imaging (excitation wavelength 532 nm; emission filter 580BP30). Fusion proteins were isolated from *E. coli* cells by affinity chromatography on amylose resin under native conditions. Five 300 μ l fractions were eluted in maltose elution buffer. Fusions were isolated from cells that were not treated with PEB (*Lanes* 1-4) and cells that were incubated with PEB (*Lanes* 6-10). Isolated proteins (40 μ l) were suspended in 40 μ l of Laemmli sample buffer and 2.5 μ l of β -mercaptoethanol. Protein solutions were heated at 95 $^{\circ}$ C for 5 minutes, centrifuged at 10,000 rpm for 1 min and heated again at 95 $^{\circ}$ C for 5 minutes. 20 μ l of protein samples and 5 μ l of MW standards were loaded on the 12 % poly acrylamide gel (Bio-Rad), and separated by using the constant current of 30 mA. After protein separation gel was first analyzed by fluorescence imaging and then stained with Bio-safe Coomassie blue (7). *Lanes* 1-4, the fourth, the third, the second, and the first purification fractions of MBP-R-PE alpha subunit fusions without PEB; *lane* 5, prestained MW standards, low range 18-106 kDa (Bio-Rad); *lane* 6-10, the fifth, the fourth, the third, the second, and the first purification fractions

of MBP-R-PE alpha subunit fusions with PEB. Results show that MBP-R-PE fusion protein with molecular weight of ~ 65 kDa is successfully purified under native conditions. Fusion proteins isolated from cells incubated with PEB were fluorescent in contrast to fusion proteins isolated from cells that were not incubated with PEB. The highest amount of fusion proteins is found in the first elution fractions. The same conclusions were obtained after isolation of cytoplasmic MBP-R-PE beta subunit fusions.

Fig. 8. Normalized excitation and emission fluorescence spectra of cytoplasmic MBP-R-PE alpha subunit fusion protein after attachment of PEB *in vivo*. Spectra were recorded by the fluorescence spectrometer. Emission wavelength used to record excitation spectrum was 610 nm. Excitation wavelength used to record emission spectrum was 530 nm. Spectra show excitation peak at 577.5 nm and emission peaks at 584.0 nm, and indicate formation of fluorescent fusions containing PEB. Fusion protein between cytoplasmic MBP and R-PE beta subunit showed the same fluorescence spectra after PEB attachment. Excitation peak at 517 nm comes from the solvent (maltose elution buffer).

Fig. 9. Photographs comparing *E. coli* cells expressing periplasmic MBP-R-PE alpha subunit fusion protein and control cells after incubation of cells with PEB chromophore. Vials from left to right contained the following cells incubated with PEB: 1. Control cells that were not induced for expression of periplasmic MBP-R-PE alpha subunit fusion, 2. Cells that were induced for expression of periplasmic MBP-R-PE alpha subunit fusion. A, Daylight colors of cells. Pink color of induced cells can be seen. B, Colors of cells under UV illumination. Orange fluorescence of induced cells can be seen. Results indicate formation of fluorescent fusion proteins that are pink in color and show orange fluorescence.

Fig 10. Subcellular localization of fusion protein consisting of periplasmic MBP and R-PE apo-alpha subunit after incubation of cells with PEB. *E. coli* cells that expressed MBP-R-PE alpha apo-subunit fusion were fixed on microscope slide after incubation with PEB. Cells were imaged by a 100 X microscope objective. Zoom lens in front of the CCD gave additional 2 X magnification. Panel A, DIC image of cells. Panel B, Fluorescence image of

cells recorded by using TRITC filter. Cells that were normal in size and cells that were elongated were noticed among induced cells. Elongated cells were much brighter than normal cells probably because they expressed more of the fusion protein. Fluorescent fusions were localized throughout cells in normal cells indicating that fusion proteins are soluble in the cell cytoplasm, and probably partially exported to periplasmic space. In elongated cells, fluorescent fusions were localized both throughout cells and at cell poles revealing the presence of both soluble and insoluble fusion proteins. Elongation of cells was not noticed in control cells and these cells were less bright than induced cells (images not shown).

Fig. 11. Fluorescence intensities of cells expressing periplasmic MBP-R-PE apo-alpha subunit fusion and control cells after incubation of cells with PEB. Fluorescence was measured by a flow cytometer by using 532 nm laser for excitation and 580nmBP30 filter for emission. Fluorescence intensities are shown on the x-axis in the logarithmic scale. Numbers of cells shown on Y-axis were normalized for the purpose of graphical presentation. Fluorescence of cells was analyzed in regions A, B, and C. Region A corresponds to highly fluorescent induced cells, while regions B and C correspond respectively to all induced and control cells. Results on the graph combined with data in Table 4 show that cells containing periplasmic MBP-R-PE subunit fusions are much brighter than control cells. As in fluorescence microscopy, two subpopulations are noticed among induced cells corresponding to less bright cells that are normal in size and more bright elongated cells.

Fig. 12. Normalized excitation and emission fluorescence spectra of PEB, and cytoplasmic MBP-alpha subunit after attachment of PEB *in vitro*. PEB solution was prepared by adding 25 μ l of 27.0 μ M PEB solution in DMSO into 500 μ l of maltose elution buffer. MBP-subunit fusion solutions were prepared by adding 25 μ l of 27.0 μ M PEB solution in DMSO in 500 μ l of MBP-fusions in maltose elution buffer. Solutions were incubated at room temperature overnight. Emission wavelength used to record excitation spectrum was 620 nm. Excitation wavelength used to record emission spectrum was 530 nm. Slit widths were 10 nm. Spectra were normalized by multiplication of fluorescence intensities in excitation spectra. A, Fluorescence spectra of PEB in maltose elution buffer. B, Fluorescence spectra of MBP-

alpha subunit fusion in maltose elution buffer after attachment of PEB. Comparison of the spectra shows an excitation peak at 574.5 nm, which is characteristic for PEB attached to MBP-subunit fusions, and much higher fluorescence intensity of fluorescent fusions than fluorescence intensity of free PEB. The same conclusion was reached from fluorescence spectra of MBP-beta subunit fusions. Results confirm that attachment of PEB to R-PE subunits fused to MBP both *in vitro* and *in vivo* yield fluorescent proteins that have PEB as sole chromophore, and show excitation maximum at ~575 nm as well as emission maximum at ~585 nm.

Fig. 13. MBP-R-PE subunit solutions after attachment of PEB compared to solution of free PEB. Samples were prepared as described in the capture of Figure 12, and photographed by a digital camera. Vials from left to right contained the following solutions: 1. cytoplasmic MBP-R-PE alpha subunit and PEB in maltose elution buffer, 2. PEB in maltose elution buffer. 3. cytoplasmic MBP-R-PE beta subunit fusion and PEB in maltose elution buffer, A, Daylight color of solutions. Solutions are pink in color due to the same color of free PEB and PEB bound to fusion proteins. B, Color of solutions under UV illumination. Orange fluorescence from solutions containing fluorescent subunit fusions is seen. These images demonstrate the large increase in fluorescence of PEB chromophore after attachment to soluble apo-subunit fusion proteins.

Table 1. Spectroscopic characteristics of holo-subunits formed after attachment of PEB to recombinant R-PE apo-subunits *in vivo*. Holo-subunits were isolated from *E. coli* cells under denaturing conditions. Absorption and fluorescence spectra of holo-subunits were measured by absorption and fluorescence spectrometers (24). Values of maxima in absorption spectra, and emission and excitation fluorescence spectra are shown. From these values and referenced literature it was concluded that attachment of PEB to cells containing R-PE apo-subunits yields holo-subunits containing both UB and PEB.

Absorption maximum (nm)	496.0	552.0	
Excitation fluorescence maximum (nm)	495.0	542.5	569.5
Emission fluorescence maximum (nm)	506.5	573.0	581.5
Phycobilin present in holo-subunit	UB	PEB	

Table 2. Average fluorescence intensities (PMT1 mean) of cells containing holo-subunits and control cells measured by flow cytometry. Fluorescence intensities of 10,000 cells were analyzed. All cells were incubated with PEB under the same conditions, but only α_{ind} and β_{ind} cells expressed apo-alpha and apo-beta subunits of R-PE respectively. These cells had, on average, several times higher fluorescence compared to cells without expressed apo-subunits (α_{con} , β_{con} , BL21(DE3)).

Cells	α_{ind}	α_{con}	β_{ind}	β_{con}	BL21(DE3)
PMT1 mean	15.1	2.9	7.9	3.0	3.1

Table 3. Fluorescence maxima of MBP-R-PE apo-subunit fusion proteins after attachment of PEB *in vivo*. Proteins were isolated from *E. coli* cells containing MBP-R-PE apo-subunit fusions after incubation of cells with PEB. Spectra of fusion proteins were recorded in maltose elution buffer by a fluorescence spectrometer ($\lambda_{exc} = 530$ nm, $\lambda_{em} = 610$ nm). From these values and referenced literature it was concluded that attachment of PEB to cells containing MBP-R-PE apo-subunit fusion proteins yields holo-subunit fusion proteins containing PEB as the sole chromophore.

Excitation fluorescence maximum (nm)	577.5
Emission fluorescence maximum (nm)	584.0
Phycobilin present in fusion protein	PEB

Table 4. Average fluorescence intensities (PMT1 mean) of cells expressing periplasmic MBP-R-PE alpha-subunit fusion protein and control cells measured by flow cytometry.

Fluorescence of induced and control cells was measured after incubation of cells with PEB. Average fluorescence intensities of cells in regions shown in Figure 11 are compared. Region A corresponds to highly fluorescent induced cells, while regions B and C correspond respectively to all induced and control cells. Average fluorescence of induced cells is 5.4 times higher than average fluorescence of control cells. Average fluorescence of highly fluorescent induced cells is 10.1 times higher than average fluorescence of control cells.

Cells	MBP- α_{ind}	MBP- α_{ind}	MBP- α_{con}
Region	A	B	C
PMT1 mean	74.0	39.4	7.3

Table 5. Excitation and emission fluorescence maxima of PEB, and MBP-R-PE apo-subunit fusion proteins after attachment of PEB *in vitro*. Spectra of free PEB and fusion proteins were recorded in maltose elution buffer by a fluorescence spectrometer ($\lambda_{exc} = 530$ nm, $\lambda_{em} = 620$ nm). From values of fluorescence maxima and shoulders (sh) and referenced literature, it was concluded that attachment of PEB to MBP-R-PE apo-subunit fusion proteins *in vitro* yields holo-subunits containing PEB.

Phycobilin	Free PEB	Bound and Free PEB
Excitation fluorescence maximum (nm)	528.0	576.0, 525.0 (sh),
Emission fluorescence maximum (nm)	579.0, 625.0 (sh)	586.5, 625.0 (sh)

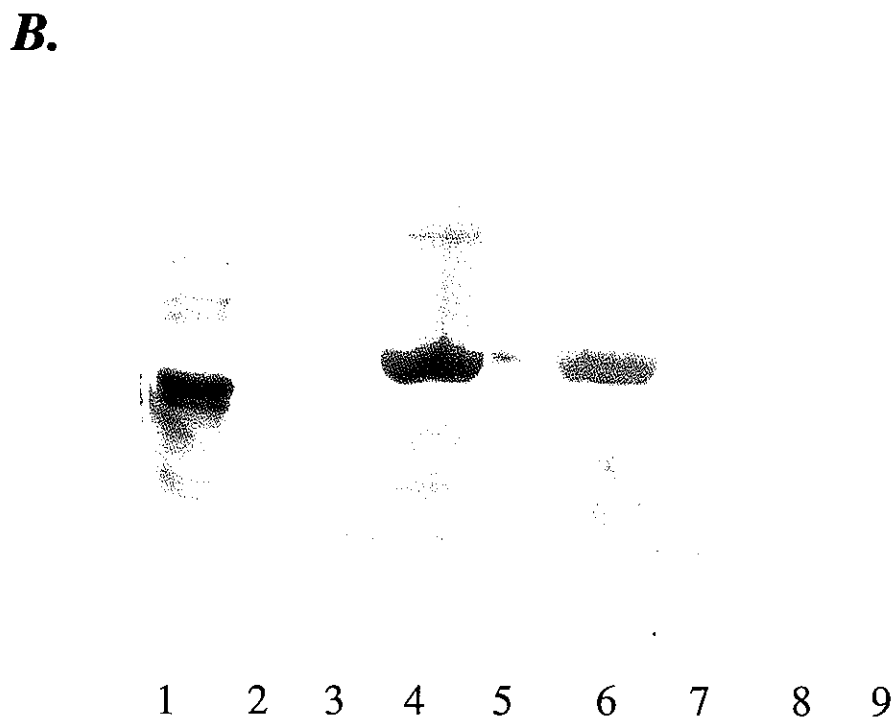
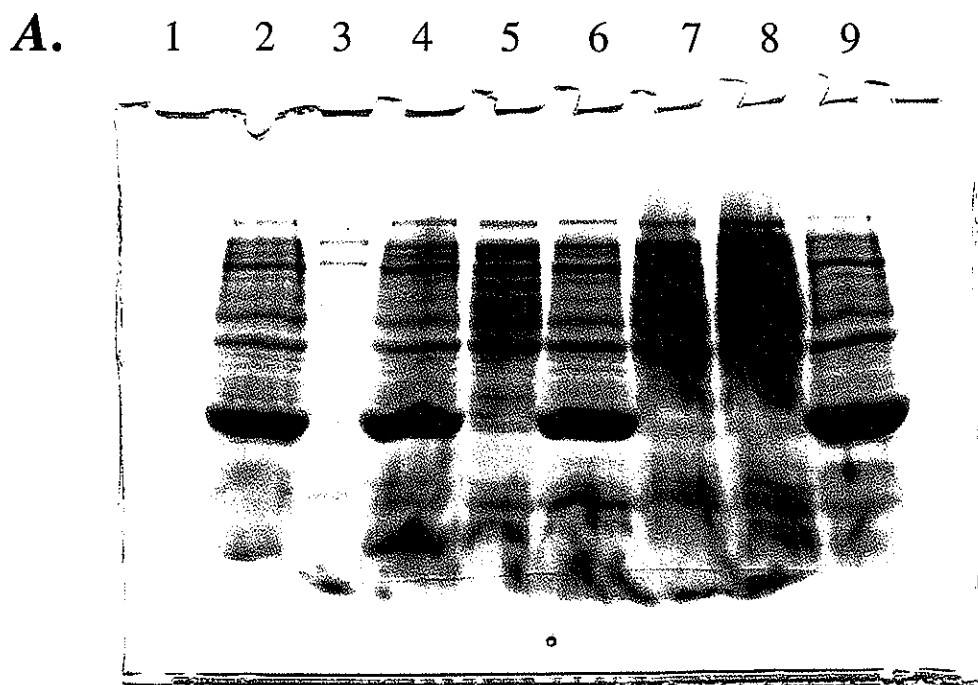
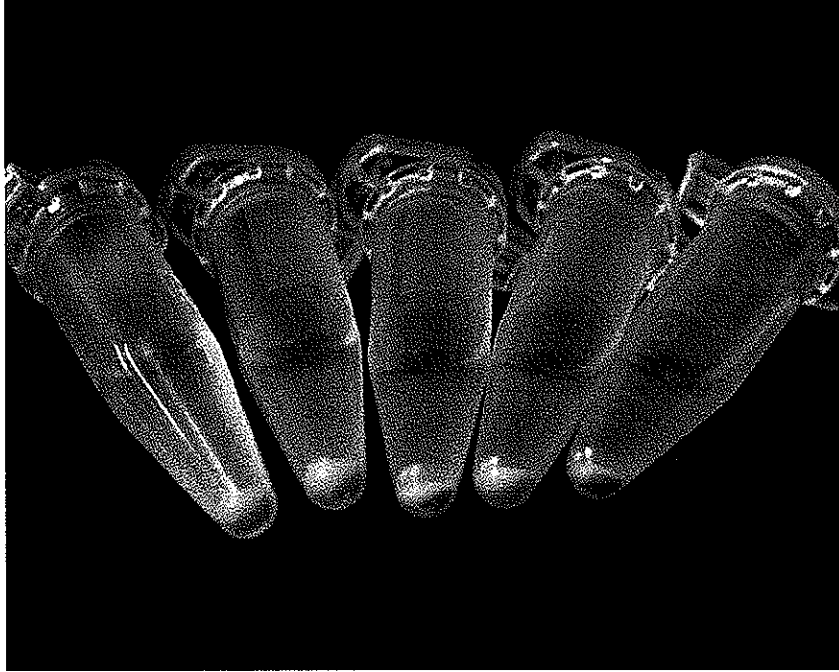


Figure 1.

A.



B.

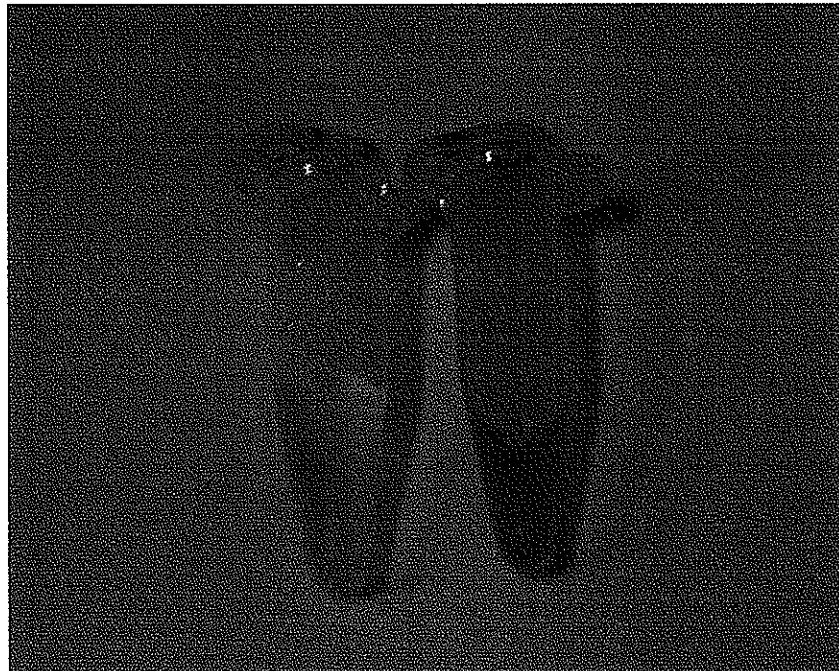
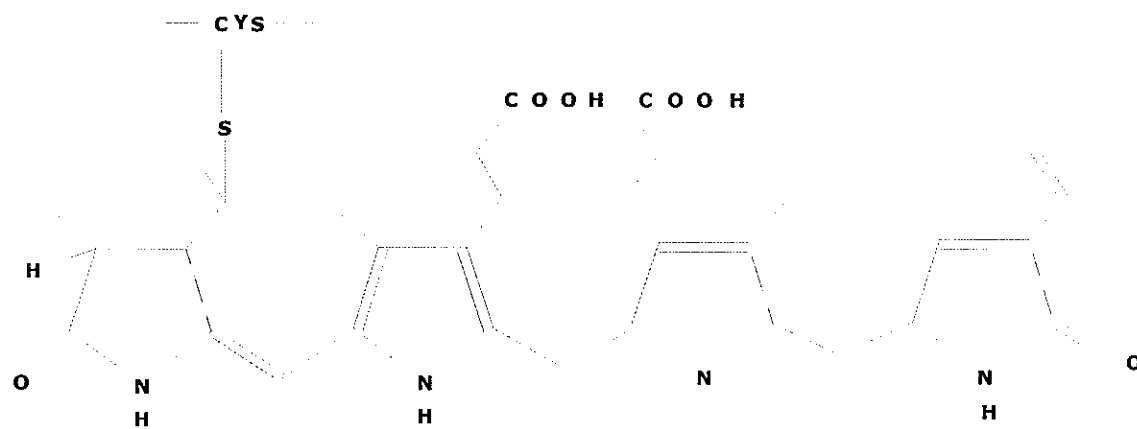
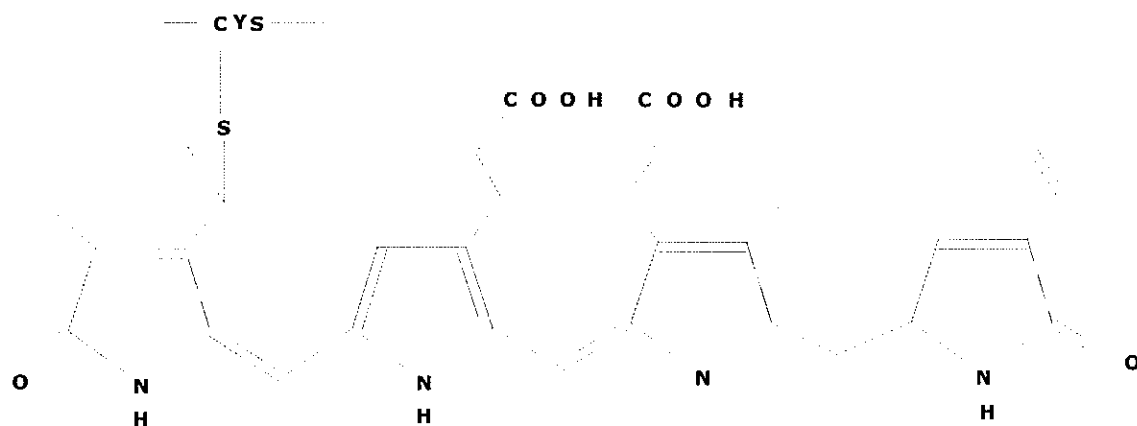


Figure 2.

A. Singly linked PUB***B. Singly linked PEB******Figure 3.***

A - C

D - F

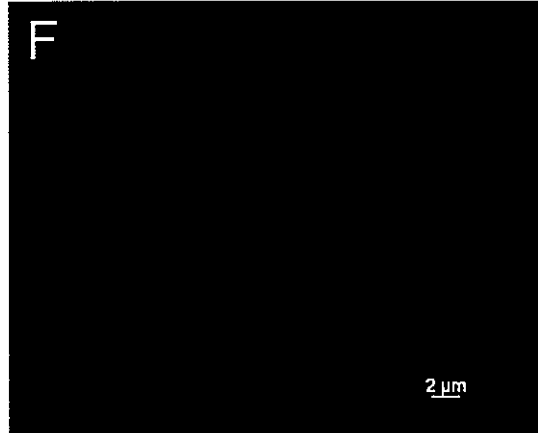
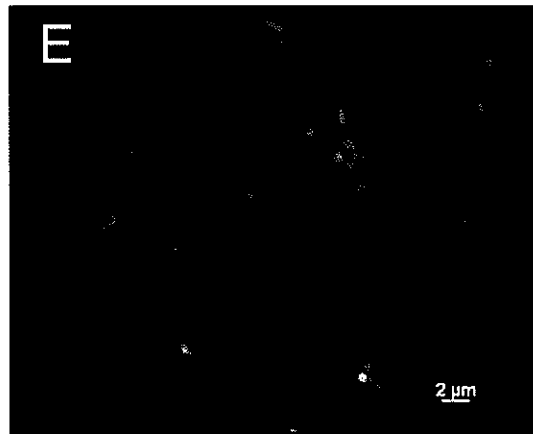
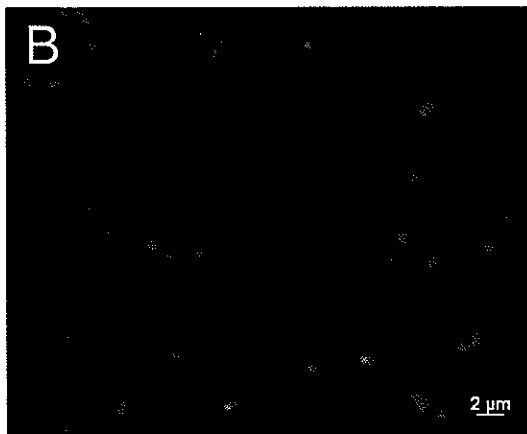
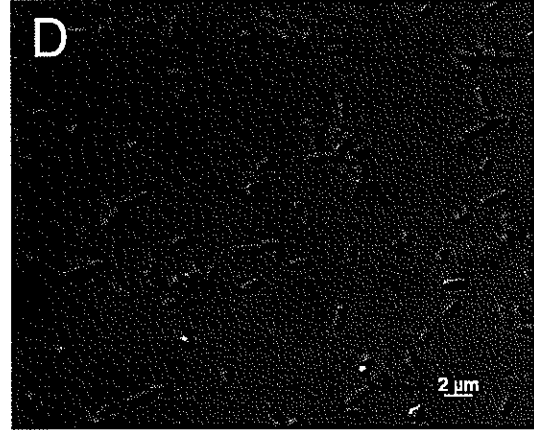
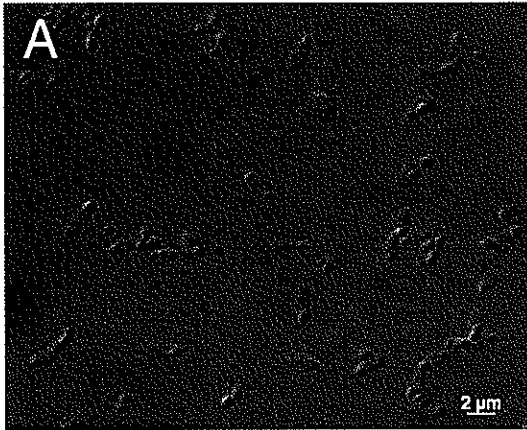


Figure 4.

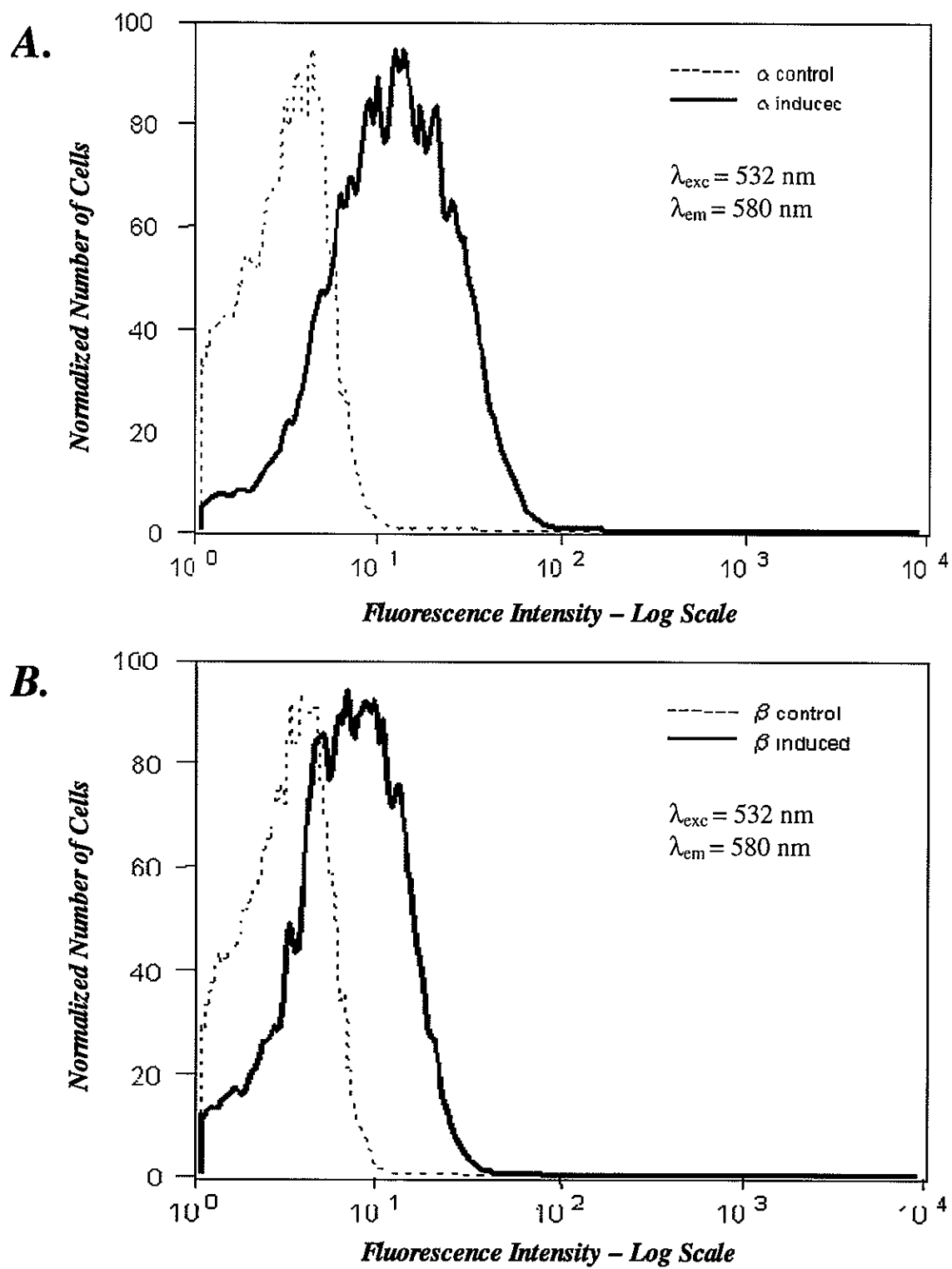
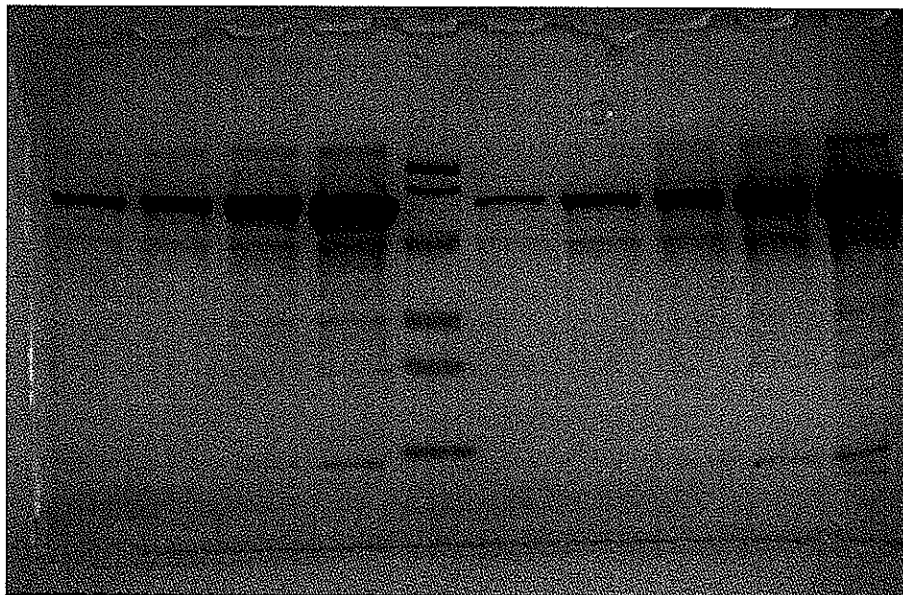
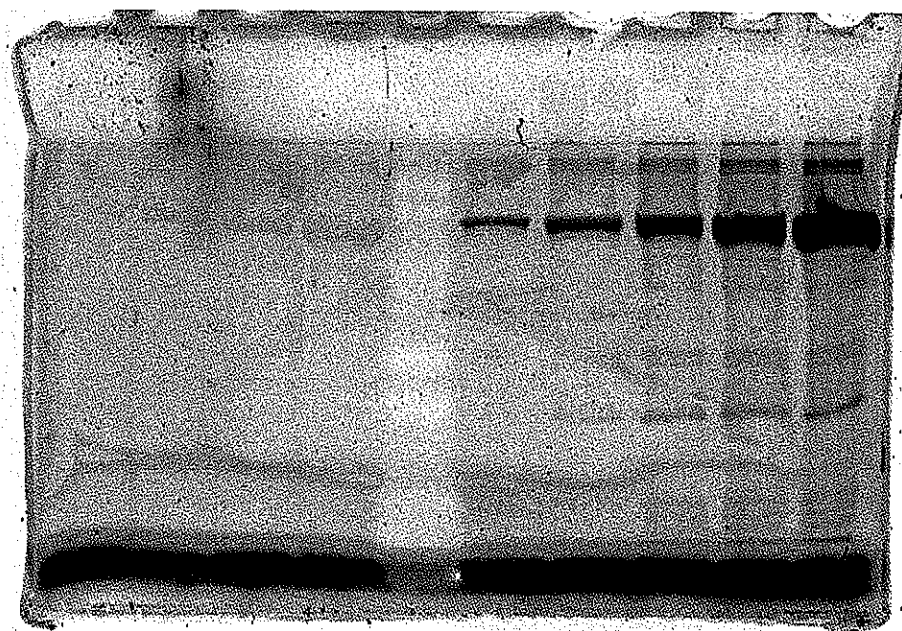


Figure 6.

A. 1 2 3 4 5 6 7 8 9 10



B.



1 2 3 4 5 6 7 8 9 10

Figure 7.

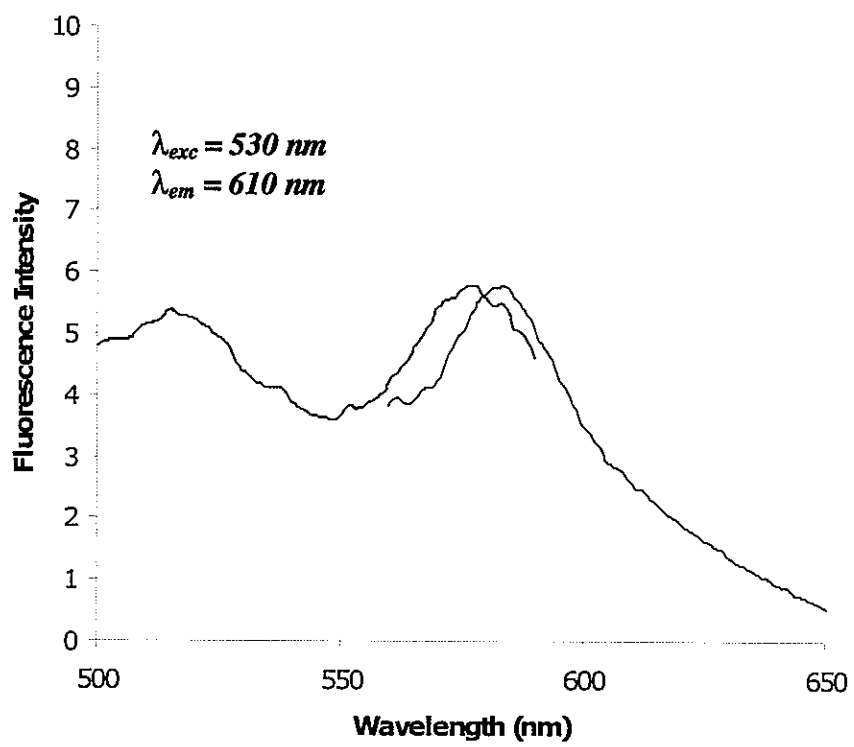


Figure 8.

A.



B.

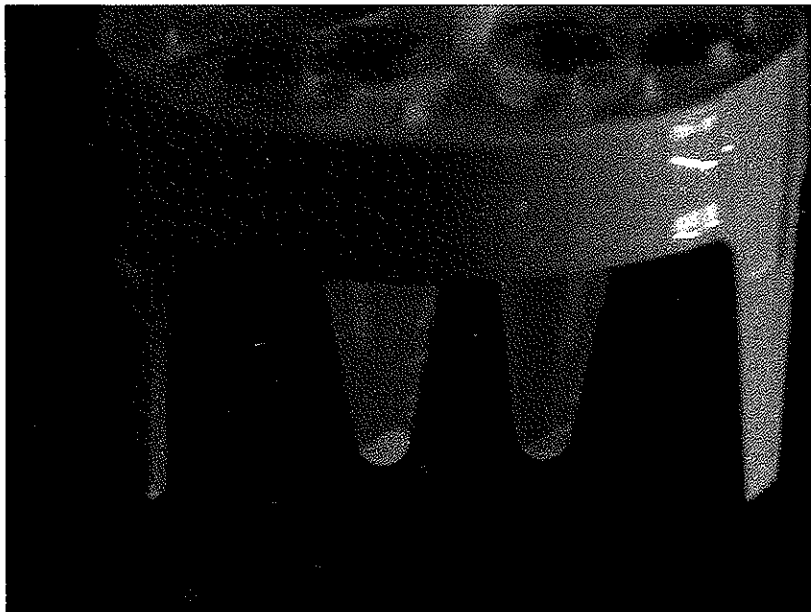


Figure 9.

A.



B.

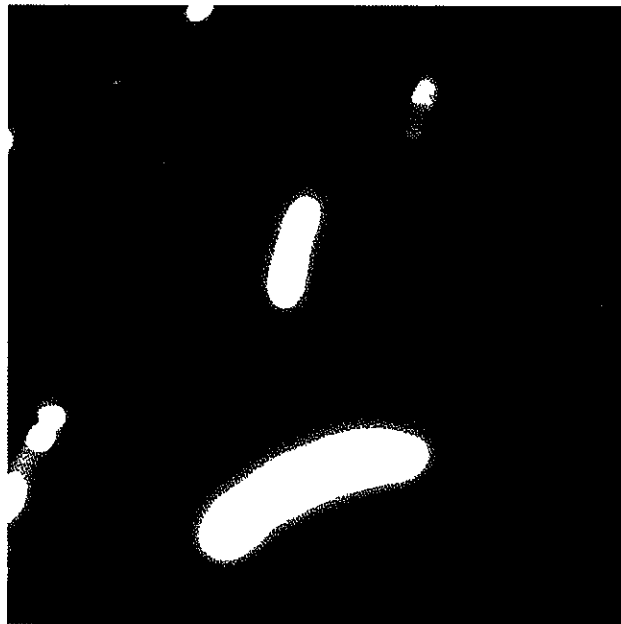


Figure 10.

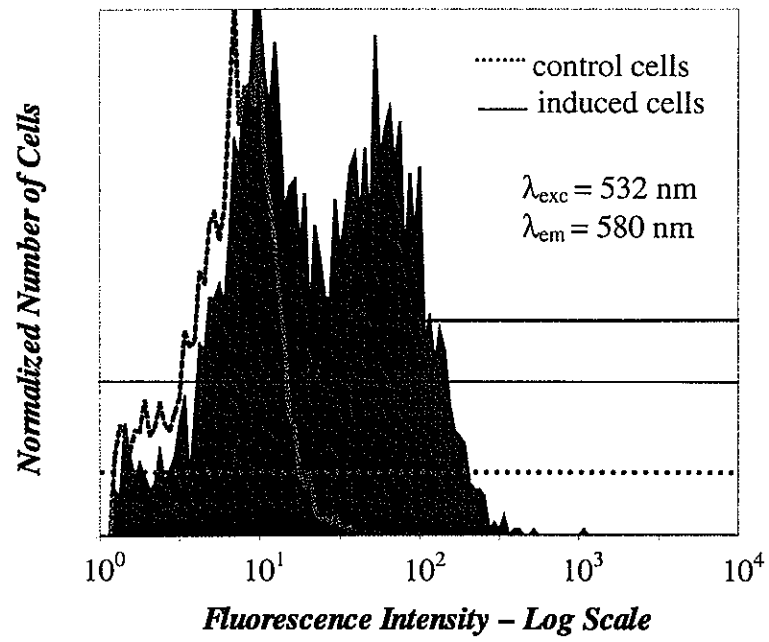
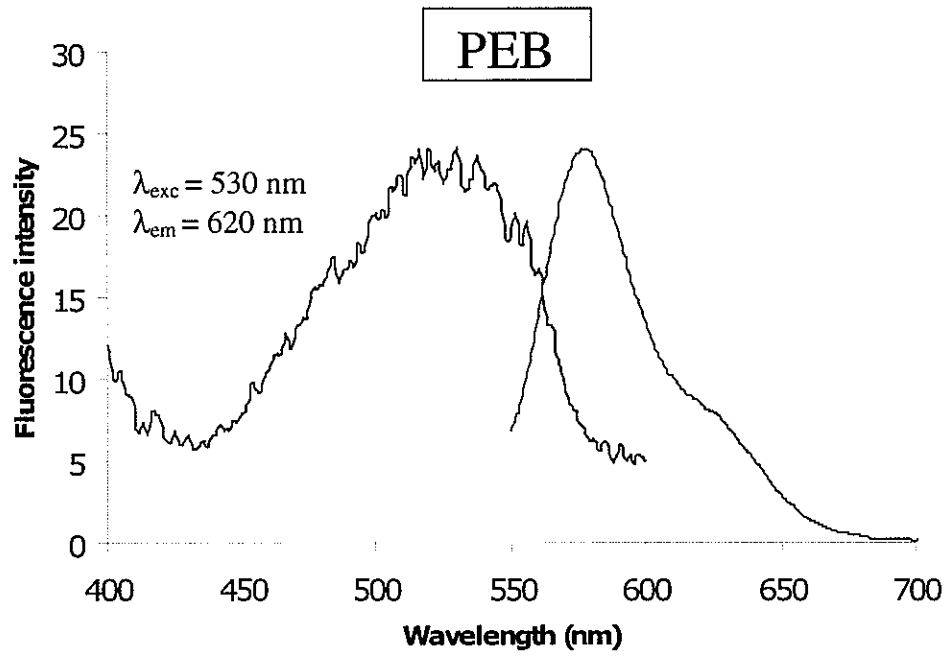
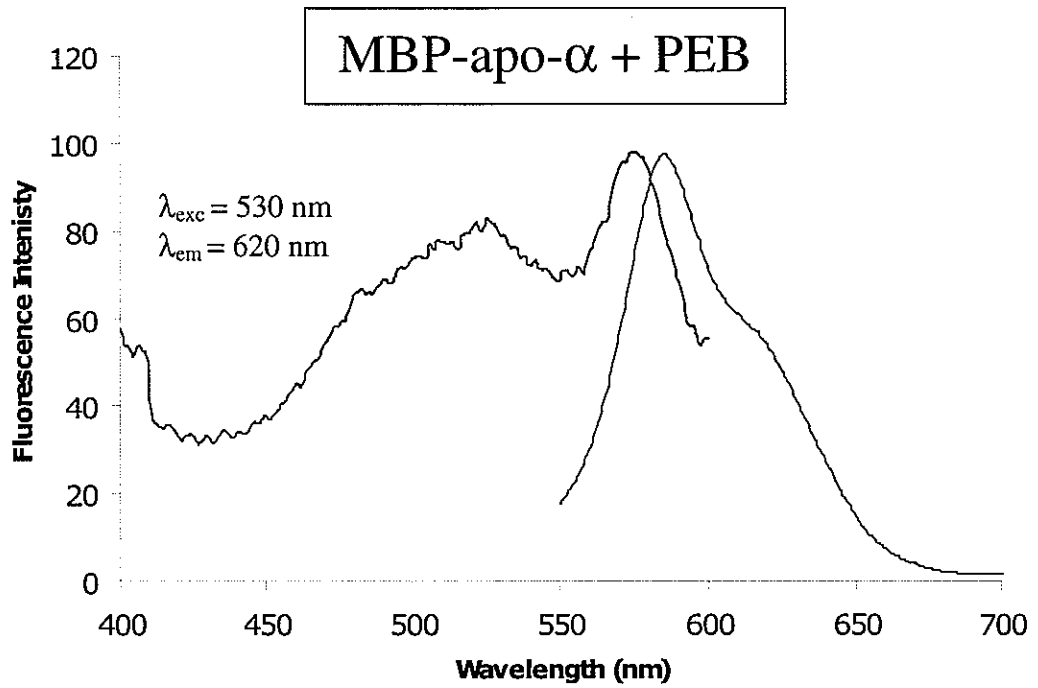
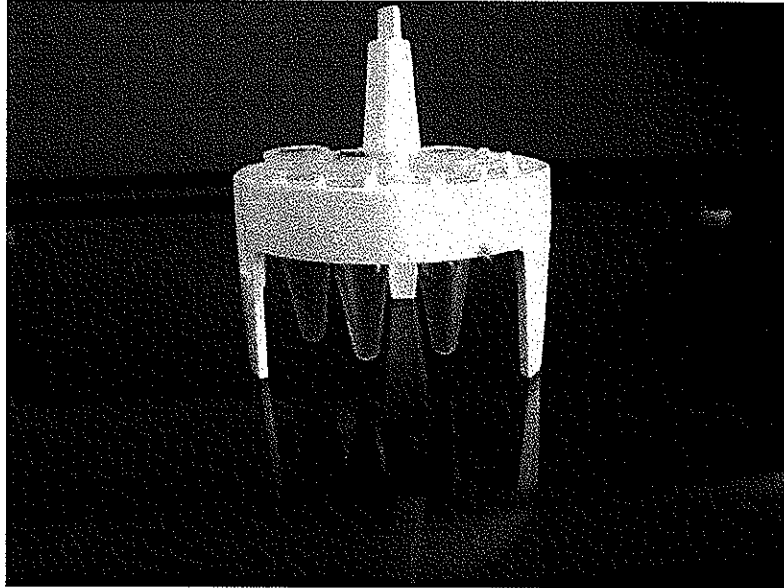


Figure 11.

A.**B.****Figure 12.**

A.



B.

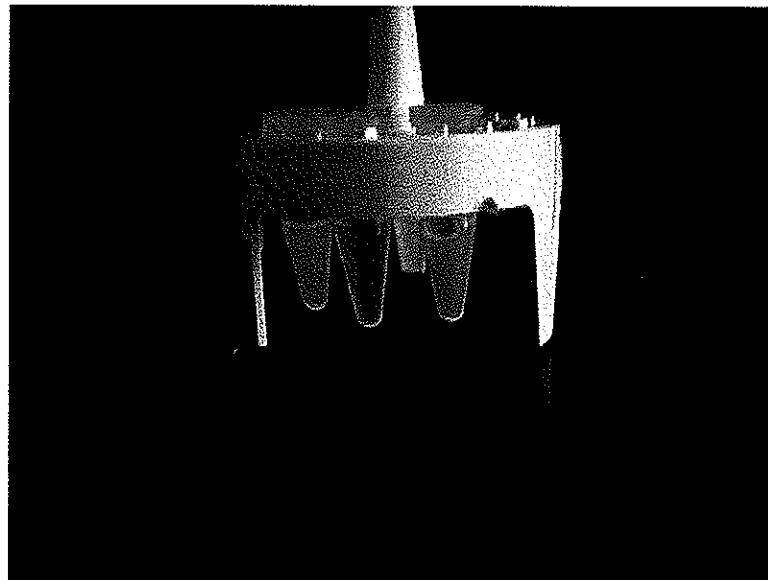


Figure 13.

**CHAPTER 4. HIGH-THROUGHPUT SINGLE-CELL FLUORESCENCE
SPECTROSCOPY**

A paper published in Applied Spectroscopy*

Dragan Isailovic, Hung-Wing Li, Gregory J. Phillips, and Edward S. Yeung

ABSTRACT

A high-throughput method for measuring single-cell fluorescence spectra is presented. Upon excitation with a 488 nm argon-ion laser many bacterial cells were imaged by a 20X microscope objective while they moved through a capillary tube. Fluorescence was dispersed by a transmission diffraction grating, and an intensified charge-coupled device (ICCD) camera simultaneously recorded the zero and the first orders of the fluorescence from each cell. Single-cell fluorescence spectra were reconstructed from the distance between zero-order and first-order maxima as well as the length and the pixel intensity distribution of the first-order images. By using this approach, the emission spectrum of *E. coli* cells expressing green fluorescent protein (GFP) was reconstructed. Also, fluorescence spectra of *E. coli* cells expressing non-fluorescent apo-subunits of R-phycoerythrin (R-PE) were recorded after incubation of the cells with phycoerythrobilin (PEB) chromophore. The fluorescence spectra are in good agreement with results obtained on the same cells using a fluorescence spectrometer or a fluorescence microscope. When spectra are to be acquired, this approach has a higher throughput, better sensitivity, and better spectral resolution compared to flow cytometry.

Index Headings: Fluorescence spectra; Single cell; *E. coli*; Transmission grating; Intensified charge-coupled device; ICCD; Green fluorescent protein; GFP; Phycoerythrobilin chromophore; PEB; R-PE apo-subunits; Holo-subunits; Flow cytometry.

INTRODUCTION

Fluorescence from a biological cell originates from its chemical components (intrinsic, native, or autofluorescence) or from chemically or genetically incorporated fluorophors (extrinsic fluorescence). Native fluorescence varies among different cells and species and can overlap the emission wavelength to interfere with the detection of a fluorescence label.¹ Sometimes the measurement of fluorescence spectra is difficult due to cell culture heterogeneity, inner filter effect, and stray light.² Depending on the application, specially designed sensitive and accurate spectroscopic methods may be needed to measure the fluorescence spectra of cells.

There are several ways to measure the fluorescence spectra of cells. Fluorescence spectrometers interrogate cells that are either suspended in a buffer in a cuvette or immobilized on a glass slide.^{2,3} The average (bulk) value of fluorescence is recorded. Spectroscopic methods that analyze properties of the individual cells could provide information that is inaccessible by population-based approaches.⁴ Single-cell fluorescence can be different from the average fluorescence of the bulk culture due to mutations, changes in the cell cycle, or different microenvironments.⁵ Hence, it could be important to measure single - cell fluorescence spectra especially in applications of fluorescence microscopy, flow cytometry, and fluorescence- activated cell sorting.

Fluorescence spectra of single cells can be acquired by fluorescence microscopy. Either a fluorescence lamp or a laser excites immobilized cells on a microscope slide, and fluorescence is collected through a microscope objective. Fluorescence light is dispersed by a spectrograph in microspectrofluorimetry^{6,7} or by an interferometer in spectral imaging.⁸⁻¹¹ Emission spectra of native and extrinsic fluorescent constituents of cells have been recorded by using these methods. Both single-cell spectra and high-resolution cell images can be obtained by spectral imaging. However, the cells may not be in their native states because they are fixed on the slide, and throughput is generally limited.

The measurement of cell fluorescence spectra in a flow stream is faster and more quantitative than the use of a microscope. Capillary electrophoresis (CE) and flow cytometry have been used to record the fluorescence spectra of cells and their components in a capillary and in a sheath flow.¹²⁻¹⁹ A laser or a lamp is used for excitation while cells or their components pass by in the liquid stream and are imaged by an objective through a window. The fluorescence is dispersed usually by a prism or a grating spectrograph, and spectra are recorded by a multichannel detector (vidicon, photodiode array, or charge coupled device (CCD)). CE separations of cells and their fluorescent components are highly efficient and sensitive.¹² However, the throughput is generally low since only one cell at a time can be in the optical path of the spectrometer.

In flow cytometry, cells are analyzed with a high throughput in a buffer that is usually a suitable environment for normal cell function. Commercial flow cytometers use photomultiplier tubes (PMTs) to measure fluorescence intensities at specific wavelengths designated by optical filters.¹³ Full cell fluorescence spectra are lost so that discrimination of cells based on minor differences in their fluorescence spectra is not possible. One way to obtain fluorescence spectra of cells in a flow cytometer is to use a scanning monochromator in front of the PMT. Fluorescence emission spectra of dyes bound for DNAs were measured by averaging scans on a population of cells.^{14,15} There were few examples that spectra of single cells were measured directly by a flow cytometer. Wade et al. observed the fluorescence spectrum of single cells by using a grating spectrograph and a vidicon detector after stopping the flow completely and waiting for the cell to drift into the laser beam.¹⁶ Besides being slow, this method required background subtraction in order to derive the spectrum of the cell.¹⁶ Spectra of single fluorescent particles were recorded by a flow cytometer using a Fourier transform interferometer for light dispersion and a PMT for detection.¹⁷ A wider use of this system was hindered by its limited throughput due to the time required for the interferometer to scan a complete spectrum.¹⁸ Gaucci et al. have recorded spectra of single cells in a flow cytometer after dispersion of light by a prism spectrograph on a photodiode array detector.¹⁸ The throughput of the system was limited to recording spectra of up to 50 cells/s.¹⁹ Spectral fingerprinting is a technique in which PMTs are replaced by a multi-channel array detector. Further improvements in instrumentation are required to

provide much higher throughput and broader use of spectral fingerprinting in flow cytometry.¹⁹

We present a high-throughput method for measurement of single-cell emission spectra in the liquid stream of a capillary by using an experimental setup developed in our lab earlier for single-molecule spectroscopy.^{20,21} Because no slits are required, the light throughput is significantly improved over spectrographs. Imaging also permitted the simultaneous acquisition of spectra from multiple cells. The goal is to record the fluorescence spectra of *E. coli* cells containing fluorescent proteins, namely GFP and holo-subunits formed after *in vivo* attachment of phycoerythrobilin (PEB) chromophore for genetically expressed R-PE apo-subunits.

EXPERIMENTAL

Chemicals. All chemicals were from Fisher Scientific (Pittsburgh, PA) or Sigma (St. Louis, MO). PEB was a generous gift of H. Scheer and M. Storf (University of Munich, Germany).

Sample Preparation. *E. coli* strain pRK6/BW25113, expressing wild-type GFP, was the gift of J. E. Cronan, Jr., and R. M. Morgan-Kiss (University of Illinois at Urbana-Champaign, IL). The strain was restreaked on low salt medium plates containing 50 mg/mL chloramphenicol, and grown at 37 °C overnight.²² A single colony was inoculated in 5 mL of low salt rich broth (LSRB) containing 50 mg/mL chloramphenicol, and cells were grown at 37 °C with shaking till an optical density (OD) of ~ 0.5 was reached. To induce GFP expression 50 mL of 20% arabinose was added and cell growth was continued for the next four hours. Then, cells were washed in phosphate buffered saline (PBS) buffer and appropriately diluted for further analysis.

Starting from the known sequence of alpha and beta apo-subunit genes of R-PE from red algae *P. boldii*²³ histidine-tagged genes were cloned in the plasmid pET-21d (+) (Novagen, Madison, WI), and plasmids were transformed in *E. coli* strain BL21 (DE3) (Novagen). Cells were grown in 50 mL of Luria-Bertani (LB) broth till an OD of ~ 0.6 was reached. After three-hour expression induction by 1 mM isopropyl β -D-

thiogalactopyranoside (IPTG), cells were washed in PBS buffer and incubated in 10 mL of the same buffer with 100 μ L of 33.7 μ M PEB solution in DMSO at 25 °C overnight. Control cells were prepared under the same conditions except that expression induction was omitted. Cells were ready for analysis after repeated washing and appropriate dilution with PBS buffer.

Histidine-tagged holo-subunits were isolated from bacterial cells under denaturing conditions using the Pro-Bond™ Purification System (Invitrogen, Carlsbad, CA) and the manufacturer's procedure.

Equipment. The experimental setup for single-cell fluorescence spectroscopy was similar to one described in Ref. 21, except that a transmission grating was inserted between the notch filter and the ICCD camera. A 75 μ m i.d. fused-silica square capillary (Polymicro, Phoenix, AZ) was washed with 0.1 M NaOH solution and PBS. Cells were injected by a syringe and moved hydrodynamically through the capillary. Their fluorescence was excited with an air-cooled 488 nm argon-ion laser (Uniphase, San Jose, CA). The power of the laser was ~5 mW. The laser beam was focused normal onto the capillary using a cylindrical lens. A Zeiss Axioscop upright microscope equipped with dry Plan-Apochromat 20X objective, NA = 0.75 (Carl Zeiss, Thornwood, NY) was used for imaging of cells in the capillary. To remove scattered light, a 488 nm holographic notch filter with O.D.> 6 (Kaiser Optical, Ann Arbor, MI) was mounted in the filter slider. Fluorescence light was dispersed through a transmission diffraction grating with 70 lines / mm (Edmund Scientific, Barrington, NJ). A Pentamax ICCD camera (Roper Scientific, Princeton, NJ) recorded the zero and first orders of the fluorescence from each cell by the program WinView 32 (Roper Scientific). The pixel size of the ICCD is 19 μ m. The distance between the ICCD and the diffraction grating was ~40 mm (d_1). The camera was operated in the external synchronization mode with the intensifier disabled open. Digitization rate and resolution of the camera were 5 MHz and 12 bits, respectively. Readout time of the camera was ~43 ms. The exposure time of the ICCD was ~5 ms in the case of GFP-containing cells and ~20 ms in the case of cells with and without expressed R-PE apo-subunits. For each cell sample 500 frames were recorded with the frame rate of 5 Hz. A Uniblitz mechanical shutter with shutter controller (Vincent

Associates, Rochester, NJ) was used to block the laser beam when the camera was off. Data analysis was done offline by software WinView 32.

The spectra of cells in the PBS buffer as well as spectra of isolated fluorescent holo-subunits were measured by a LS 50B Luminescence Spectrometer (Perkin Elmer Instruments, Beaconsfield, Buckinghamshire, UK). Fluorescence was measured in increments of 0.5 nm. Absorption spectra were measured by the 8452A diode array spectrophotometer (Hewlett Packard, Palo Alto, CA) in increments of 2 nm. A flow cytometry sorter EPICS ALTRA (Beckman Coulter INC, Fullerton, CA) was used for analysis of cells containing GFP and holo-subunits. A 488 nm argon-ion laser with a power of 15 mW was used for excitation. A 525 nm band pass filter was used for detection of fluorescence from GFP containing cells, while 525 nm, 575 nm and 620 nm band-pass filters were tried for detection of cells containing holo-subunits. In addition, cells were analyzed by another flow cytometer (Guava PCA, Guava Technologies, Hayward, CA) that used 532 nm laser for excitation and a 580 nm band-pass filter for fluorescence detection, and by fluorescence microscopy.²⁴

RESULTS AND DISCUSSION

The emission spectrum of *E. coli* cells expressing GFP recorded on the fluorescence spectrometer shows a single emission maximum at 513.0 nm upon excitation at 488.0 nm (Fig. 1). The first-order spectral image of single *E. coli* cells expressing GFP measured by our setup also shows a single maximum (Fig. 2 and Movie 1, see SAS web page). If we assign to this peak the wavelength (λ) of 513.0 nm, the value of the first-order diffraction angle calculated from the grating equation ($n\lambda = d \sin \theta$) is $\theta = 2.0588$. The distance between zero-order and first-order maxima measured for twenty cells was 78.0 ± 0.5 pixels, i.e., 1.482 mm (d_2). The distance between the ICCD and the diffraction grating ($d_1 = d_2/\tan \theta$) is equal to 41.24 mm. This value is close to the measured distance d_1 and will be used for further calculations, since it includes the thickness of the camera window that we could not measure. In this way the single-cell spectrometer was calibrated using *E. coli* cells expressing GFP.

The emission spectrum of *E. coli* cells containing holo-alpha subunits shows a maximum at 583.0 nm upon excitation at 488.0 nm in the fluorescence spectrometer (Fig. 3). Using the same instrument, no fluorescence maxima were seen in the spectra of *E. coli* cells containing holo-beta subunits. These results were not in agreement with the wavelengths of the fluorescence filters used for single-cell microscopy.²⁴ When a single-cell fluorescence spectrometer was used, two first-order fluorescence maxima were obtained in the emission spectra of cells containing both alpha and beta holo-subunits (Fig. 4 and Movies 2 and 3, see SAS web page). As measured for twenty cells, the first peak was 77.0 ± 0.5 pixels away from the zero-order peak and the second peak was 88.5 ± 0.5 pixels away from the zero-order peak. Using the above equations and parameters, the value for the first order peak diffraction angles are 2.0328° and 2.3358° . Wavelengths corresponding to these peaks are at 506.5 nm and 582.0 nm, respectively, and they are the same for both holo-subunits. The length of the first-order streaks for cells containing holo-subunits is longer than the length of the first-order streaks for GFP-containing cells (Figs. 2 and 4). This fact implies that emission bands of cells containing holo-subunits are wider than the emission spectrum of GFP-containing cells. *E. coli* cells without expressed R-PE apo-subunits showed little or no fluorescence under the same experimental conditions. This confirms that cell fluorescence is coming from the formation of fluorescent holo-subunits after binding of PEB for expressed R-PE apo-subunits. Also, we were able to image cells containing holo-subunits by fluorescence microscopy using filters whose spectral characteristics fitted our results obtained with the single-cell fluorescence spectrometer.²⁴

Additional experiments proved that the cell spectra on the single-cell level are actually more accurate than the spectra measured for cells in bulk. Since holo-subunits were histidine-tagged and made inclusion bodies they were isolated using immobilized metal affinity chromatography under denaturing conditions.²⁴ Fluorescent subunit products, with identical fluorescence spectra for both alpha and beta holo-subunits, were found by the fluorescence spectrometer (Fig. 5). The first fluorescence spectra show an excitation maximum at 495.0 nm and an emission maximum at 506.5 nm, as found in the single-cell spectrometer. The second spectra show an excitation maximum at 542.5 nm and an emission maximum at 573.0 nm, while the third fluorescence spectra show an excitation maximum at 569.5 nm and an

emission maximum at 581.0 nm. Besides overlap of emission peaks, a possible reason that the single-cell spectrometer records just the peak at 582.0 nm is fluorescence resonance energy transfer (FRET) between these electronic states *in vivo*. An absorption spectrum of isolated subunits measured in the spectrophotometer shows two maxima at 496.0 and 552.0 nm (Fig. 6). This spectrum is a superposition of the excitation spectra of holo-subunits and a mirror image of the single-cell emission spectrum. These fluorescent products imply *in vivo* formation of urobilin and phycoerythrobilin containing holo-subunits after incubation of cells containing R-PE apo-subunits with PEB. Similar fluorescent products were found after incubation of C-phycoerythrin apo- α subunit with PEB *in vitro*.²⁵

The single-cell fluorescence spectrometer is more sensitive than the EPICS ALTRA flow cytometry sorter. While this instrument was able to detect fluorescence from the GFP-containing cells (data not shown), it could not detect fluorescence from cells containing holo-subunits. Latter experiments have been tried with different band-pass filters. As in our setup, the commercial flow cytometer uses a 488-nm argon-ion laser for excitation. Since the power of the laser used there was higher than the power of the laser used in our experiments, we can conclude that our system has higher light throughput and is more sensitive than this flow cytometer. Many commercial flow cytometers have a multi-channel configuration similar to EPICS ALTRA. The two-channel flow cytometer Guava PCA was able to distinguish fluorescence from cells containing holo-subunits from control cells.²⁴ This indicates that the optical configuration of a spectral flow cytometer is critical for its selectivity. The high-sensitivity of our system was proven in single-molecule spectroscopy and capillary electrophoresis experiments.^{20, 21} Although laser excitation gives sensitive detection, a fluorescence lamp and appropriate filters could be used for excitation in our setup as well.

The spectral resolution of our system was ~ 6.5 nm per pixel, which is better than in standard flow cytometers that use optical filters for wavelength selection. Spectral resolution in our setup can be improved if the distance between the grating and ICCD is increased, if a grating with shorter groove spacing (d) is used, or if an ICCD camera with smaller pixels is used.

As could be seen in the accompanying movies (see SAS web page), many single cells were imaged when they move through the capillary. In fact, there is no reason why the flow

rate cannot be increased substantially. So, this method has high-throughput capabilities even though the rate here was ~7 cells/s. Also, unlike in Ref. 18 where the spectra of some cells are omitted, a spectrum for each cell is recorded by our setup.

CONCLUSION

The single-cell fluorescence spectrometer was successfully applied in fluorescence spectra measurement of bacterial cells containing fluorescent proteins. Fluorescence proteins were either genetically expressed (GFP) or were formed upon cell incubation with the appropriate chromophore (holo-subunits). In the case of cells containing holo-subunits the results were more reliable than the results obtained from the fluorescence spectrometer, emphasizing the importance of analysis at the single-cell level.

The single-cell fluorescence spectrometer has higher throughput, better sensitivity, and improved spectral resolution compared to previously described setups for single-cell spectroscopy and standard flow cytometers. The setup is straightforward in construction and operation. It could be applied whenever fluorescence spectral recognition of cells or single molecules is desirable. Potential application areas are high-throughput cell screening (for example, in aquatic microbiology), gene expression analysis, cell–dye interaction, new fluorophore development, or fluorescence *in situ* hybridization (FISH). Emission spectra of native or extrinsic fluorophores can be measured from the cells of different dimensions with little or no modification in the experimental setup.

ACKNOWLEDGMENTS

The authors thank H. Scheer and M. Storf for the gift of PEB, J. E. Cronan, Jr. and R. M. Morgan-Kiss for the gift of the *E. coli* strain expressing GFP, and S. M. Rigby (Flow Cytometry Facility, Iowa State University) for work on flow cytometry experiments. E.S.Y. thanks the Robert Allen Wright Endowment for Excellence for support. The Ames Laboratory is operated for the U.S. Department of Energy by Iowa State University under Contract No. W-7405-ENG-82. This work was supported by the Director of Science, Office

of Basic Energy Sciences, Division of Chemical Sciences, and the Office of Biological and Environmental Research.

SUPPLEMENTARY MATERIAL

The three movie clips mentioned in the text have been posted on the web page of the Society for Applied Spectroscopy, www.s-a-s.org.

Movie 1. AVI file showing analysis of GFP-containing *E. coli* cells by the single-cell fluorescence spectrometer.

Movie 2. AVI file showing analysis of *E. coli* cells containing alpha holo-subunits by the single-cell fluorescence spectrometer.

Movie 3. AVI file showing analysis of *E. coli* cells containing beta holo-subunits by the single-cell fluorescence spectrometer.

REFERENCES

1. N. Billinton and A. W. Knight, *Anal. Biochem.* **291**, 175 (2001).
2. C. L. Bashford and D. A. Harris, Eds., *Spectrophotometry and Spectrofluorimetry: A Practical Approach* (Press Limited, Enysham, Oxford, England, 1987), p. 115.
3. <http://www.fluorescence.com/products/cuvette/cuvette-acc.htm>, on July 18, 2005
4. B. F. Brehm-Stecher and E. A. Johnson, *Microbiol. Mol. Biol. Rev.* **68**, 538 (2004).
5. H. M. Davey and D. B. Kell, *Microbiol. Rev.* **60**, 641 (1996).
6. L. Ying, X. Huang, B. Huang, J. Xie, J. Zhao, and X. S. Zhao, *Photochem. Photobiol.* **76**, 310 (2002).
7. R. Marangoni, R. Cubeddu, P. Taroni, G. Valentini, R. Sorbi, E. Lorenzini, and G. Columbetti, *J. Photochem. Photobiol.* **34**, 183 (1996).
8. X. F. Weng and B. Herman, Eds., *Fluorescence Imaging Spectroscopy and Microscopy* (John Wiley and Sons, New York, 1996), p.87.
9. <http://www.spectral-imaging.com/technology.asp>, on July 18, 2005.
10. L. Greenbaum, D. Schwartz, and Z. Malik, *J. Histochem. Cytochem.* **50**, 1205 (2002).

11. M. L. Slovak, L. Tcheurekdjian, F. F. Zhang, and J. L. Murata-Collins, *Cancer Res.* **61**, 831 (2001).
12. X. Zhang, J. N. Stuart, and J. V. Sweedler, *Anal. Bioanal. Chem.* **373**, 332 (2002).
13. A. J. Beavis and R. F. Kalejta, *Cytometry* **37**, 68 (1999).
14. H. B. Steen and T. Stokke, *Cytometry* **7**, 104 (1986).
15. C. L. Asbury, R. Esposito, C. Farmer, and G. van den Engh, *Cytometry* **24**, 234 (1996).
16. C. G. Wade, R. H. Rhyne, W. H. Woodruff, D. P. Bloch, and J. C. Bartholomew, *J. Histochem. Cytochem.* **27**, 1049 (1979).
17. T. N. Buican, *SPIE* **1205** (1990).
18. M. R. Gaucci, G. Vesey, J. Narai, D. Veal, K. L. Villiams, and J. A. Piper, *Cytometry* **25**, 388 (1996).
19. D. A. Veal, D. Deere, B. Ferrari, J. Piper, and P. V. Atfield, *J. Immunol. Meth.* **243**, 191 (2000).
20. Y. Ma, M. R. Shortreed, and E. S. Yeung, *Anal. Chem.* **72**, 4640 (2000).
21. J. Zheng and E. S. Yeung, *Anal. Chem.* **74**, 4536 (2002).
22. R. M. Morgan-Kiss, C. Wadler, and J. Cronan, *Proc. Natl. Acad. Sci. U.S.A.* **99**, 7373 (2002).
23. M. K. Roell and D. E. Morse, *Plant Mol. Biol.* **21**, 47 (1993).
24. D. Isailovic, G. J. Phillips, and E. S. Yeung, manuscript in preparation (2004).
25. C. D. Fairchild and A. N. Glazer, *J. Biol. Chem.* **269**, 28988 (1994).

FIGURE CAPTIONS

FIG. 1. Normalized excitation and emission fluorescence spectra of GFP-containing *E. coli* cells recorded on the fluorescence spectrometer ($\lambda_{\text{exc}} = 488 \text{ nm}$, $\lambda_{\text{em}} = 540 \text{ nm}$).

FIG. 2. Fluorescence spectra of GFP-containing *E. coli* cells recorded on the single-cell fluorescence spectrometer. A frame of Movie 1 (see SAS web page) is shown using the program WinView 32. The ICCD camera records zero-order images (bright dots) and first-order spectral images (bright horizontal streaks) for each cell during cell movement through

the capillary as shown in the upper panel and Movie 1. Distribution of intensities in a row of pixels (bottom panel) was used to reconstruct the emission spectrum of the cells containing GFP as described in the text.

FIG. 3. Normalized excitation and emission fluorescence spectra of *E. coli* cells containing R-PE apo-alpha subunits after incubation with PEB chromophore. Spectra were recorded on the fluorescence spectrometer ($\lambda_{\text{exc}} = 488 \text{ nm}$, $\lambda_{\text{em}} = 600 \text{ nm}$).

FIG. 4. Fluorescence spectra of *E. coli* cells containing (left) alpha and (right) beta holo-subunits recorded on the single-cell fluorescence spectrometer. Frames from Movies 2 and 3 (see SAS web page) are shown using the program WinView 32. The ICCD camera records zero-order images (bright dots) and first-order spectral images (bright horizontal streaks) during movement of cells through the capillary as shown in the upper panels and Movies 2 and 3. Distribution of intensities in a row of pixels (bottom panels) was used to reconstruct the emission spectra of cells containing holo-subunits as described in the text.

FIG. 5. Normalized excitation and emission fluorescence spectra of isolated holo-subunits. The excitation and emission wavelengths used to record these spectra were (from the top to the bottom): $\lambda_{\text{exc}} = 470 \text{ nm}$, $\lambda_{\text{em}} = 530 \text{ nm}$; $\lambda_{\text{exc}} = 532 \text{ nm}$, $\lambda_{\text{em}} = 570 \text{ nm}$; and $\lambda_{\text{exc}} = 550 \text{ nm}$, $\lambda_{\text{em}} = 620 \text{ nm}$. Spectra correspond to holo-subunits containing covalently bound urobilin (top spectra) and phycoerythrobilin (middle and bottom spectra) chromophores.

FIG. 6. Absorption spectrum of isolated holo-subunits recorded on the absorbance spectrophotometer.

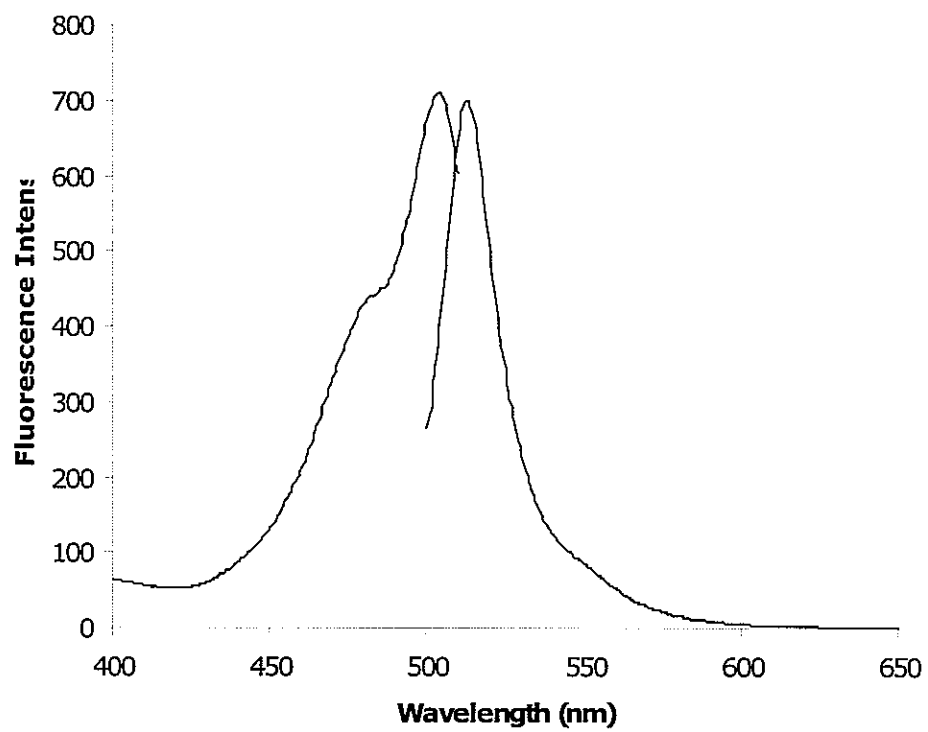


Figure 1.

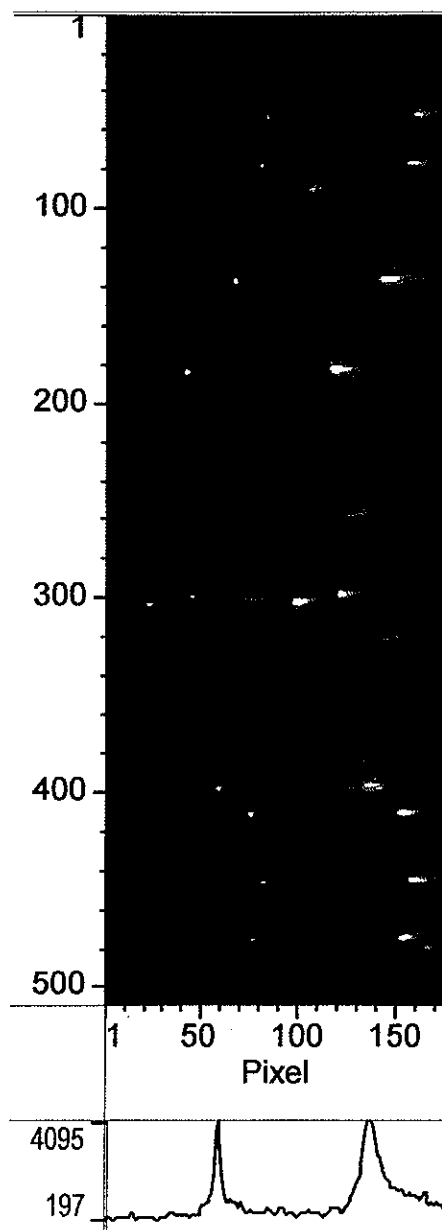


Figure 2.

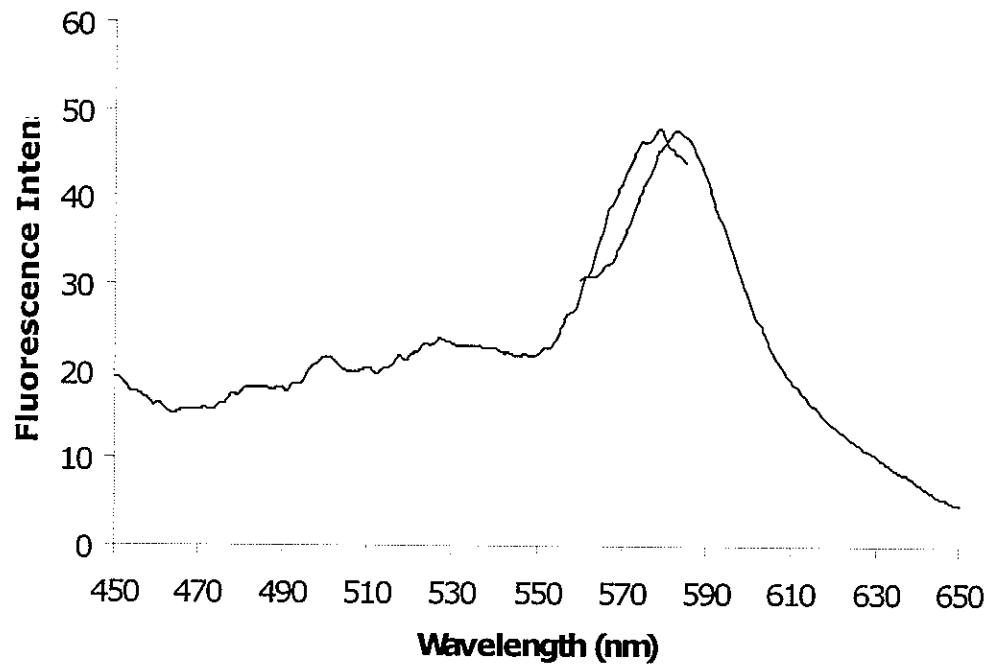


Figure 3.

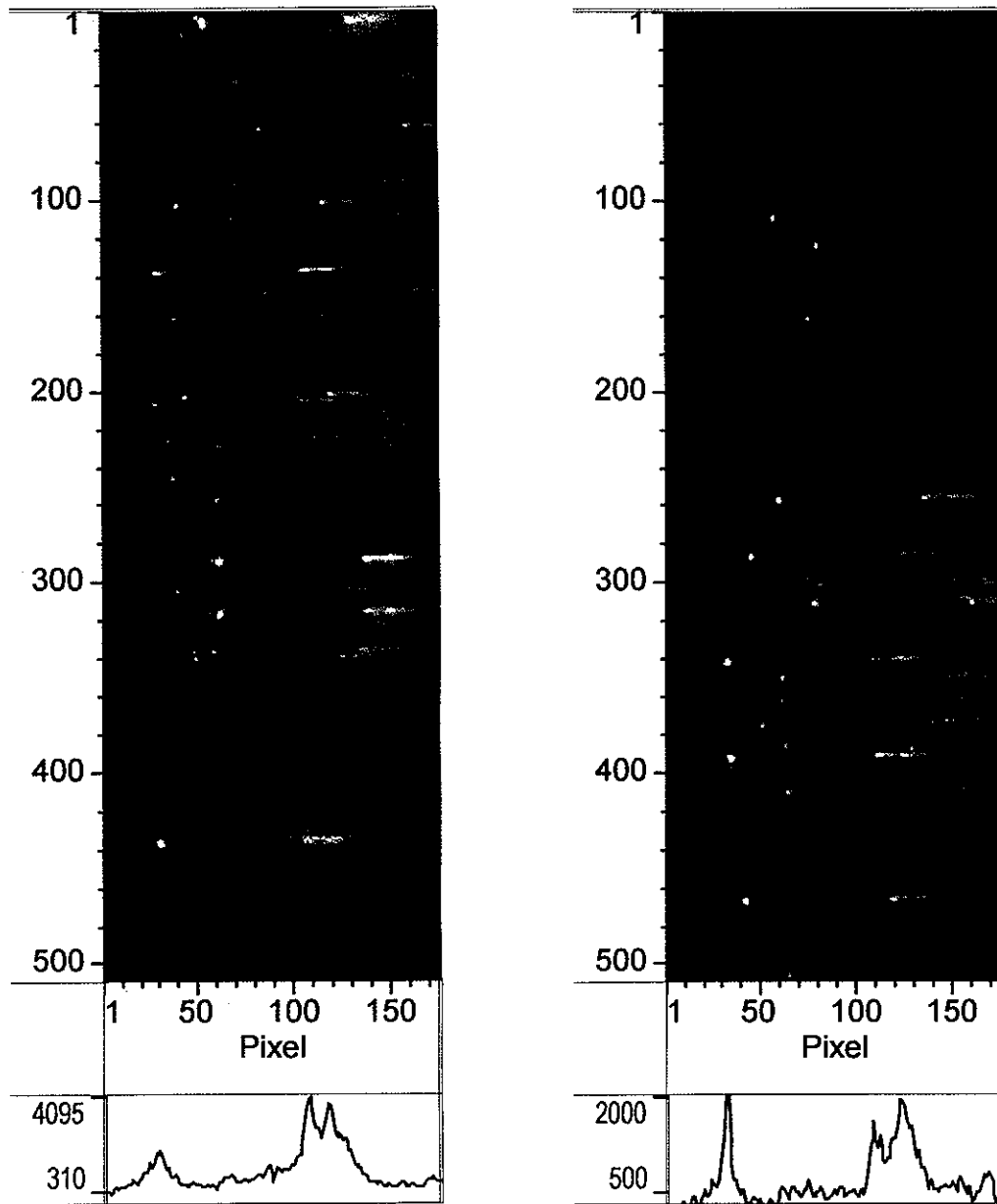


Figure 4.

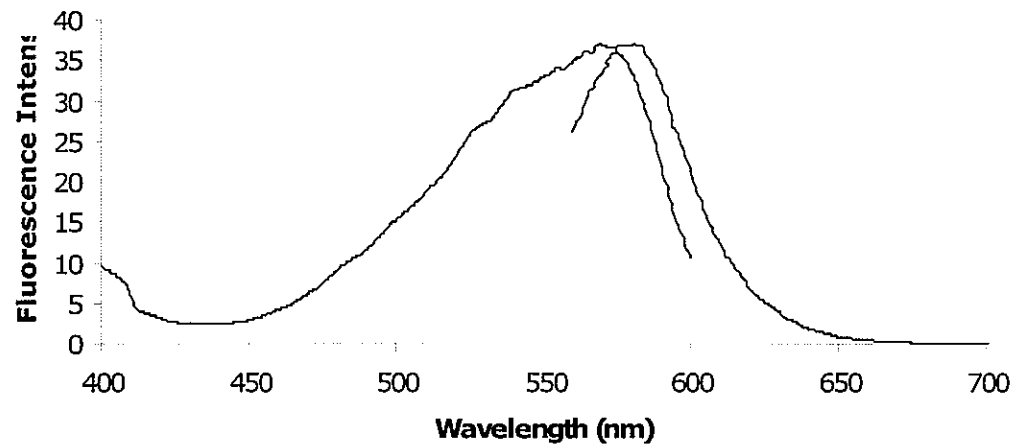
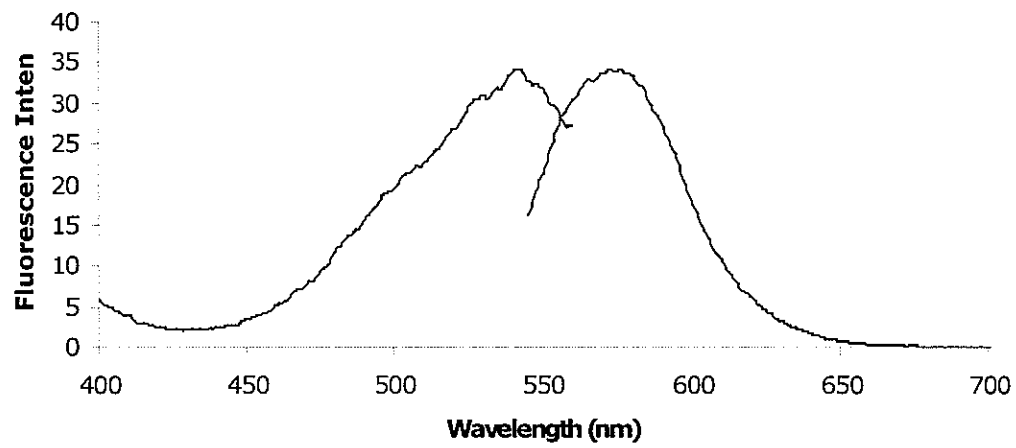
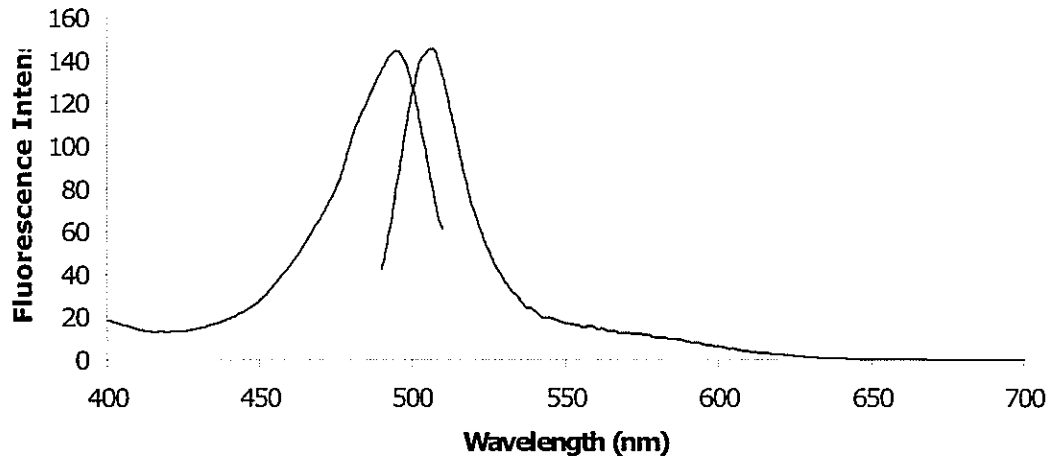


Figure 5.

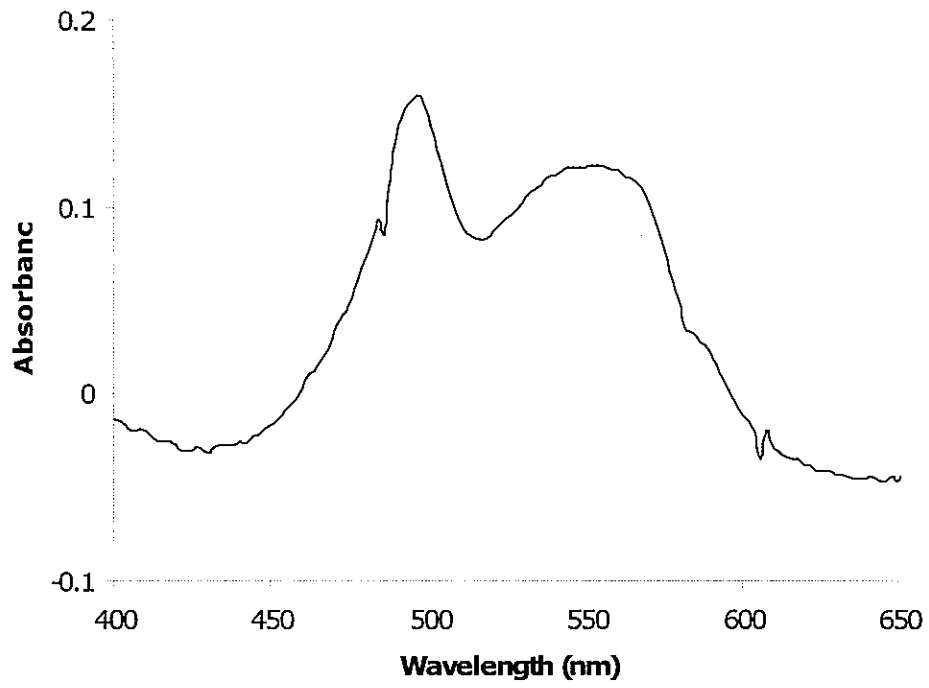


Figure 6.

CHAPTER 5. GENERAL CONCLUSIONS

Development of novel fluorescent probes with excellent spectroscopic properties will contribute to new discoveries in single-cell analysis and single-molecule detection.

Phycocerythrins are the most fluorescent molecules found to date. Their high fluorescence has proven extremely useful in many bioanalytical applications including flow cytometry and fluorescence microscopy. However, the large size of these 240 kDa trimeric proteins poses problem of steric effects and restricts use of phycobiliproteins for labeling of cells and molecules. Also, the cloning and expression of these complex proteins in cells would be very difficult. Our approach to overcome these difficulties was to investigate possible applications of R-PE subunits for SMD and labeling of cells.

Several separation and detection methods have been optimized in order to characterize R-PE subunits as well as their enzymatic digests. These highly fluorescent molecules were readily isolated from R-PE by semi-preparative chromatography. Detection of R-PE subunits at the single-molecule level confirmed their excellent absorption and fluorescence properties. R-PE subunits and chromophore-containing peptides showed good potential for use as fluorescence probes in single-molecule detection and single-cell analysis. In contrast to GFP, they remain fluorescent even under denaturing conditions and at low pH values. This is making them suitable for labeling of single-molecules as well as acidic organelles or other cellular compartments that are under specific physiological conditions. Attachment of R-PE subunits to antibodies or other biologically active moieties could yield new applications in immunofluorescent microscopy and flow cytometry. They would interfere less with the system under interrogation (for example molecules, cells or surfaces) than R-PE because of the absence of interactions associated with quaternary structure and much smaller size compared to R-PE. It would be interesting to investigate how efficiently R-PE digest peptides could be used as fluorescence probes, because they will decrease steric interactions during labeling to a minimum.

To further improve the potential of R-PE subunits for labeling of cells and molecules we designed fluorescent holo-subunits by attachment of PEB chromophore to recombinant alpha and beta apo-subunits. We cloned apo-subunit genes of R-PE from red algae

Polisiphonia boldii into bacterium *Escherichia coli*. Although expression yielded to aggregation of apo-subunits in inclusion bodies, fluorescent holo-subunits were surprisingly formed after incubation of the bacterial cells with PEB *in vivo*. Spectroscopic characterization of isolated holo-subunits showed that they contained not only PEB but also its isomer urobilin. Polar location of inclusion bodies in bacterial cells was unambiguously confirmed by high-resolution and high-contrast images acquired by both DIC and fluorescence microscopy. Inclusion bodies are usually located in cells by transmission electron microscopy (TEM). A fluorescent reporter of inclusion bodies based on attachment of PEB to R-PE apo-subunits could be a less expensive and less time consuming alternative for TEM. Since 70 to 80% of all recombinant proteins form inclusion bodies such a fluorescent reporter could be a sensitive and selective marker of protein aggregation, readily adapted to high-throughput applications.

Fluorescent proteins were also formed after attachment of PEB chromophore to fusions of *E. coli* maltose binding protein (MBP) and R-PE apo-subunits *in vitro* and *in vivo*. Both cytoplasmic and periplasmic versions of MBP formed orange-fluorescent fusions with apo-alpha and apo-beta subunits that were soluble. Attachment of PEB to fusion proteins happened without isomerization of the chromophore and lead to high increase in the brightness of the fluorophore. Fluorescence microscopy revealed that fusion proteins were localized either throughout the cells or on cell poles. Our future goal is to optimize the expression of periplasmic MBP-subunit fusion so that most of the protein is exported to the periplasmic space of *E. coli*. If MBP-fusions are functional in this subcellular compartment attachment of PEB chromophore should yield fluorescence signal located mainly in periplasmic space. While GFP was active in periplasmic space when exported by the TAT secretion pathway, it was not functional when targeted by the Sec pathway. Ideally, R-PE-subunit fusions might work as reporters of protein transport in both pathways. This could help us to answer important biological questions related to secretion and transport of proteins from the cytoplasm into periplasmic space of bacteria.

Fluorescent subunits were successfully used in flow cytometry and fluorescence microscopy, and show promise for use in photodynamic therapy of cancer. Possibilities are fully open for use of recombinant R-PE apo-subunits as reporters of gene expression and

protein localization after incubation of cells with PEB chromophore. Good properties of R-PE apo-subunit fluorescent fusions include: broad excitation and emission fluorescence spectra, high fluorescence in the orange region of the electromagnetic spectrum (away from cellular autofluorescence), and functioning both *in vitro* and *in vivo*. The unique property of such a reporter is that it works despite the way R-PE apo-subunits are folded. There is still much room for improvement of fluorescent properties of holo-subunits through mutagenesis, as well as the use of other phycobilins in the attachment. The need for exogenous supply of PEB chromophore could be overcome if the complete biosynthetic pathway for formation and attachment of PEB to apo-subunits of R-PE can be expressed in a heterologous system. Such a project would yield both to new and improved recombinant phycobiliproteins and help to reveal details about biogenesis of these highly fluorescent compounds in nature.

In addition to development of novel fluorescent protein probes we realize that improvements in bioanalytical technologies are very important for analysis of cells and molecules. We demonstrated a high-throughput technique for measurement of fluorescence spectra of bacterial cells containing fluorescent proteins that were either genetically expressed (GFP) or formed after cell-dye interaction (holo-subunits). Useful applications of the technique could be envisioned in gene expression analysis, cell-dye interaction, new fluorophore development, or fluorescence *in situ* hybridization (FISH). The setup could be used for high-throughput cell screening based on both cell fluorescence or scattered light in aquatic microbiology, biodefense, or clinical chemistry. The single-cell fluorescence spectrometer could have higher throughput, better sensitivity, and improved spectral resolution compared to spectral flow cytometers. The setup was successfully applied for fluorescence spectroscopy of single-molecules that confirms the exceptional sensitivity of the method. Improvements in the setup optics and imaging software could make this instrument a real state-of-art spectral imager, and provide also cell-sorting capabilities.

Analysis of cells and molecules is crucial for development of basic sciences as well as for discoveries in technology and medicine. Since the amount of some substances in cells is limited down to the single-molecule level, developments and improvements in the sensitivity and the selectivity of experimental methods is always beneficial. In addition, improvements in the throughput of a method will provide shorter analysis time making a technique very

suitable for clinical or industrial applications. We hope that results shown in this thesis will contribute to improvements in single-cell analysis and single-molecule detection.

ACKNOWLEDGEMENT

First of all, I want to thank my major professor Dr. Yeung for the generous support during my graduate studies. He had given me the chance to work in his group, and enjoy the research that I really liked. Besides very interesting lectures in spectroscopy class, he helped me in my research and my quest for knowledge. He encouraged me to attend conferences and helped to defray costs. Also, I was fortunate to have access to high-technology equipment and supplies. Thanks to Dr. Yeung I received skills and experiences that will be extremely valuable for my future career.

I want to thank Dr. Phillips for an enormous help in research. From him I received an excellent training in microbiology. Moreover our discussions of science behind experiments and issues that arose from research helped me to broad and strengthen my scientific experience. He demonstrated to me how to succeed as a teacher and a scientist. I am very thankful for the feedback that I received from him. The work with Dr. Phillips will be a great experience for my whole career.

I would also like to thank other members of my POS committee. They were opened for discussions and gave me great advices. Dr. Hong was my first adviser at ISU and from her I learnt how to succeed as a graduate student. She taught me much about great NMR experiments, and she is the most deserving for a paper that we published together. Dr. Houk gave me an excellent background in mass spectrometry, and Dr. Porter did the same in electrochemistry class. Dr Lin's presence in my POS committee was also valuable.

I am thankful very much to members of Dr. Yeung, Dr. Phillips and Dr. Hong's research groups for the help in the research. I learnt something new from all of them and spent enjoyable time with these hard-working scientists. Especially I would like to thank Hung-Wing, Ishrat, Slavica, Craig and Chanan for help with experiments described in this thesis and useful discussions. It was great experience to work with them.

There are many people at Iowa State University and around the world who also deserve credit for supporting the research described in this thesis. I acknowledged to some of them in the manuscripts, and I would like to thank all of them again. It was my honor and privilege to collaborate with them and learn from them.

In the end I would like to thank my family and friends for all support and nice moments that we spent together during last five years. My parents-in-law, who spent much time with us during this period, and my parents also helped to get close to graduation. They and especially my wife Slavica and our son Petar made my life in graduate school harmonic and beautiful.